OPTIMUM OIL PALM SHELL CONTENT AS COARSE AGGREGATE IN CONCRETE BASED ON MECHANICAL AND DRYING SHRINKAGE PROPERTIES

MEHDI MAGHFOURI

DISSERATION SUBMITTED IN FULFILMENT OF THE REQUIREMENTS FOR THE DEGREE OF MASTER OF PHILOSOPHY

FACULTY OF ENGINEERING
UNIVERSITY OF MALAYA
KUALA LUMPUR

2019

UNIVERSITY OF MALAYA

ORIGINAL LITERARY WORK DECLARATION

Name of Candidate: Mehdi Maghfouri

Matric No: KGA140018

Name of Degree: Master of philosophy

Title of Dissertation:

"Optimum oil palm shell content as coarse aggregate in concrete based on mechanical and drying shrinkage properties"

Field of Study: Engineering science based

I do solemnly and sincerely declare that:

(1) I am the sole author/writer of this Work;
(2) This Work is original;
(3) Any use of any work in which copyright exists was done by way of fair dealing and for permitted purposes and any excerpt or extract from, or reference to or reproduction of any copyright work has been disclosed expressly and sufficiently and the title of the Work and its authorship have been acknowledged in this Work;
(4) I do not have any actual knowledge nor do I ought reasonably to know that the making of this work constitutes an infringement of any copyright work;
(5) I hereby assign all and every rights in the copyright to this Work to the University of Malaya ("UM"), who henceforth shall be owner of the copyright in this Work and that any reproduction or use in any form or by any means whatsoever is prohibited without the written consent of UM having been first had and obtained;
(6) I am fully aware that if in the course of making this Work I have infringed any copyright whether intentionally or otherwise, I may be subject to legal action or any other action as may be determined by UM.

Candidate's Signature Date:

Subscribed and solemnly declared before,

Witness's Signature Date:

Name:

Designation:

ABSTRACT

Oil palm shell (OPS) is a bio-solid waste in palm oil industry in tropical region which could be used as aggregate in concrete mixture. For more than three decades, OPS has been experimented as lightweight aggregate to produce lightweight aggregate concrete (LWAC). The use of this solid waste is not only a practical way to reduce the negative impact of the construction industry but also leads to a low-cost material. Medium and high strength LWAC using of OPS as coarse aggregate was successfully produced and reported by the researchers. However, high drying shrinkage at early and later ages is considered as a drawback for this type of concrete. From previous studies it was concluded that increasing the volume of OPS in concrete mixtures, leads to lower mechanical properties and higher drying shrinkage. In this regard, comprehensive experimental study was carried out to investigate the effect of partial replacement of crushed granite aggregates in normal-weight concrete (NWC) with OPS on mechanical properties and drying shrinkage behaviour in order to obtain the optimum level of OPS contribution in concrete mixture. For this study, six concrete mixes were designed using crushed granite and the OPS as coarse aggregates. The NWC by using of crushed granite aggregate and density of 2340 kg/m^3 was considered as control concrete, and for all other mixes, crushed granite was partially replaced with OPS from 0 to 100% (by volume) with interval of 20% and a constant water to cement ratio of 0.33. The influence of curing condition on mechanical properties and drying shrinkage of concretes was also considered. Three different conditions of curing, namely, air curing (AC) to simulate the practical curing condition, 28 days' water curing (28D) and 7 days curing in water and then air drying (7D) in the laboratory environment, are employed to examine 28-day compressive strength. The results of the study clearly indicated that up to 60% replacement of crushed granite aggregates by OPS in NWC, structural lightweight

aggregate concrete with maximum drying shrinkage strain of approximately 500 micro-strain can be produced which is in allowable limit for drying shrinkage. Whereas in long-term ages (275 days) the value of drying shrinkage was 33% higher than the control mix. For mixes containing OPS beyond 60% the increment of shrinkage was significantly higher. Furthermore, for mixes containing up to 60% OPS, mechanical properties and final water absorption were satisfactory.

ABSTRAK

Oil Palm Shell (OPS) adalah sisa bio-pepejal dalam industri minyak sawit di rantau tropika yang boleh digunakan sebagai agregat dalam campuran konkrit. Lebih 3 dekad yang lalu, OPS telah dikaji sebagai agregat ringan semulajadi dalam penyelidikan untuk menghasilkan konkrit agregate ringan (LWAC). Penggunaan sisa pepejal ini bukan sahaja merupakan penyelesaian praktikal untuk mengurangkan kesan negatif industri konkrit tetapi juga membawa kepada bahan kos rendah. Kekuatan LWC pada kadar sederhana dan tinggi dengan menggunakan OPS sebagai agregat kasar berjaya dihasilkan. Walau bagaimanapun, pengecutan pengeringan yang tinggi pada usia awal dianggap sebagai kelemahan untuk jenis konkrit ini. Daripada kajian terdahulu, kesimpulan bahawa peningkatan jumlah OPS dalam konkrit membawa kepada sifat mekanikal yang rendah dan pengecutan pengeringan yang lebih tinggi. Dalam kaitan ini, kajian eksperimen yang komprehensif telah dijalankan untuk mengkaji kesan penggantian sebahagian daripada agregat granit yang dihancurkan dalam konkrit berat normal atau normal-weight Concrete (NWC) dengan OPS pada sifat mekanik dan kelakuan pengerasan pengeringan untuk mendapatkan keputusan maksima terhadap sumbangan OPS dalam campuran konkrit. Untuk kajian ini, enam campuran konkrit telah direka menggunakan granit yang dihancurkan dan OPS sebagai agregat kasar. NWC dengan kepadatan 2340 kg/m^3 dengan menggunakan agregat granit yang dihancurkan dianggap sebagai konkrit kawalan, dan untuk semua campuran lain, granit yang dihancurkan sebahagiannya diganti dengan OPS dari 20 hingga 100% (mengikut kuantiti) dengan selang 20 % dan air berterusan kepada nisbah simen 0.33. Pengaruh keadaan pengawetan terhadap sifat-sifat mekanik dan pengecutan pengeringan konkrit juga dipertimbangkan. Tiga keadaan pengawetan yang berbeza, iaitu pengawetan udara atau air curing (AC) untuk mensimulasikan keadaan pengawetan praktikal, 28 hari pengawetan air atau water curing (WC) dan 7 hari pengawetan di dalam air (AC) dan kemudian pengeringan udara (AC) (7 hari) dalam

persekitaran makmal, digunakan untuk memeriksa 28 kekuatan mampatan sehari. Keputusan kajian menunjukkan dengan jelas bahawa sehingga 60% penggantian agregat granit dihancurkan oleh OPS di dalam NWC, konkrit agregat ringan struktur dengan ketegangan pengecutan maksimum kira-kira 500 micro-strain boleh dihasilkan yang mempunyai had yang dibenarkan untuk pengecutan pengeringan. Sedangkan dalam jangka masa panjang (275 hari) nilai pengecutan pengeringan adalah 33% lebih tinggi daripada campuran kawalan untuk campuran yang mengandungi OPS melebihi 60% kenaikan dalam pengecutan adalah jauh lebih tinggi. Tambahan pula, untuk campuran sehingga 60% daripada kadar penggatian, sifat-sifat mekanik dan penyerapan air akhir berada dalam julat yang memuaskan.

ACKNOWLEDGEMENTS

I would like to express my gratitude to all those who gave me the possibility to complete this dissertation.

My first and sincere appreciation goes to my supervisor, Dr. Payam Shafigh for the encouragement, advices and continues support on my research. I would also like to thank Prof. Ir. Dr. Mohd Zamin Bin Jumaat for his good advices and support.

A special thanks to my parent for every single support in my research, carrier and life. I also would like to express my gratitude to Mr. Vahid Alimohammadi, Ir. Choon Teck Kiang and all the members in the Engineering Faculty for their help and supports in this research.

TABLE OF CONTENTS

LIST OF FIGURES

LIST OF TABLES

LIST OF SYMBOLS AND ABBREVIATIONS

ACI	:	American Concrete Institute
BS	:	British Standard
CV	:	Coefficient of Variation
EP	:	Error Percentage
EPA	:	Expanded Perlite Aggregate
EPAC	:	Expanded Perlite Aggregate Concrete
GBR	:	Green Building Rating
HSLC	:	High Strength Lightweight Concrete
LWA	:	Lightweight Aggregate
LWC	:	Lightweight Concrete
LWAC	:	Lightweight Aggregate Concrete
MS	:	Malaysian Standard
NWA	:	Normal Weight Aggregate
NWC	:	Normal Weight Concrete
OPBC	:	Oil Palm Boiler Clinker
OPC	:	Ordinary Portland Cement
OPS	:	Oil Palm Shell
OPSC	:	Oil Palm Shell Concrete
PAC	:	Pumice Aggregate Concrete
RH	:	Relative Humidity
SP	:	Super-plasticizer
W/C	:	Water to Cement ratio

CHAPTER 1: INTRODUCTION

1.1 Background of the Study

Concrete is a common structural material in construction industry which is made by mixing of binders, sand, aggregate and water. In most of countries the consumption of the concrete is 10 times greater than steel. Due to three main factors concrete is the most popular engineering material. First, the ability of water resistance which is significant specially for the hydraulic structures. The second factor is workability and ability of fresh concrete that can be easily shaped, placed and formed. The third reason is the low cost and availably of this material. With production of more than 10 billion tons of concrete annually it is considered the most important building material (Meyer, 2009; Swamy, 2007). It has been predicted that the world's population will increase to about 9 billion by the year 2050, which will result in a remarkable increase in the demand for natural resources, energy and services (Rosković & Bjegović, 2005). The demand for concrete also is expected to grow to approximately 18 billion tons a year by 2050 (Mehta & Monteiro, 2006). Consequently, the concrete industry is going to use a considerable amount of natural resources to produce cement and concrete. The green rating for infrastructure and buildings has become increasingly widespread in the last decade. Generally, the current green building rating (GBR) systems evaluate the sustainability of buildings according to various categories, of which the construction material is one such category in most of the systems. Issues like carbon dioxide emissions during the production of Portland cement, along with a significant amount of energy, water, aggregate and fillers used for production of concrete as well as construction waste from the demolition of concrete structures, makes this important construction material look less compatible with the environmental requirements of a modern sustainable construction industry. Ramezanianpour et al. (2009) demonstrated that the current state of the concrete industry is not sustainable. However, the utilization of industrial and agricultural waste

components can be a breakthrough to make the industry more environmental friendly and sustainable. Waste materials, such as fly ash, silica fume, ground granulated blast furnace slag, recycled concrete, post-consumer glass, recycled tyres, and recycled plastics, have been successfully used in concrete for decades (Meyer, 2009; Rosković & Bjegović, 2005). Also, recent studies have shown the successful use of agricultural solid waste as aggregate in structural and non-structural concrete. Oil palm shell (or palm kernel shell), coconut shell, rice husk, corn cob, pistachio shell, spent mushroom substrate and tobacco wastes are among the wastes used for this purpose. Since aggregate (sand as fine and gravel as coarse) makes up about 60 to 80% of the volume of concrete (Badur & Chaudhary, 2008), the successful use of such agricultural solid wastes, as whole or partial replacement of conventional aggregates, contributes to energy saving, conservation of natural resources, and a reduction in the cost of construction materials. It also solves the disposal problem of the wastes, and, hence, helps environmental protection (Harimi et al., 2005).

The oil palm industry is one of the most important agro-industries in certain countries, such as Malaysia, Indonesia, Thailand and Nigeria. Malaysia and Indonesia are respectively the world's largest palm oil producing countries. Malaysia is producing more than half of the world's total output of palm oil, planted over 4.05 million hectares of land, yielding about 18.88 tons/hectare of fresh fruit bunches (Teo et al., 2006). In the oil palm industry, waste is normally disposed through incineration and at times, the shell is left to rot in huge mounds that will ultimately cause pollution and is harmful to the ecosystem. Exploitation of this waste material as sustainable building material in the construction industry not only solves the problem of disposing this solid waste but also helps conserve natural resources and maintain the ecological balance. The great mass of oil palm shells (OPS) in the palm oil mill area is shown in figure 1.1. Results from previous studies show that OPS can be used as LWA for production of LWAC (Teo et

al., 2006). For OPS lightweight concrete the compressive strength in the range of 13-22 MPa was observed by many researchers. Also with the inclusion of fly ash, silica fume and admixtures, compressive strength of 37 MPa has been obtained. Furthermore, high strength lightweight concrete with 28-day compressive strength up to 48 MPa with dry density of about 1870 and 1990 kg/m^3 using of the crushed OPS and limestone powder has been reported (Alengaram et al., 2013; Shafigh et al., 2014a and 2014b).

Figure 1-1: A massive volume of oil palm shell in the palm oil mill yard (Shafigh et al., 2010)

1.2 Problem Statement

Using of the lightweight aggregate is a popular way to produce lightweight concrete. The oil palm shell as a solid waste from the palm oil industry is one of the natural lightweight aggregate that is abundantly available in most tropical countries. Recently, researchers (Aslam et al., 2015, 2016c; Aslam et al., 2016a) studied the behavior of structural lightweight aggregate concrete by using by-product materials from palm oil industry.

They stated that it is possible to produce environmentally-friendly and high-strength structural LWAC by incorporating high volume waste LWAs from the palm oil industry. They also reported that lightweight concrete by using OPS as coarse aggregate has satisfactory mechanical properties. However, there are some major drawbacks that need to be addressed before it can be used to produce lightweight concrete (LWC) mixture for structural purposes. First, higher water absorption of the OPS aggregates as a result high water absorption and low durability of the oil palm shell lightweight concrete. Teo et al (2007) reported that water absorption of OPS concrete with normal strength is higher than 10%. Whereas, water absorption for other types of structural LWCs such as pumice aggregate concrete (PAC), polystyrene aggregate concrete (EPAC) and expanded clay ranged from 3-6% and 14-22% respectively (Babu & Babu, 2003; Gündüz & Uğur, 2005). Furthermore, Ranjbar et al. (2013) categorized the quality of concrete as good, average and poor based on the initial water absorption values of 0-3%, 3-5%, and above 5%, respectively. It has been reported by Gribniak et al. (2013) that the LWAs with high rate of the water absorption tend to increase the shrinkage deformations. Second drawback of the OPS lightweight concrete is higher drying shrinkage compare to the conventional concrete (Abdullah, 1996). Drying shrinkage occurs in all type of concretes but the use of LWA has a significant impact on drying shrinkage of the LWC. Bogas et al. (2014) reported that when the internal curing of the LWC becomes less, the shrinkage rate would be increased compare to the normal weight concrete (NWC). It was also demonstrated that the drying shrinkage of LWC depends on the water lost by evaporation and ambient condition. In fact, the rate of the shrinkage on lightweight concrete is correlated to the curing condition. Basically, using of the LWAs increases the rate of drying shrinkage due to lower restriction effect on the paste deformations. With regard to the mentioned matters above, this study is an effort to give the optimum level of the OPS substation in concrete

in order to achieve satisfactory results for mechanical properties, water absorption and drying shrinkage strain.

1.3 Goals and Objectives

The main objective of this research is to investigate the effectiveness of oil palm shell as partly and fully substitution of coarse aggregate in conventional concrete on drying shrinkage and mechanical properties of oil palm shell lightweight concrete. The related objectives of the present research are as follows:

I. To optimize the drying shrinkage in concrete with varied oil palm shell substitution ratios.
II. To investigate the effect of different curing condition on drying shrinkage strain of OPS concrete.
III. To compare actual drying shrinkage of the OPS concrete at early and long-term ages with theoretical results from different drying shrinkage prediction models and selection of the best model for prediction.

1.4 Chapter Outline

This thesis comprises of five (5) main chapters and the content of these chapters are outlined in this section.

Chapter 1: Introduction

This section covered a historical background and general concepts of the oil palm shell lightweight aggregate concrete and concerned issues for application of this type of concrete are presented. The research goals and objective, research significant and methodology of the research are also presented in this chapter.

Chapter 2: Literature review

This chapter presents a literature review studies of lightweight concrete as well as different approaches to obtain lightweight concrete. Various types of lightweight

aggregates with focusing on oil palm shell as agro waste by-product lightweight aggregate for production of oil palm shell lightweight concrete were reviewed. Drying shrinkage as a main drawback of oil palm shell lightweight concrete and factors affecting drying shrinkage were discussed technically.

Chapter 3: Research methodology

This chapter presents the methodology used to carry out the experiments studies for investigation of mechanical and time-dependent properties of oil palm shell lightweight aggregate concrete. It introduces the materials used in this research as well as its properties. It covers the procedures used in concrete mixing and specimen curing. It also provides test method and curing conditions for all concrete specimens.

Chapter 4: Results and discussion

This section presents the analyzed results of laboratory test for six different concrete mixes using of oil palm shell as replacement of crushed granite from 20 to 100% (by volume) with interval of 20%. The results for concrete slump, density, compressive strength in different curing conditions, splitting tensile strength, initial and final water absorptions and drying shrinkage of cured and uncured specimens of all concrete mixes were analysed, compared and discussed. Furthermore, actual drying shrinkage of mixes in 2 groups (including 12 mixes), at early and long-term ages (275 days) was compared with theoretical results from five different drying shrinkage prediction model such as ACI209R, EN1992, GL2000, B3 and SAK in other to select the best predictor for drying shrinkage of the OPS lightweight concrete.

Chapter 5: Conclusion

This chapter presents the conclusions drawn from the finding of this research and suggest the optimum level of the OPS substation as coarse aggregate in concrete.

CHAPTER 2: LITERATURE REVIEW

2.1 Lightweight Concrete

Concrete as a composite material which is made from a mixture of Portland cement, sand, aggregate and water, simulates the properties of rock. Concrete is considered as second most used material on earth after water. Based on density, it is classified into three types. First, heavy-weight concrete with density more than 3200 kg/ m^3 which is mainly being used for radiation shielding. Second, normal-weight concrete with density about 2400 kg/m^3 containing natural normal-weight sand and aggregates. It is most commonly used concrete for conventional construction and structural purposes. The third type is lightweight concrete with density less than 1800 kg/m^3. During Roman Empire, the first lightweight concrete was produced in the Mediterranean region by using of natural volcanic aggregates together with ordinary hydrated burned as binder for the mixture. Although that type of concrete did not have satisfactory mechanical properties, it was amazingly durable. The use of lightweight concrete was limited after the fall of the Roman Empire until the 20th century when industrial manufactured, expanded shale lightweight aggregate introduced for commercial use. In 1918, the first artificial lightweight aggregate made by the expansion of shale came into production in America and was used for manufacturing of ships in World War I. Due to shortage of steel and lightweight materials during World War II, engineers again utilized the lightweight aggregate concrete for shipbuilding program in north of America (Sarabèr et al., 2012). In 1958, the first building by using of reinforced lightweight concrete was constructed in United Kingdom. Since then, this method had been applied for production of concrete precast components, pre-stressed and reinforced lightweight concrete structures. After 1965, many concrete structures such as tall billings and bridges specially by using of lightweight concrete elements were built. Expanded clay and shale were the main lightweight aggregates employed for production of lightweight concrete. In 1972, for the first time construction

of a floating dock in Italy began by using of LWAC with density of 1870 kg/m^3 for lightweight concrete structural members consist of top and bottom raft caisson slabs, longitudinal walls of raft caisson and side walls. Maximum compressive strength for concrete was 17 MPa at the age of 28-day.

Nowadays, any structure is designed intelligently to be as light as possible. Its function is to support live and imposed loads. The use of lightweight concrete is an effective way to minimize the loads of the structures. In many cases, lightweight concrete using for structures offers economic advantages, since the higher cost of the artificial aggregate is often offset by the reduction in size of the structural components and by the savings in reinforcing steel. The reduction in dead weight also can be resulted in savings in the cost of falsework and foundations (Yasar et al., 2004). Similarly, by application of the lightweight concrete in precast industry, the cost of transporting and handling of the precast concrete components is reduced because lighter vehicles and lifting appliances can be employed. Moreover, reduction of the lateral forces related to the seismic condition, high strength/weight ratio, superior sound and heat insulation characteristics, frost and fire resistance and low coefficient of thermal expansion (Shafigh et al., 2010), making lightweight concrete more competitive material in construction industry. There are also some disadvantages for this type of concrete such as lower mechanical properties, more cement content is required to achieve same strength as normal-weight concrete, greater shrinkage, creep and pre-stressing loss in pretension structures and high risk for corrosion of the reinforcement due to the depth of carbonation (Shafigh et al., 2011). Generally, the mechanical properties of lightweight concrete (LWC) are lower than conventional concrete. However, production of high strength low density concrete with a compressive strength of 50–100 MPa has been successfully investigated with several types of lightweight aggregate concrete (LWAC) (Hassanpour et al., 2012).

Using of the lightweight aggregate (LWA) together with normal-weight sand as fine aggregate in concrete mixtures is an effective approach for production of LWAC. Basically, LWAs can be broadly classified into three general groups: natural, artificial and by-product aggregates. The main natural LWAs are diatomite, basaltic pumice, volcanic cinders, scoria and tuff (Neville, 2008). Basaltic and eruptive rocks are formed by the cooling of molten matter from the earth's crust, which flowed out of cracks. Such rocks may have widely differing properties, depending on their chemical composition, the fluidity of the lava from which they were formed, and the mode of cooling. Molten rock from volcanoes cooled at a relatively slow rate. Lava with an average temperature of between 900 °C and 1200 °C flowed rather fast. In some cases, the volcanic matter was thrown into the air and fell back on to the ground, where it subsequently solidified to form a loose-textured rock (volcanic tuff or tufa). In other cases, cooling took place under water (when lava flowed or was hurled into the sea). The slaggy material has a cellular, sometimes spongy, structure caused by the gases contained in the molten rock. Figure 2.1 shows a volcanic rock namely pumice which is used as lightweight aggregate for production of the lightweight concrete.

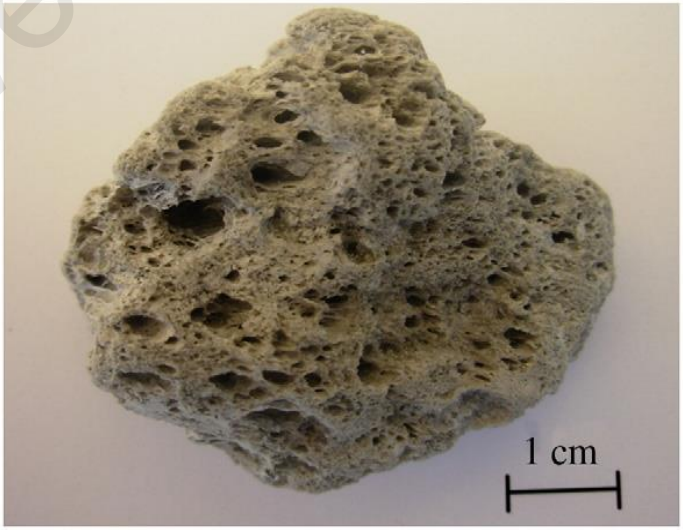

Figure 2.1: The pumice volcanic rock

The artificial aggregate is second category of the LWA. It further grouped into two different categories, the modified naturally arising materials and the industrial by-products. The naturally arising materials or factory-made aggregates are obtained through the heat treatment such as expanded clay, shale, slate, vermiculite and perlite. Nowadays, modern manufacturing plants are becoming highly automated, and the aggregates produced by them have uniform quality. Research is being carried out with a view to giving these aggregates greater strength without increasing their weight and making them less and less hygroscopic. There is no doubt that such lightweight aggregates will be manufactured in ever larger quantities, since adequate supplies of good natural heavy aggregates are becoming more difficult to find. The range of lightweight aggregates manufactured for use in structural concrete is very wide, and the products are vary according to their origins and the countries in which they are produced. The process flow diagram for production of expanded clay as a factory-made aggregate is shown in Figure 2.2.

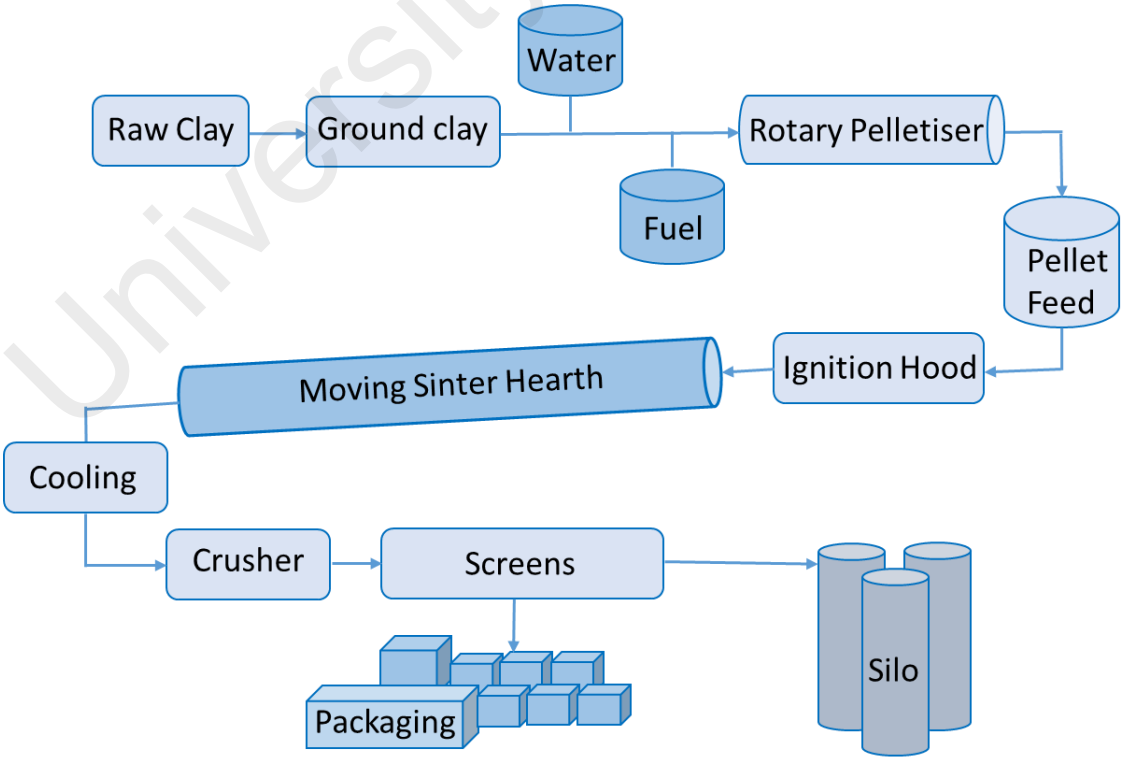

Figure 2.2: The process flow for production of expanded clay

The by-product materials such as sintered slate, sintered pulverized fuel ash, colliery waste, foamed or expanded blast furnace and oil palm shell from oil palm industry are also utilized as LWAs for production of concrete in construction industry (Shafigh et al., 2010). For instance, sintered pulverized fuel ash is one of the type of LWA in this group which is originated from fly ash. Generally, fly ash is used as cementitious material in concrete mixtures or as an additive to cement clinker for making pozzolanic cements. It can also be used for the manufacture of lightweight aggregates for concrete. For production of this aggregate, the ash is homogenised and stored in one or more holding silos. lt is then pelletized agglomerated into spherical pellets in rotating pans. This is similar to the procedure of pelletizing used in certain methods of cement manufacture (semi-dry process), these pellets then being calcined on a travelling grate whence they are fed to a short rotary kiln. Pelletizing is also used for the agglomeration of finely granular iron prior to smelting, as well as in other widely differing industrial processes such as the manufacture of certain types of chocolate-coated sweets. The pelletiser is an inclined pan or dish, 2 to 4 m in diameter, with a flat or a stepped bottom, which rotates at a certain speed. The powder to be pelletized and water are fed into the pan. The powder particles cling together and agglomerate into larger spherical pellets which are well compacted by the centrifugal force. The size, hardness and density of the pellets depend on the distinctive features, operating conditions and control of the pelletizing pan, on the granulometric composition of the powder and on the water content. If necessary, the pellets can be screened to remove excessively oversize or under-size ones. A pellet typically has a fairly densely compacted core surrounded by a more porous outer part. The pellets are delivered by a belt conveyor on to a horizontal burning grate on which they form a bed 20 to 40 cm in depth. This grate, from 40 in length, comprises a drying zone where drying is effected by hot gas obtained from the burning zone; a burning or sintering zone where a temperature of 1200°-1300° C is produced. In most installations

the grate is of the travelling type, while the gas-fired or oil-fired burners are stationary; sometimes, however, the grate is stationary and the battery of burners moves along. Fans circulate hot air through the bed of pellets, which remain in the burning zone for a period ranging from 15 to 25 minutes; a cooling zone. The sintered pellets are then screened (after being crushed if necessary) and stored in different particle size fractions (Mehta & Monteiro, 2006; Neville, 2008) The process flow diagram for production of sintered pulverized fuel ash as industrial by-product aggregate is shown in Figure 2.3.

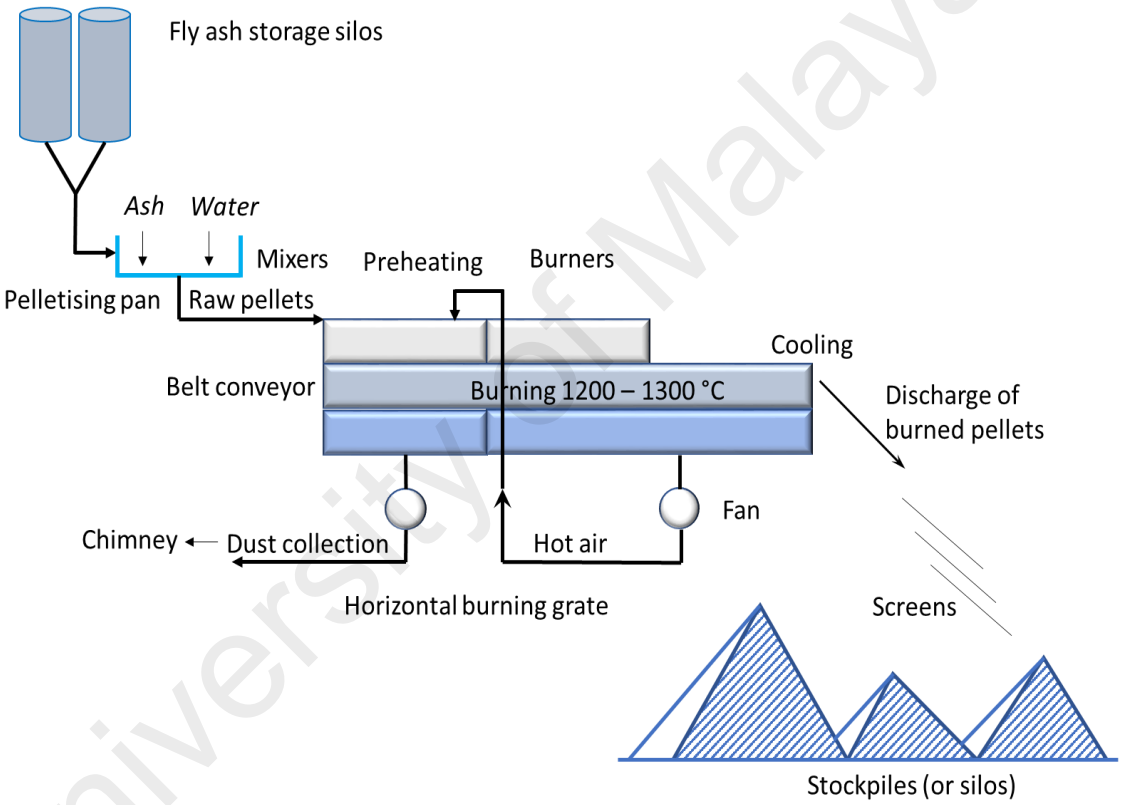

Figure 2.3: The process flow diagram for production of sintered pulverized fuel ash

Growing of the human population and consumption of the natural resources leads to produce of large quantities of the waste which caused resource and environmental issues. Many of non-decaying waste materials will be remained in the environment for thousands of years. Therefore, waste management is an effective way to reduce negative environmental effect and make the waste materials more sustainable (Alimohammadi et al., 2017a; Batayneh et al., 2007). Its simplicity lies in the fact that concrete constituents

are ubiquitous almost anywhere. Nowadays only 10-12 billion tonnes of sand and rock together are consumed as aggregate in concrete industry annually. This fact shows that enormous amount of raw material and natural resources have being used for production of concrete worldwide (Aslam et al., 2016c). In regard to the huge daily production of concrete, even a small reduction in using of the natural raw material leads to remarkable benefit to the environment and avoid ecological imbalance (Silva et al., 2016). Therefore, recently the emphasis on sustainable material in order to substitution the natural material has been intensified (Alengaram et al., 2013). In the long run, sustainable development will happen only with dramatic improvements to resource efficiency, thereby many researchers have been motivated to investigate utilization of wastes and by-product materials into potential construction materials (Mo et al., 2015). Oil palm shell with its availability in tropical countries is considered as remarkable replacement for natural resources specially as lightweight aggregate for construction industry.

2.2 Oil Palm Shell Lightweight Concrete

Oil palm shell (OPS) is one of several types of waste resulting from the palm oil industry. This agro waste is mainly obtained in tropical countries with palm oil industry such as Malaysia, Indonesia, Nigeria and Thailand. The contribution of these countries for the palm oil production is about 90% of the total world's palm oil industry in the year 2009 (Islam et al., 2016; Liu et al., 2014). At the oil palm mills, after extraction process of the oil from the fresh fruit bunches, solid residues are generated which is including empty fruit bunches, shell and fibers. Figure 2.4 shows the process of the oil palm shell extraction from the palm fruit.

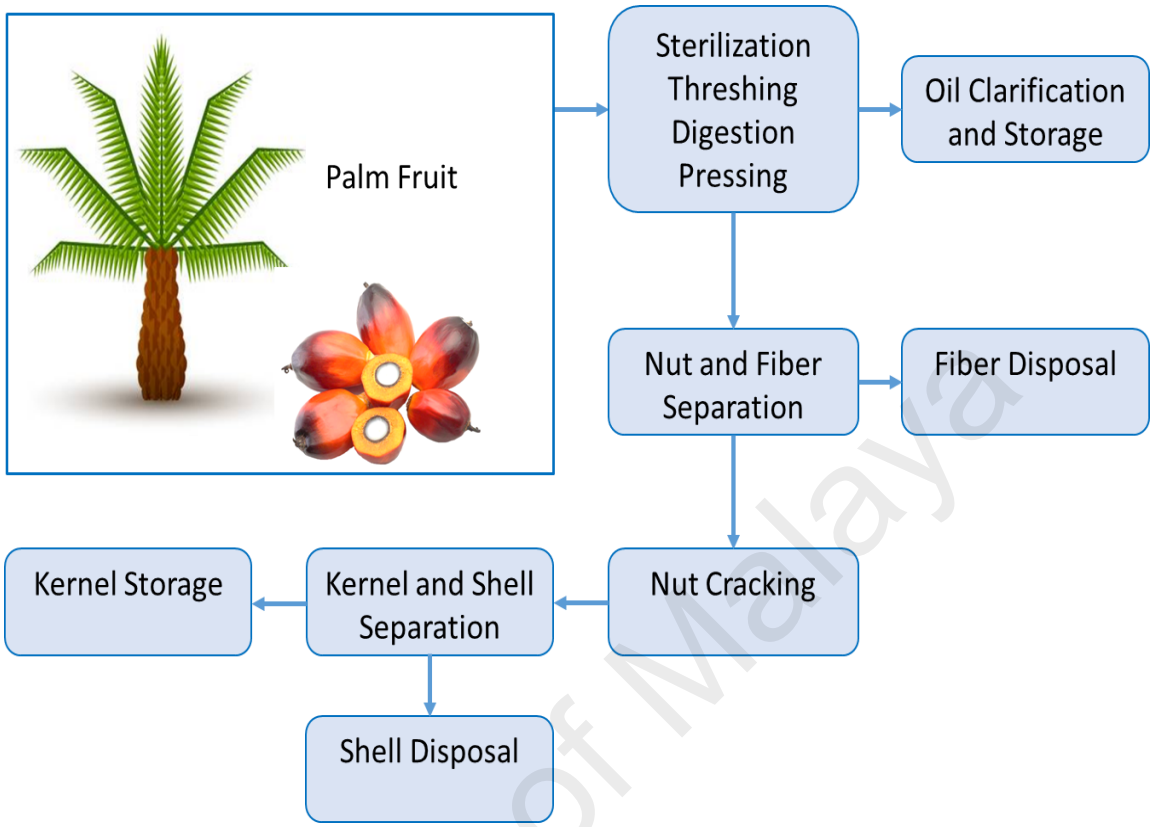

Figure 2.4: Extraction process of the oil palm shell from the palm fruit

Due to hardness of the shell, it can be used as coarse aggregate in concrete mixtures. The chemical composition of the OPS lightweight aggregate is presented in Table 2.1. As shown in Figure 2.5, OPS is available in various shapes, such as curved, flaky and elongated. Usually, due to extraction process some oil coating is present on the surface of fresh OPS; therefore, in order to remove oily surface of the OPS pretreatment is necessary. For this purpose, different approaches are proposed such as washing by using of detergent, boiling in water or keep the OPS in an open area to be dried under the sun.

Table 2.1: Chemical composition of OPS aggregate (Teo et al., 2007)

Elements	Results
Ash	1.53
Nitrogen (as N)	0.41
Sulphur (as S)	0.000783
Calcium (as CaO)	0.0765
Magnesium (as MgO)	0.0352
Sodium (as Na2O)	0.00156
Potassium (as K2O)	0.00042
Aluminium (as Al2O3)	0.130
Iron (as Fe2O3)	0.0333
Silica (as SiO2)	0.0146
Chloride (as Cl-)	0.00072
Loss on Ignition	98.5

Figure 2.5: Oil palm shell lightweight aggregate

Salam and Abdullah (1987) for the first time in Malaysia introduced the method of using OPS as a LWA for manufacture of LWAC. Several researchers have pointed out that conventional coarse aggregate can be replaced with OPS to produce structural grade of LWC. Mannan & Ganapathy (2001) studied the failure pattern of oil palm shell concrete (OPSC) under 7 and 90-day water curing condition. They observed that failure patterns in early ages are depending on strength of the OPS aggregate while in the later age, at 90-day the strong bonding of OPS and paste is governed. Researchers over last twenty years have proven that LWC containing OPS has satisfactory mechanical properties and durability (Teo et al., 2010). For OPSC the compressive strength in the range of 13-22 MPa was observed by many researchers. Okafor (1991) reported the performance of a superplasticizer (SP) in OPS concrete. He concluded that the compressive strength of OPS lightweight concrete in water to cement ratios of 0.45 and 0.50 increases with the increase in dosage level of the SP from 0 to 2.5% of cement weight. Basri et al. (1999) highlighted that the compressive strength of OPS concrete is approximately 50% lower than that of conventional concrete. Mannan et al. (2006) demonstrated that with improvement of the OPS aggregates quality, it would be possible to decrease the water absorption of OPS up to about 82% (from 23.3 to 4.2%) and achieving better bonding between the OPS and cement matrix. This improved the compressive strength to 35.3, 38.8 and 39.2% for 3, 7 and 28-day respectively.

With the inclusion of fly ash, silica fume and admixtures, compressive strength of 37 MPa has been obtained. Furthermore, high strength lightweight concrete with 28-day compressive strength up to 48 MPa with dry density of about 1870 and 1990 kg/m^3 using of the crushed OPS and limestone powder has been reported (Alengaram et al., 2013; Shafigh et al., 2014) did a study to compare expanded clay and the OPS lightweight aggregate concretes in terms of drying shrinkage and mechanical properties. Result show that, the OPSC has 44% higher compressive strength and 30% greater flexural strength.

However, the dry density of the expanded clay LWC is 5% lower than the OPSC. It was demonstrated that there is a linear relationship between early-age and 28-day compressive strength of OPSC made with crushed OPS aggregate (Shafigh et al., 2014). The studies (Teo et al., 2006; Abdullah, 1996; Alengaram et al., 2008) showed that the splitting tensile strength of the continuously water cured OPS concrete at 28-day varied from about 1.1 to 2.4 MPa. The modulus of elasticity of OPS concrete is in the range of about 5 - 11 GPa for a compressive strength range of 24 - 37 MPa (Teo et al., 2006; Alengaram et al., 2008). In general, the modulus of elasticity of concrete is primarily affected by the stiffness and volume of components (Gao et al., 1997). In general, the modulus of elasticity of concrete is primarily affected by the stiffness and volume of components (Gao et al., 1997). For the same strength the modulus of elasticity of LWAC is 25 - 50% lower than normal weight concrete (Neville & Brooks, 2008). In another experimental study, OPS lightweight concrete was utilized to cast reinforced concrete beams. The result shows satisfactory shear and flexural performances (Ahmed & Sobuz, 2011; Alengaram et al., 2011). This type of concrete also has been used to supply industrialized building system (IBS) components such as precast lightweight wall panel for affordable housing in Malaysia. Figure 2.6 shows a low-cost affordable house which was built by using of the oil palm shell lightweight concrete in Malaysia.

Figure 2.6: Low-cost house by using of oil palm shell concrete (Teo et al., 2006)

Previous studies revealed that LWC by using the OPS has a good mechanical properties and durability performance. However, a good mechanical property is not the only indicator to evaluate the quality of OPS lightweight concrete. This type of concrete has some drawbacks such as high rate of drying shrinkage which need to be taken into consideration and rectified before it is applied.

2.3 Shrinkage in Concrete

Shrinkage in concrete can be defined as reduction in the volume or the length of hardened concrete with time, which is mainly due to moisture and chemical changes in the concrete (ACI Committee 209, 1997). There are several types of the shrinkage, but some of them with high magnitude have got remarkable influence on durability of concrete such as plastic shrinkage, chemical shrinkage, autogenous shrinkage and drying shrinkage. Other types of shrinkage with less magnitude are carbonation shrinkage and thermal shrinkage. Plastic shrinkage normally occurs during unhardened state and early ages of concrete. Basically, during compaction of concrete the water move upward and solid constituents of concrete tend to move downward and settle down, which causes bleeding on the

surface. However, the evaporation also can be happened on the surface of concrete by some external factors such as sun or wind. Therefore, the plastic shrinkage occurs when the rate of evaporation for discharged and placed concrete exceeds the rate of bleeding. Furthermore, the plastic cracks will be appeared when tensile stresses exceed the fresh concrete tensile strength (Neville, 2000).

The chemical shrinkage is described as "the phenomenon in which the absolute volume of products due to hydration process is less than the total volume of unhydrated cement." (Tazawa et al., 1993). Chemical reaction in the concrete mixture as well as hydration process cause chemical shrinkage. At the early ages of drying, when the concrete is still in plastic phase, the chemical shrinkage results in overall reduction of the concrete volume. However, at the stage where the concrete begins to be stiffer, chemical shrinkage tends to create more pores in the cement matrix (Lura et al., 2003).

According to the Japan Concrete Institute, (Tazawa, 2014) autogenous shrinkage is defined as the macroscopic volume reduction of the cement matrix after initial setting. The autogenous shrinkage is a volume reduction of the concrete with no moisture transfer with the outer environment. Basically, the low water to cement ratio is the main reason for the autogenous shrinkage in concrete. This type of shrinkage is a concern for the concretes with water to cement ratio (w/c) less than 0.42 (Holt, 2001). The typical value of autogenous shrinkage is suggested about 40 micro-strain at the age of one month (Davis, 1940; Tazawa et al., 1993) highlighted that at very low w/c ratios, the rate of autogenous shrinkage would be very high. The value of 700 micro-strain was reported for concrete with a w/c ratio of 0.17. A higher w/c ratio for the concrete mixture can minimize the autogenous shrinkage and mitigate this issue.

The drying shrinkage is the time-dependent volume reduction of concrete which is occurred due to water movement and moisture losses from the concrete structure in long-

term ages (Hansen, 1987). This type of shrinkage plays an important role in the contraction of concrete as its driving force causes the removal of adsorbed water from the hydrated cement paste (Aslam et al., 2018). During early ages of drying, the free moisture transfers from the concrete mass to the surface as a bleed water (Holt, 2001). The moisture evaporation from the interior of the concrete mass will generate empty pores and as a result negative pressure inside of the concrete and capillary pores (Khairallah, 2009). The tensile stresses resulted from the negative pressure in the pores are equilibrated by compressive forces in the surrounding concrete. Eventually, these compressive forces lead to the drying shrinkage (Cement and Concrete Association of Australia, 2002). Basically, both drying and autogenous shrinkage are similar in mechanism due to loss of moisture and internal relative humidity, where in drying shrinkage the moisture is exchanged with the surrounding environment in long-term ages, whereas for autogenous type, the exchange of the moisture is occurred internally within the pore structure at early ages. Normally, the drying shrinkage of the conventional concrete is ranging from 200 to 800 micro-strain. In order to avoid the development of drying shrinkage, it is necessary to keep that water from evaporating from the concrete (Zia et al., 1997).

All the types of discussed shrinkages are important as they cause one of the most objectionable defects, which is the appearance of cracks, particularly in pavements, slabs and floors. Thus, to check the safety, durability and serviceability of concrete structures, prediction and control the rate of shrinkage over the long term is highly important (Sakata et al., 2001).

2.3.1 Factor affecting drying shrinkage

Factors that affect the drying shrinkage of concrete can be categorized into two main categories: external and internal. The external factor is related to the environmental condition such as level of humidity, ambient temperature or wind velocity (Cement and

Concrete Association of Australia, 2002). In low ambient relative humidity (RH), strong gradients are produced on the surface of concrete, thus increasing the rate of drying. Compare to the RH the effects of ambient temperature and wind velocity are lesser. Curing also is considered as an external factor. Beside of the mix design and quality of the raw material, properties of concrete are dependent of temperature and humidity especially during the period of curing. The main purpose of curing is to keep the concrete moisture in order to complete the hydration process (Mannan et al., 2002). Basically, durability and mechanical properties of concrete are influenced by curing condition which greatly affects the hydration of cement. Generally, the hydration of cement is decreased by reduction of the relative humidity within capillaries in concrete (Neville, 1995). When hydration process becomes slow, the development of the calcium silicate hydrate which is the main factor for concrete strength will be slower. Therefore, providing sufficient moisture and efficient curing are inevitable to prevent the moisture movement or evaporation of water from concrete surface.

The hydration process begins during mixing and continues throughout the time the concrete reaches its ultimate strength. Basically, the rate of hydration is controlled by the quality and quantities of the cementitious materials present in the mix as well as by the ambient temperature and the availability of moisture in the mix (Mannan et al., 2002). A researcher (Aminur et al. 2010) have discussed the effects of water and vapor curing conditions on short and long-term concrete properties. In the event water is not readily available for curing purposes, the conventional curing method is not practiced and delayed curing may occur. Sometimes in the normal construction project, curing may also be delayed due to many factors. Therefore, various types of curing conditions on mechanical properties and drying shrinkage of OPS concrete is important to be investigated. The internal factor includes the characteristic (intrinsic) properties of the

material used for concrete mixtures such as cement and aggregates content, their composition as well as their proportions in the mix design (Smadi et al.,1987).

Basically, the water to cement ratio (w/c) is a criterion to determine how much water there is in the cement matrix. A lower ratio leads to higher strength and durability but lower workability. Meanwhile, low w/c ratio will lead to a remarkable decrease in the shrinkage strains and the porosity of the cement paste. However, that rate of shrinkage is increased by high cement content in concrete mix.

The effect of aggregate on drying shrinkage is also significant. The overall deformation of concrete is restricted by presence of aggregates in the concrete mixture. Due to the restraining effect, it can be stated that the higher aggregate to cement ratio causes the lower rate of the shrinkage. Stiffness of the aggregates also plays an important role on drying shrinkage since the restraining effect highly depends on this factor. Generally, for the lower stiffness of the aggregates, higher shrinkage strain is expected. Meanwhile, the size of the aggregates can influence the shrinkage, where using of larger aggregates lead to higher drying shrinkage strain (Bisschop & Van Mier, 2002).

Other internal factor which can affect drying shrinkage is addition of additive and cementitious materials such as fly ash, ground granulated blast furnace, palm oil fuel ash and silica fume. Due to pozzolanic reaction of the cementitious materials, the drying shrinkage of concrete in some cases might be reduced (Haque, 1996; Li & Yao, 2001). For instance, using of fly ash in concrete mixture reduces the water requirement, as a result reduces the rate of shrinkage. Using of the mineral admixtures beyond certain limit, may augments the rate of drying shrinkage due to lower specific gravity and higher paste in the concrete mixtures (Khairallah, 2009).

The addition of chemical admixtures such as water reducing agents or workability agents also influence the drying shrinkage. Plasticizer and Super-plasticizer as water reducing agent breaks the cement and paste agglomeration in fresh concrete and reduce inter-particle friction among solid particles, therefore it can increase the rate of shrinkage (Omar et al., 2008).

2.4 Drying Shrinkage of Oil Palm Shell Lightweight Concrete

Drying shrinkage is the time-dependent volume reduction due to loss of water at constant temperature and relative humidity (Hansen, 1987). For structural members, drying shrinkage strain of the concrete plays very important role and it would be harmful when it is restrained. However, it is not critical when used for insulation or filling purposes (Kosmatka et al. , 2002). For the lightweight concrete, high drying shrinkage is one of the main drawbacks compared to the NWC. Reports (Neville, 2008; Satish & Berntsson, 2002) show that the LWC has higher drying shrinkage than NWC. It is mainly influenced by volume of aggregate as well as aggregate's properties. Basically, lightweight aggregate concretes are containing less rigid, porous aggregate and high volume of cement paste. The high cement content is mainly due to enhancement of mechanical properties of hardened concrete as well as modification of the workability and stability of the mixtures (Aslam et al., 2016a; Holm & Bremner, 2000). Therefore, the long-term shrinkage value of LWC should be greater than the NWC of the same grade. Clarke (2002) reported that for general structural design, the shrinkage of LWAC is suggested in the range of 1.4 to 2 times that of NWC.

The drying shrinkage of OPSC was first investigated by Abdullah (1996), who reported that drying shrinkage of this type of concrete is about 5 times higher than the NWC. Mannan and Ganapathy (2002) also investigated the drying shrinkage of OPSC and NWC up to the age of 90-day. They reported that the drying shrinkage of both types

of concretes was increased with age but higher increment was for OPSC by about 14% higher compared to NWC. Drying shrinkage for several types of low-density concrete using OPS with 28-day compressive strength in the range of 22-38 MPa was measured by Alengaram and Awam (2009). They reported that drying shrinkage of OPS at the age of 90 days is in the range of 540-1300 microstrain. Shafigh et al. (2014) pointed out that drying shrinkage of OPSC is greater than expanded clay low-density concrete of about 100% at the early ages and about 35% at the age of 90-day and beyond.

Generally, high cement content and OPS percentage in OPSC are key reasons for its high value of drying shrinkage. Therefore, one of the effective method to control the drying shrinkage of OPSC is reduction of the volume of OPS aggregate in the concrete mixture (Aslam et al., 2016a). From the previous studies, it was found that there is not any information concerning the optimum OPS content in concrete with acceptable drying shrinkage. Because of the importance of OPS content in concrete, in order to achieve satisfactory mechanical properties and less drying shrinkage, this investigation was carried out to find out the optimum substitution of oil palm shell in conventional concrete to produce durable structural lightweight aggregate concrete. The results of present study can be effectively used as a reference for production of structural OPS lightweight concrete in precast and construction industry since there is an optimum level of OPS to meet requirements of both mechanical properties and drying shrinkage.

CHAPTER 3: METHODOLOGY

This section mainly declares the methods of this research which consist laboratory works and experiments. The purpose of the laboratory works and experiments are basically to emphasize the effect of using of oil palm shell in conventional concrete on drying shrinkage and mechanical properties.

3.1 Selection of and preparation of materials

The crushed granite and locally available agro-waste material from the palm oil industry namely OPS was used as coarse aggregates in this study. OPS aggregates were stored at the friendly atmosphere for approximately 6-8 months to properly dry them and remove the fibers from the OPS surface. After that the OPS aggregates were washed in the concrete mixer by using a detergent powder to remove the oil and other impurities from the surface. Then, both aggregates were sieved to achieve the same grading. According to BS 5075 the chloride free admixture Sika ViscoCrete compatible with all types of Portland cements was used as super-plasticizer in this study. The portable tap water was utilized for mixing and the curing of concrete specimens.

3.2 Selection of suitable mix design

In order to achieve a suitable mix design and accurate results for mechanical properties and drying shrinkage of the mixes, few trail mix were prepared and six mix designs were finalized to be applied for this research. The six concrete mixes were prepared using crushed granite and the OPS as coarse aggregates. The normal-weight concrete (CM mix) was considered as control concrete, and for all other mixes, crushed granite aggregate was partially replaced with OPS at 20, 40, 60, 80, and 100% by volume. The volume of aggregates, cement and admixture contents were constant for all the mixes.

3.3 Preparation and testing of concrete and specimens

Sampling and testing of fresh and of hardened concrete were carried out in accordance with the relevant parts of BS 1881, BS EN 12390 and MS 26. For the drying shrinkage test two specimens with the size of 100 × 100 × 300 mm were prepared to measure the drying shrinkage strains of all the designed concrete mixes according to ASTM C157 (2008) (Figure 3.1).

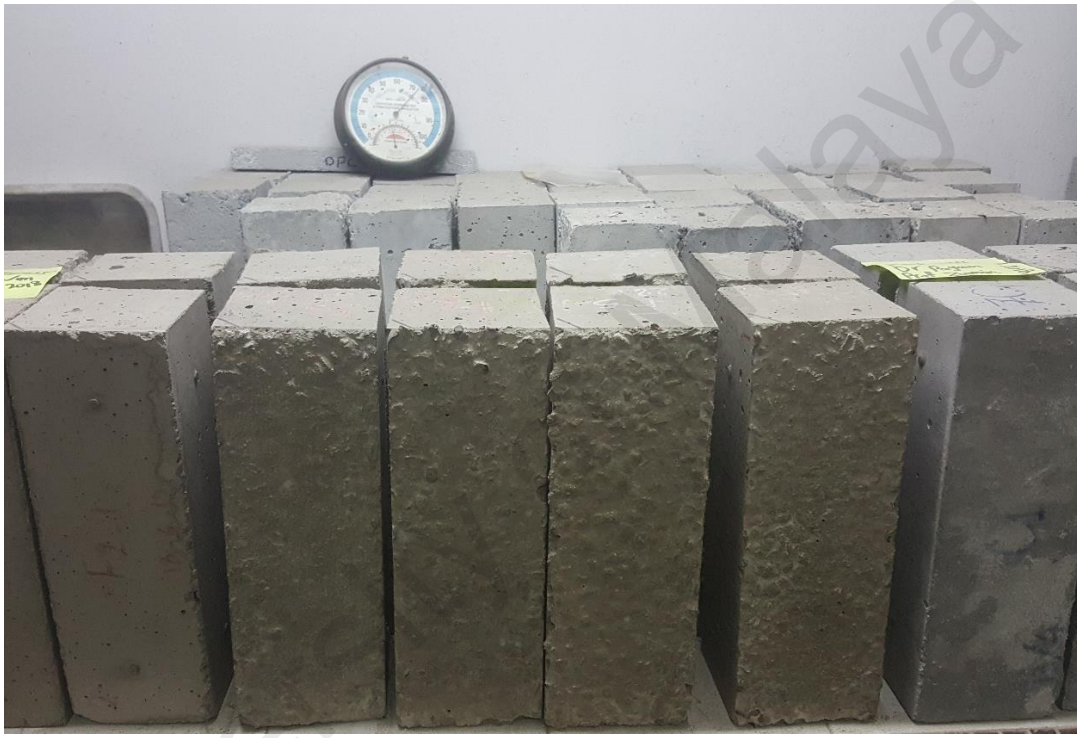

Figure 3.1: Drying shrinkage prisms

Right after placing of concrete, the specimens were covered with plastic sheets and stored in the laboratory atmosphere. After demoulding and proper curing, the pre-drilled stainless steel discs namely DEMEC points (Figure 3.2) were attached with adhesive on three sides of the prisms with spacing of 200 mm.

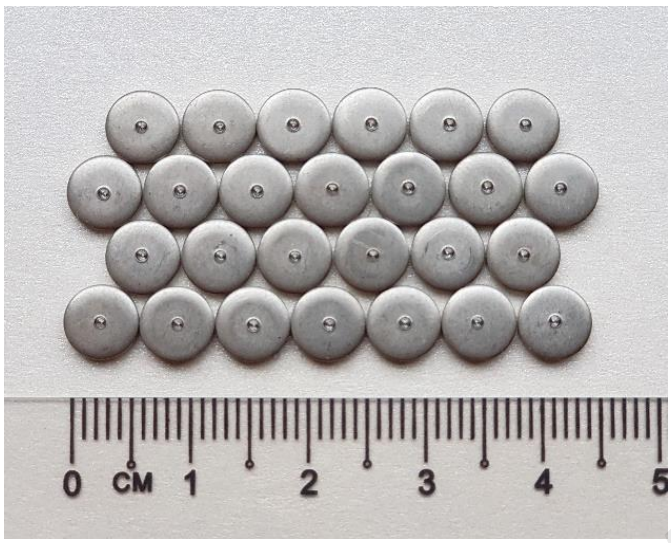

Figure 3.2: Pre-drilled stainless steel discs (DEMEC points)

Drying shrinkage strains of the concrete prisms were precisely measured by the digital version of the DEMEC Mechanical Strain Gauge which was calibrated to measure based on micro-strain. As shown in Figure 3.3, the DEMEC gauge consist of an invar main beam with two conical locating points, one fixed and the other pivoting on a special accurate knife edge. The gauge points locate in the DEMEC points.

Figure 3.3: DEMEC Mechanical Strain Gauge

3.4 Data collection and analysis

The data obtained from the lab as below were studied and analysis.

i. The compressive strength for all mixes at 1, 3, 7, 28, 56, 90 and 120 days
ii. The water absorption of all concrete mixes at 28-day age for 30 minutes and 72 hours
iii. The splitting tensile strength for all the mixes under moist curing at different ages and under air drying at 28-day age
iv. The development of drying shrinkage of all concrete mixes under air-dry condition up to 275-day age

3.5 Materials

3.5.1 Cement

Ordinary Portland Cement (OPC) which complies to the requirements of MS EN 197-1:2014 CEM 1 52.5N standards with a 2-, 7- and 28-day compressive strength of 25, 41 and 55 MPa respectively, was used as binder in this investigation. The specific gravity and Blaine specific surface area of the cement were 3.15 and 3710 cm^2/g, respectively.

3.5.2 Aggregate

The OPS and crushed granite and were utilized as coarse aggregates in this study. In order to remove the fibers from the OPS surface, it was stored in an open area for approximately 7 months (Shafigh et al., 2011). Oil palm shell with and without fibers is shown in Figure 3.4. OPS aggregates were washed in the concrete mixer using a detergent powder to remove the oil and other impurities from the surface. Then, for having same grading, both granite and OPS were sieved.

For the fine aggregate, mining sand with fineness modulus of 2.89 and maximum grain size of 5.0mm was used. The mechanical and physical features of the aggregates are represented in Table 3.1.

Table 3.1: Physical and mechanical properties of aggregates

Physical and mechanical properties	Coarse aggregate		Fine aggregate
	OPS	Granite	Mining sand
Specific gravity	1.20	2.65	2.68
Compacted bulk density (kg/m^3)	610	1490	1657
24-hour water absorption	20.5	< 1	1.2
Crushing value (%)	0.2	18.0	-
Impact value (%)	5.5	15.5	-
Abrasion value (%)	5.7	22.4	-

Figure 3.4: Oil palm shell with and without fibers

3.5.3 Superplasticizer

The chloride free admixture Sika ViscoCrete was used as superplasticizer in present research. According to BS 5075, admixture's dosage should be within the range of 500-2000 ml per 100kg of cement, based on strength and workability requirements.

3.5.4 Water

The portable water was utilized for the concrete mixtures and the curing of concrete specimens.

3.5.5 Concrete mixing and mix proportions

OPS and crushed granite as coarse aggregate were used for Six different concrete mixes. The OPS aggregates were pre-soaked in water for 1 day and used in saturated-surface-

dry condition. The normal weight concrete (mix CM) was considered as control mix, and for other mixes, crushed granite was partially replaced with OPS at 20, 40, 60, 80, and 100% by volume. The volume of aggregates, cement and superplasticizer (SP) contents was placed constantly for all the mixes. Mix proportions of all mixes are given in Table 3.2.

Table 3.2: Concrete mix proportions

Mix ID	Cement (kg/m^3)	Water (Litre)	SP (kg/m^3)	Sand (kg/m^3)	Coarse aggregate (kg/m^3)	
					Granite	OPS
CM	480	163	4.8	819	898	0
C20					715	81
C40					540	163
C60					359	244
C80					179	325
C100					0	406

3.6 Test methods and specimen sizes

To produce each concrete mixture, raw materials were combined in a rotating drum mixer and mixing was continued for two minutes. Then a mixture of 70% mixing water with SP was added, and mixing continued for another three minutes. Another 5 minutes were applied for mixing of remaining water. After mixing process, the slump test was carried out and followed by taking 100mm cubes for compression test, cylinders of 100mm diameter and 200mm height for splitting tensile test as well as prisms of 100 × 100 × 300 mm for drying shrinkage strain. A vibrating table was used in order to proper compaction of the specimens. After sampling, covered specimens were kept in the laboratory condition and demoulded after 24-h. The demoulded density of all the mixes was measured right after demoulding, whereas, the oven density was measured at the age of

28-day. To evaluate precise value of the mechanical properties, three test specimens were prepared for early-ages and 28-day. Drying process of the specimens was carried out in the oven at 105 ± 5 ºC for the water absorption test. The dried specimens then, were immersed in water at 23 ± 3 ºC for the initial (30 minutes) and final (72 h) water absorption tests.

3.7 Curing conditions

The 28-day compressive strength of the prepared specimens was also examined under different curing conditions. For that purpose, three different curing conditions were applied as following:

- 28D: immersed the specimens in water for 27 days.
- 7D: cured the specimens in water for 6 days and then air dried in the laboratory with 31 ± 3 ºC temperature and 84 ± 3 % of relative humidity, until the age of testing.
- AC: kept the specimens in the laboratory with 31 ± 3 ºC temperature and 84 ± 3 % of relative humidity, until the age of testing.

CHAPTER 4: RESULTS AND DISCUSSION

4.1 Slump

The slump values of all the concrete mixes are indicated in Table 4.1. It was found that the control conventional concrete showed the highest workability of about 205mm. However, the partial substitution of OPS in CM, consistently decreased the slump value. It was mainly because of the organic nature of OPS with many pores on the surface which resulted in high water absorption than the crushed granite aggregates as well as flaky shape of the OPS aggregates. (Ahmad et al., 2007) reported that it is essential to obtain the water absorption of the aggregates due to aggregate may significantly reduce the concrete's workability and consistency. Results show that the partial substitution of OPS up to 80% in the control NWC still shows good workability. As reported by Mehta and Monteiro (2006), slump value for acceptable workability of LWAC is ranging from 50 to 75 mm.

Table 4.1: The slump value of all the mix proportions

Mix Code	Slump (mm)
CM	205
C20	130
C40	90
C60	70
C80	65
C100	40

4.2 Density

The compacted bulk density of conventional coarse aggregate is 40% higher than OPS coarse aggregate. Therefore, the partial substitution of OPS in conventional concrete should significantly reduce the density with the average difference between the demoulded and oven-dry density of about 68 kg/m^3. In substitution levels of 0 to 40%, the concretes can be considered as semi-lightweight concretes with the oven-dry density ranging from 2100 to 2200 kg/m^3. Hassan and Ismail (2015) reported that the concretes

with the density from 2000 to 2200 kg/m^3 is categorized as semi-lightweight. Results show that at 60, 80 and 100% replacement levels, the oven-dry density was about 2015, 1988 and 1900 kg/m^3, respectively. BS EN 206-1 (2001) specified the LWC as a concrete with the oven-dry density from 800 to 2000 kg/m^3. Therefore, by replacing more than 60% of normal weight aggregates with OPS, a lightweight aggregate concrete can be produced.

A linear relationship with strong correlation was achieved between the densities and the percentage of OPS substitution as shown in Figure 4.1. Compared to the density of NWC (2337 kg/m^3), there is a saving in self-weight of about 14, 15 and 19% for concretes with 60, 80 and 100% substitution of OPS, respectively. Figure 4.2 shows relationship between the 28-day compressive strength and the oven-dry density. It was found that as the substitution level of OPS in conventional concrete increased, the density and the 28-day compressive strength were constantly reduced and the linear equation with a very superior coefficient of determination ($R^2 = 0.99$) value was found.

The regression statistics for obtained equations for six tests in figures 4.1 and 4.2 were evaluated and shown in Tables 4.2 and 4.3, respectively. In the model, linear parameters were significant with p-value < 0.05. Any p-value smaller than 0.05 shows that the model is significant at the 95% confidence limit. In addition, if the p-value is less than 0.05, it shows a significant difference does exist between the tests, and the null hypothesis is rejected. If the p-value is larger than 0.05, means that a significant difference exists between the tests (Alimohammadi et al., 2017b).

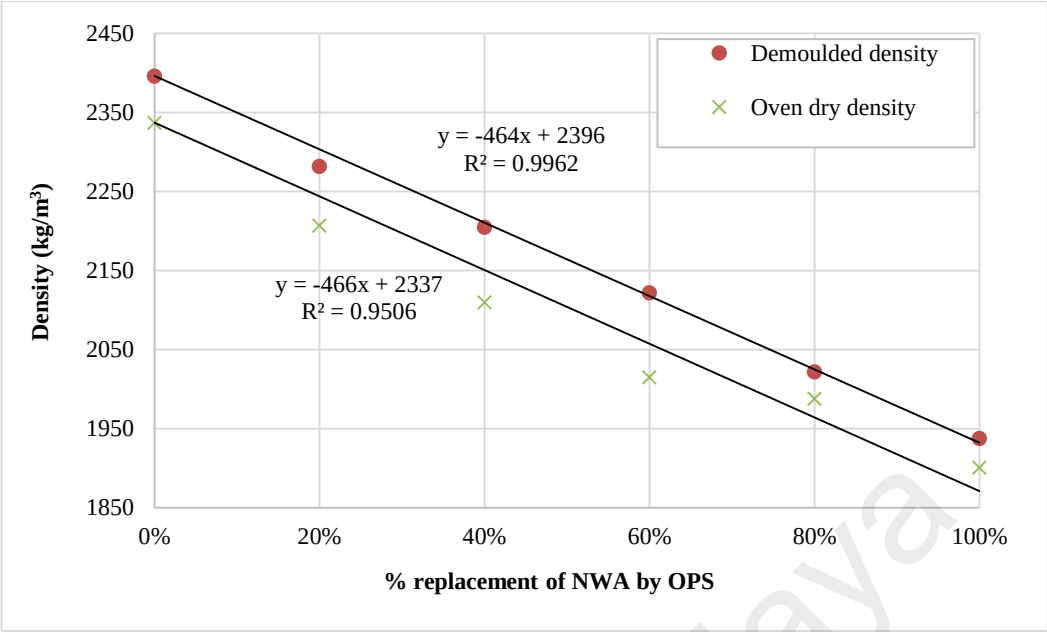

Figure 4.1: Relationship between the density and the substitution of OPS in NWC

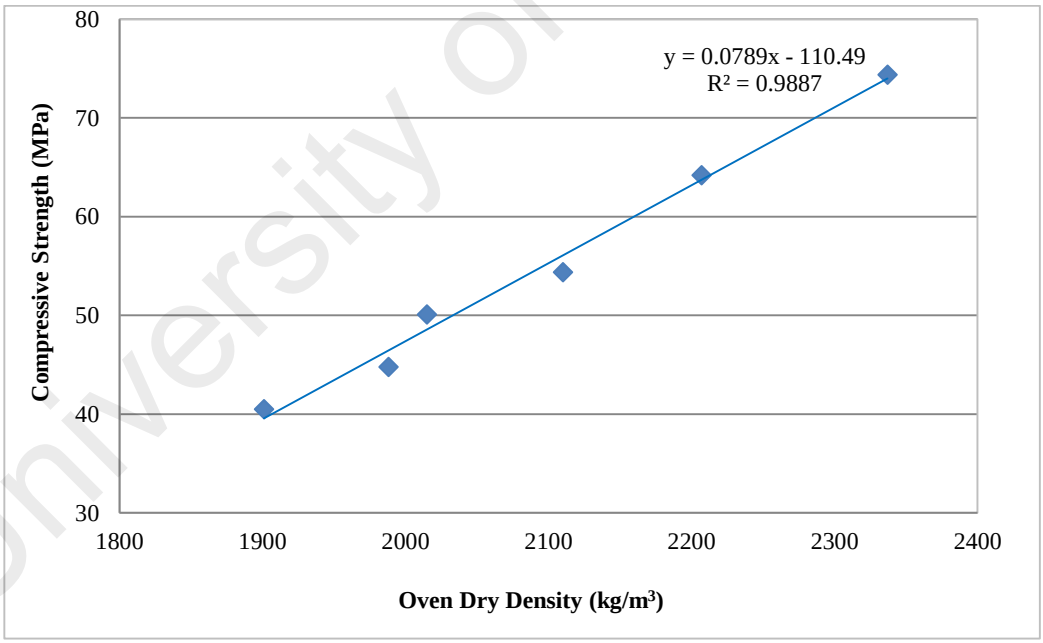

Figure 4.2: Relationship between 28-day compressive strength and the oven-dry density

4.3 Compressive Strength

4.3.1 Compressive strength under standard curing

The development of compressive strength for all mixes at 1, 3, 7, 28, 56, 90 and 120 days are shown in Figure 4.3. In all mixes the compressive strength was increased with age. However, the results showed that with increasing the OPS incorporation level, the compressive strength of mixes was reduced. With the percentage replacement of 60, 80 and 100%, the decrease in compressive strength at 1, 3, 7 and 28 days were found in the range of 26-33% for C60, 35-47% for C80 and 40-49% for C100 concrete mixes, respectively. Moreover, Basri et al. (1999) stated that compressive strength of OPSC at 28-day was lower than conventional concrete by about 42-55%, depending on the curing condition.

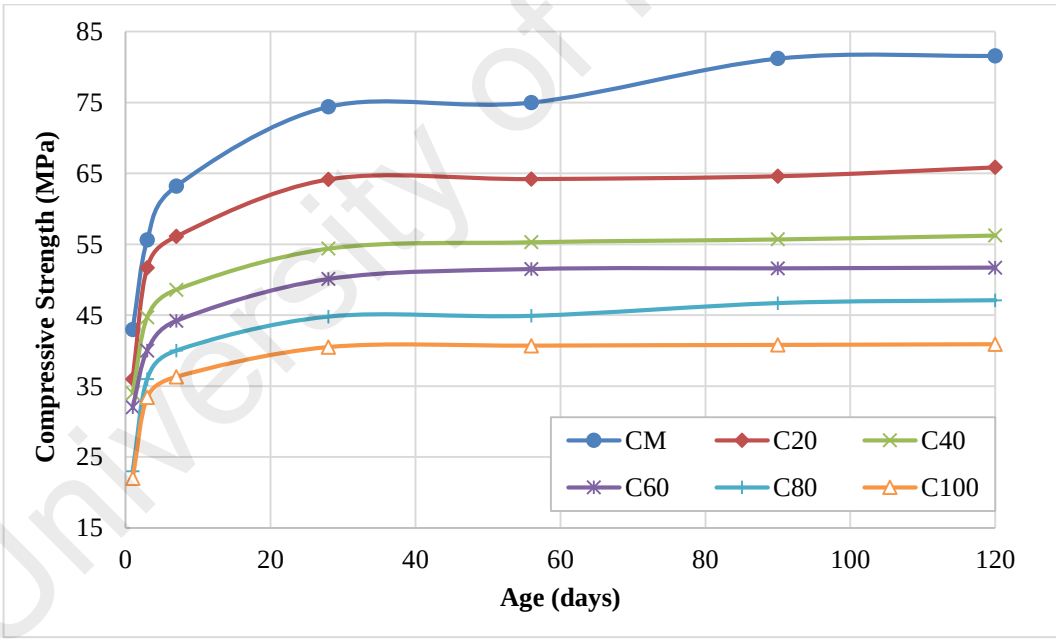

Figure 4-3: Compressive strength development of concrete mixes

Obtained results show that, the 28-day compressive strengths of all concretes containing OPS, is comparable with structural LWC. Reduction on the compressive strength of OPS concrete is due to smooth surface texture of the OPS aggregates which resulted weaker interfacial zone (Aslam et al., 2016; Mannan et al., 2002). Mannan et al.

(2002) investigated the compressive strength of OPSC. They reported that the main reason of the failure in this type of concrete is because of adhesion between the shells and the cement matrix. Some pre-treatment techniques were introduced by them to enhance the quality of the shells in order to achieve high compressive strength of the concrete. Shafigh et al. (2011) developed high strength lightweight concrete (HSLC) using aged OPS as an aggregate with pre-treatment techniques. They reported that use of aged OPS provided a stronger interfacial mechanical bond and as a result high 28-day compressive strength up to 48 MPa with the oven-dry density less than 2000 kg/m^3.

The comparison of early-ages and 28-day compressive strengths under full moist curing is shown in Table 4.2. It was determined that, by using of OPS in NWC, all the mixes achieved 51-64% of their 28-day compressive strength at 1 day, 75-82% at the age of 3-day and 85-90% at 7-day age. Fujji et al. (1998) pointed out that, 7 to 28 days compressive strength ratio is in the range of 80 to 90% for HSLC, whereas, in another study reported by Holm and Bremner (2000), this ratio is between 80 to 90% for HSLC. However, for an artificial LWAC, the ratio of 7 to 28 days compressive strengths was found between 76 to 87% (Wilson, 1988). Therefore, in the present research it was found that the OPS lightweight concretes showed the similar 7 to 28-day compressive strength ratios to the other types of structural lightweight aggregate concretes.

In structural engineering, the prediction models for 28-day compressive strength from early-ages are greatly required. Despite the fact that for high-strength concretes it is difficult to determine the specific prediction equation for the 28-day compressive strength because of the behavior and type of the aggregate (Shafigh et al., 2012). The obtained relationship between compressive strength at 28-day and premature early-age at 1, 3, and 7 days is indicated in Figure 4.4. The linear prediction models were made for all mixes to compute the 28-day compressive strength from the early-ages. It was found that all the

prediction models for early-ages showed satisfactory reliability with $R^2 > 0.90$ Furthermore, statistics analysis for the estimated relationships which obtained from six observations in different ages (shown in Figure 4.4), confirmed that the regression model is significant.

Table 4.2: Early-ages and 28-day compressive strengths under continuous moist curing

Mix Code	1 day	3 days	7 days	28 days
CM	43 (58%)	55.6 (75%)	63.2 (85%)	74.4
C20	36 (56%)	51.7 (81%)	56.1 (87%)	64.2
C40	34 (63%)	44.7 (82%)	48.6 (89%)	54.4
C60	32 (64%)	40.0 (80%)	44.2 (88%)	50.1
C80	23 (51%)	36.0 (80%)	40.0 (89%)	44.8
C100	22 (54%)	33.4 (82%)	36.3 (90%)	40.5

* Value in parenthesis presents early ages compressive strength ratio to 28 days

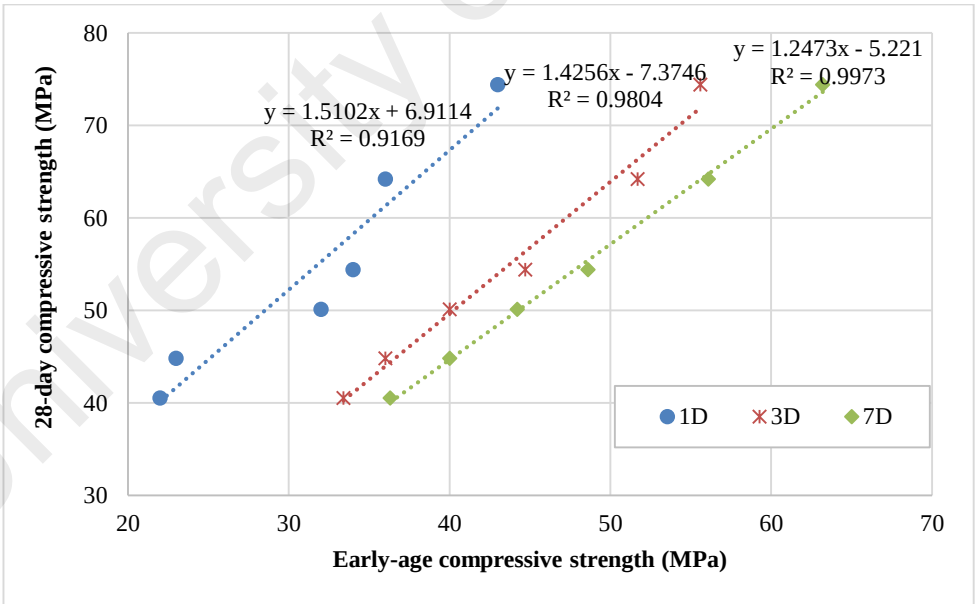

Figure 4.4: Relationship between early age (1, 3 and 7 day) and 28-day compressive strength for mixes

4.3.2 Compressive Strength under partially early curing

Curing of concrete is a process to keep moisture and temperature in concrete during its initial stages to confirm that it develops its desired properties (ACI 308, 1980). In Figure

4.5, the comparison of the 28-day compressive strength of the mixes under 7-day water curing (7D), 28-day water curing and air-curing/drying (AC) is illustrated. From this figure, almost similar compressive strength can be observed for the mixes containing OPS from 20 to 60% (semi-lightweight concrete) under 7- and 28-day curing conditions. However, as the substitution level of OPS exceeds 60%, the compressive strength reduced under 7D curing condition with the average difference of about 7% compared to continuous moist-cured specimens (28D). Whereas, generally under AC condition, compressive strength of the mixes was reduced, compared to 7D moist-cured specimens. Control concrete showed the lowest reduction in compressive strength under AC condition. However, as the substitution level of OPS increased, the reduction in compressive strength also increased. All concretes containing OPS showed the average reduction of about 9% under AC condition compared to the 7D cured specimens. Therefore, for OPS concrete at least 7 days moist curing is essential to develop compressive strength properly. Mehta and Monteiro (2006) also pointed out that minimum 7 days moist curing is required for the concretes containing ordinary Portland cement.

As can be seen in Figure 4.5, a reduction of the 28-day compressive strength was observed for all the specimens cured under air-drying condition (AC). Compare to continuous moist curing (28D), the C20 and C40 mixes showed almost similar ratio (about 9%) of reduction in compressive strength compared to the CM. However, as the substitution level of OPS increased from 40%, the reduction in compressive strength also significantly increased. With the substitution of 60, 80 and 100 % of OPS aggregate in NWC, the compressive strength value was reduced by 14%, 16%, and 17%, respectively.

The obtained prediction model between continuous moist and air-drying curing condition for all concretes (NWA-OPS) at 28-day of compressive concrete are

demonstrated in Figure 4.6. This relationship was also proposed by previous researchers for NWC containing silica fume (NC-SF) and OPS concrete made by fly ash (OPS-FA) (Atis et al., 2005; Shafigh et al., 2013). It was noted that (NWA-OPS) could have better compressive strength under AC condition than NC-SF and OPS-FA concretes.

Obtained regression statistics for the relationship between compressive strength of NWA-OPS mixes with and without curing (five samples) in Figure 4.6 which are corresponding to this study shown that the model of regression is significant.

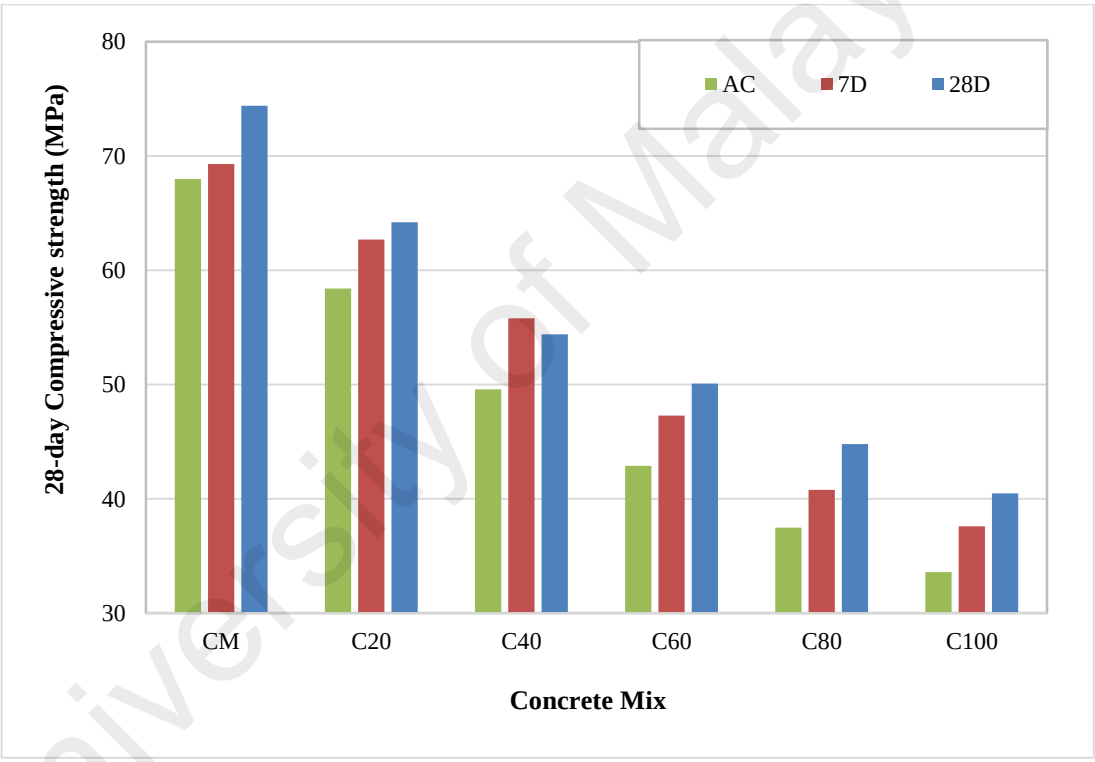

Figure 4.5: 28-day compressive strength under different curing conditions

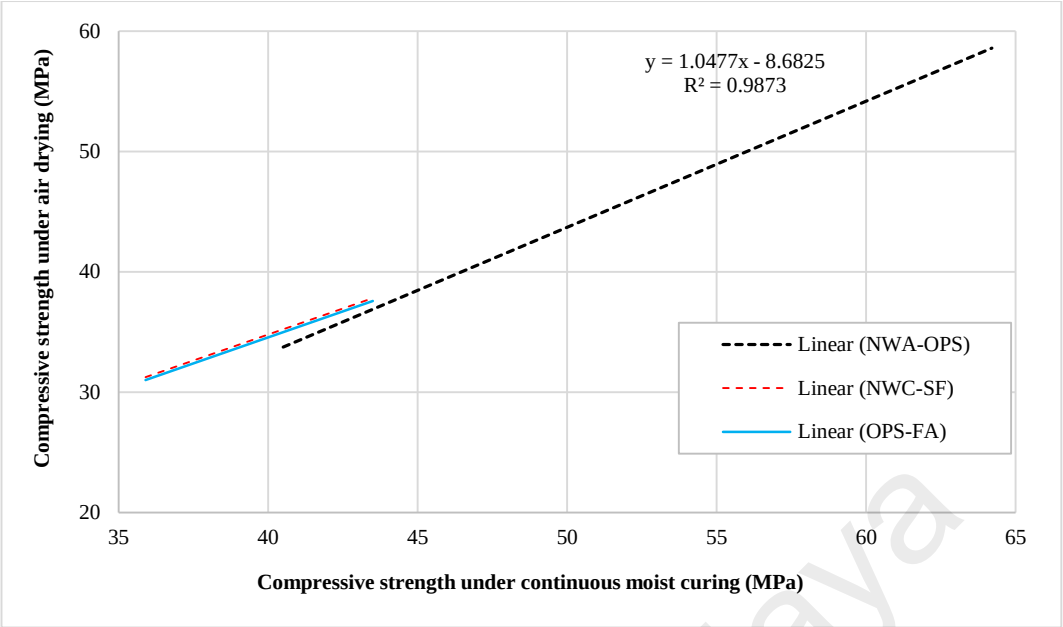

Figure 4.6: The relationship between compressive strength of NWA-OPS mixes with and without curing and comparison with normal concrete containing silica fume (NC-SF) (Atiş et al., 2005) and OPS concrete containing fly ash (OPS-FA) (Shafigh et al., 2013).

4.4 Splitting Tensile Strength

Basically, to address the issue of low tensile strength of concrete, designers consider steel reinforcement in their designs in order to increase the tensile capacity of the concrete structures. Whereas, for some structures such as airfield slabs, highways, concrete pavements, dams, employ of the reinforced concrete is impractical. Therefore, it is quite necessary to select a trustworthy of the splitting tensile strength value of the concrete, particularly for plain concrete structures such as dams under seismic behavior (Mehta & Monteiro, 2006; Neville, 2008). Further, it was reported by Bhanja and Sengupta (2005) that, if the concrete has low tensile strength, cracks under tension regions may affect serviceability and durability of the concrete structure.

The splitting tensile strength for all the mixes under moist curing at different ages and under air-drying at the age of 28-day are shown in Table 4.3. As shown in this table, the values of splitting tensile strengths for all the mixes are more than 2 MPa at 1-day age

and it gradually increased with the increment of the compressive strength. According to ASTM C 330 (2006), for the structural-grade of LWC, 2.0 MPa is the minimum value of the splitting tensile strength.

The control mix CM achieved 75% splitting tensile strength of its 28-day strength. Whereas, by the incorporating of OPS from 20 to 100%, all the mixes achieved more splitting tensile strength at early-ages. Furthermore, Table 4.3 also presents the comparison of splitting tensile strength under continuous moist curing and air-drying conditions. Results show that if the OPS content in concrete exceeds 20%, significant reduction on the tensile strength can be observed in concrete under air-drying condition.

Table 4.3: Splitting tensile strength for all the mixes under continuous moist and air curing conditions

Mix codes	Moist curing			Air dried	Reduction in tensile strength compared to moist curing (%)
	1 day	7 days	28 days	28 days	
CM	3.53 (69%)*	3.85 (75%)	5.10	4.80	6.0
C20	3.20 (78%)	3.50 (85%)	4.10	3.90	5.0
C40	3.00 (81%)	3.50 (95%)	3.70	3.20	14.0
C60	2.60 (71%)	3.40 (93%)	3.65	3.10	15.0
C80	2.50 (70%)	3.30 (94%)	3.50	2.80	20.0
C100	2.40 (71%)	3.20 (94%)	3.40	2.70	21.0

*Value in parenthesis presents ratio of the splitting tensile strength compare to 28-day result

Figure 4.7 shows a relationship between the incorporation level of OPS and the splitting tensile strength of concrete with normal coarse aggregate. This figure indicates that as the substitution level of OPS increased, the splitting tensile strength decreased at all ages. Concrete containing 100% coarse OPS aggregate has a splitting tensile strength more than 2 MPa which shows that it has standard requirement in term of tensile strength, although this value for concretes containing OPS is less than control mix. As can be seen from the regression analysis for predicted relationships in Figure 4.7 (for six observations

in each curing condition), the calculated equations are reliable. For mixes C60 to C80 which are categorized as lightweight concrete, the ratio of 28 days splitting tensile strength to the compressive strength is on average 8%. However, this ratio for NWC is generally from 8 to 14% (Kosmatka et al., 2011; Shafigh et al., 2014). Therefore, the prepared lightweight concretes can still be considered as good quality concrete with the ratio of splitting tensile to compressive strength similar to the NWC.

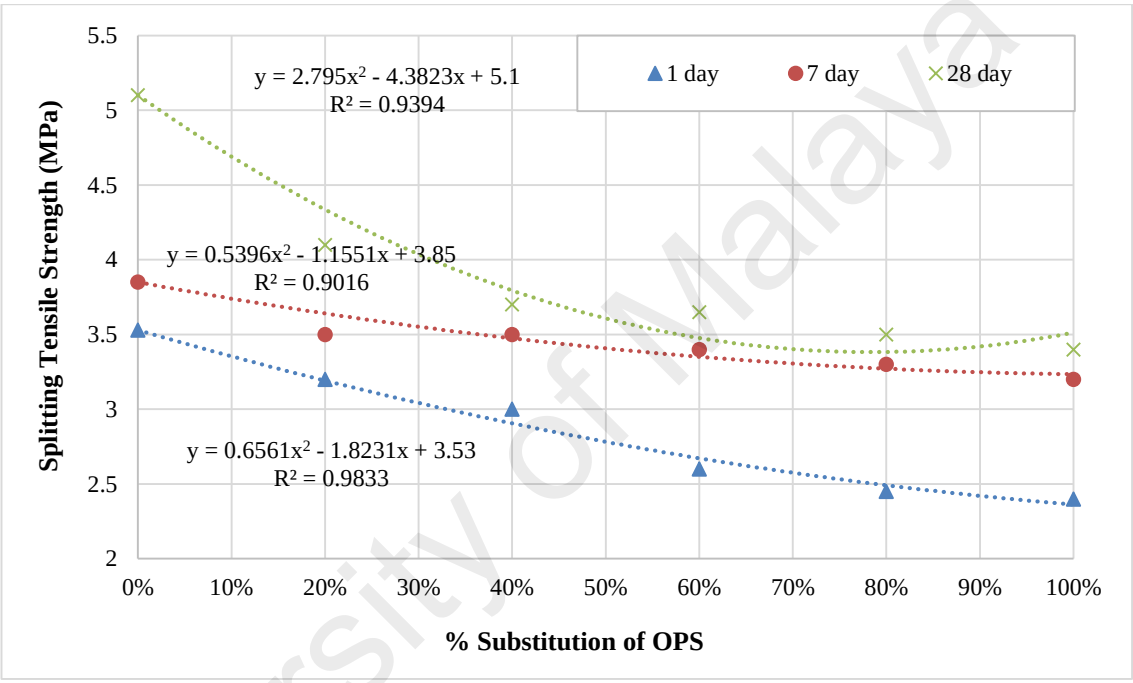

Figure 4.7: Relationship of splitting tensile strength and OPS substitution level for all mixes

The The comparison of splitting tensile test results with the predicted results from different proposed models by various researchers and standards are shown in Figure 4.8. Shafigh et al. (2014) proposed Eq. (1) for the LWC produced by using solid wastes from the palm oil industry. Arioglu et al. (2006) proposed Eq. (2) for the NWC with a cylinder compressive strength in the range of 40-120 MPa. ACI Committee (2005) proposed Eq. (3) for the NWC with a cylinder compressive strength ranging from 21 to 83 MPa. For OPSC with cube compressive strength in the range of 35 to 53 MPa, Eq. (4) was proposed (Shafigh et al., 2012), whereas, Eq. (5) was presented for NWC (FA, 1991). Shafigh et

al. (2010) proposed Eq. (6) for OPSC containing original OPS aggregates with cube compressive strength from 17 to 37 MPa. Neville (2008) reported Eq. (7) for pelletized blast furnace slag LWAC, with cube compressive strength in the range of 10 to 65 MPa. For LWAC containing cold-bonded fly ash with cube compressive strength between 20 to 47 MPa, Eq. (8) was proposed by Gesoglu et al. (2004). Smadi and Migdady (1991) studied the natural Tuff lightweight aggregate concrete with high compressive strength and proposed Eq. (9) for prediction of the splitting tensile strength. Whereas, the Eq. (10) was made for high-strength lightweight concrete (Slate et al.,1986).

$$f_t = 0.27\,(f_{cu})^{0.63} \tag{1}$$

$$f_t = 0.387\,(f_{cy})^{0.63} \tag{2}$$

$$f_t = 0.59\,(f_{cy})^{0.5} \tag{3}$$

$$f_t = 0.4887\,\sqrt{f_{cu}} \tag{4}$$

$$f_t = 0.20\,(f_{cy})^{0.70} \tag{5}$$

$$f_t = 0.20\,\sqrt[3]{f_{cu}^2} \tag{6}$$

$$f_t = 0.23\,\sqrt[3]{f_{cu}^2} \tag{7}$$

$$f_t = 0.27\,\sqrt[3]{f_{cu}^2} \tag{8}$$

$$f_t = 0.46\,\sqrt{f_{cy}} \tag{9}$$

$$f_t = 0.51\,\sqrt{f_{cy}} \tag{10}$$

Where, ft is the splitting tensile strength, fcu and fcy are the cube and cylindrical compressive strengths, respectively. As showed in Figure 8, some of the equations such

as Eq. (3) and Eq. (8) present forecast results close to the experimental results, with 90% reliability.

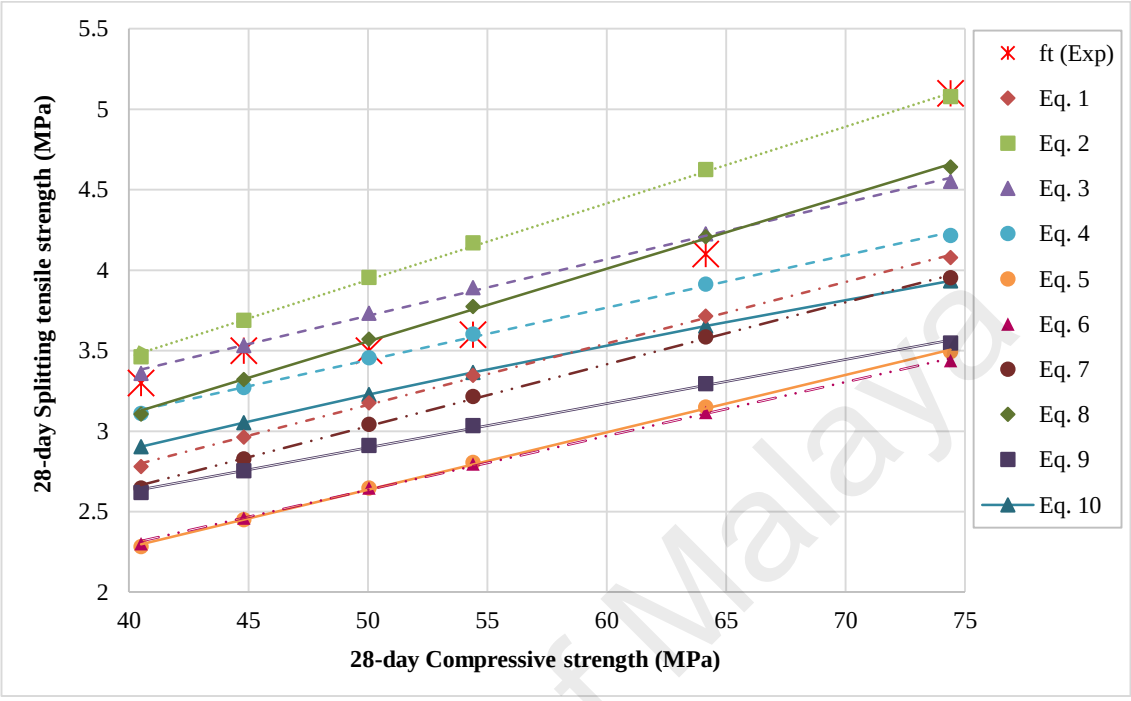

Figure 4.8: Experimental and theoretical splitting tensile strength of all concrete mixes

4.5 Water Absorption

The water absorption test was carried out for all concrete mixes at the age of 28-day for 30 minutes (initial water absorption) and 72 hours (final water absorption), as shown in Figure 4.9. Normal-weight concrete mixture (CM) showed the initial water absorption less than 3%. However, as NWA was replaced with OPS aggregate, the water absorption was consistently increased due to high water absorption of the OPS aggregate. As can be seen in Table 3.1, compare to crushed granite, the water absorption of the OPS aggregate is significant higher. Teo et al. (2007) concluded in his report that the water absorption of normal strength OPS concretes is higher than 10%. Whereas, other types of structural LWACs like pumice and expanded polystyrene aggregate concrete have the water absorption ranging from 14% to 22% and 3-6%, respectively (Babu & Babu, 2003;

Gündüz & Uğur, 2005). The investigations on analysis of statistics for six samples shown that the predicted models in Figure 4.9 are trustworthy.

The quality of concrete is categorized as good, average and poor based on the initial water absorption values of 0-3%, 3-5%, and above 5%, respectively (Ranjbar et al., 2013). It has been specified that a good quality concrete has final water absorption less than 5%. Based on the mentioned criteria it can be concluded that incorporation of OPS as coarse aggregate in concrete should be less than 50% of total volume of coarse aggregate.

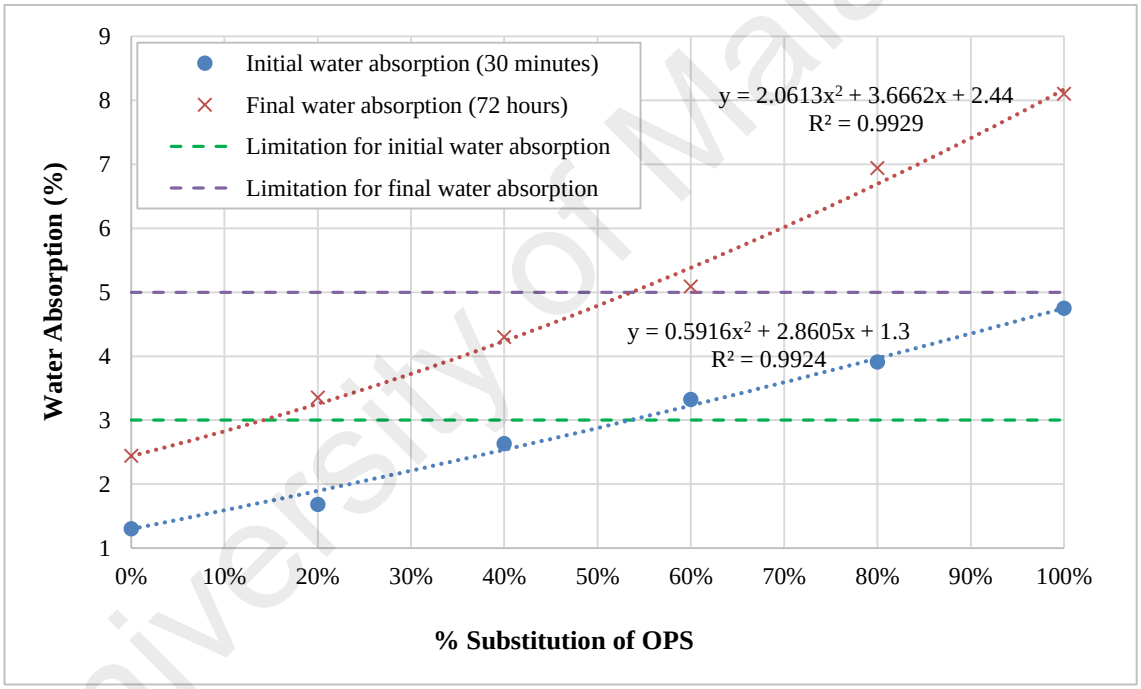

Figure 4.9: Relationship between OPS content in NWC and water absorption

4.6 Drying Shrinkage Development

For structural members, the drying shrinkage strain of the concrete plays very important role and is possibly harmful when it is restrained. However, it is not critical when used for insulation or filling purposes (Kosmatka et al., 2002). Reports (Neville, 2008; Satish & Berntsson, 2003) show that the LWC has higher drying shrinkage than NWC. It is

mainly influenced by volume of aggregate as well as aggregate's properties. In these reports, the impact of partial substation of crushed granite with OPS on concrete's drying shrinkage was investigated under cured and uncured conditions.

4.6.1 Drying shrinkage of uncured specimens

In order to evaluate precise value of the drying shrinkage strain, two test specimens for each mix were prepared and the average results were applied for analysis. As shown in Figure 4.10, according to ASTM C157 (2008), drying shrinkage strains of the concrete prisms were precisely measured by the digital version of the DEMEC Mechanical Strain Gauge which was calibrated to measure based on micro-strain.

Figure 4.10: measurement of drying shrinkage by using of DEMEC Mechanical Strain Gauge

Drying shrinkage development of concrete mixes under air-drying condition up to 275 days' age is presented in Figure 4.11. Control concrete (CM) showed the long-term shrinkage strain of 318 microstrain, which is significantly lower than the other mixes. Generally, normal-weight concrete showed the drying shrinkage ranging from of 200-800 microstrain (Zia et al., 1997). It was noted that the OPS's incorporation in conventional concrete consistently increased the drying shrinkage strain of the mixes. As the

substitution level increased beyond 60% (C80 & C100 mixes), the significant increase for shrinkage strain was observed even after 2 days of drying. During first 28 days, the increasing rate of shrinkage strain for mixes C20 to C60 was found moderate compared to the CM mix. The average difference between the mixes was found about 21%. However, this ratio was considerably higher for mixes C80 and C100 which is about 47% and 52%, respectively, higher compared to control conventional concrete. After 4 months, the drying shrinkage values for CM to C60 mixes were found constant. However, the C80 and C100 mixes were showing the consistent increase in the shrinkage strain at the similar ages. After around 10 months, the C20, C40, C60, C80 and C100 mixes showed about 19%, 31%, 57%, 96%, and 118%, higher drying shrinkage against the CM, respectively.

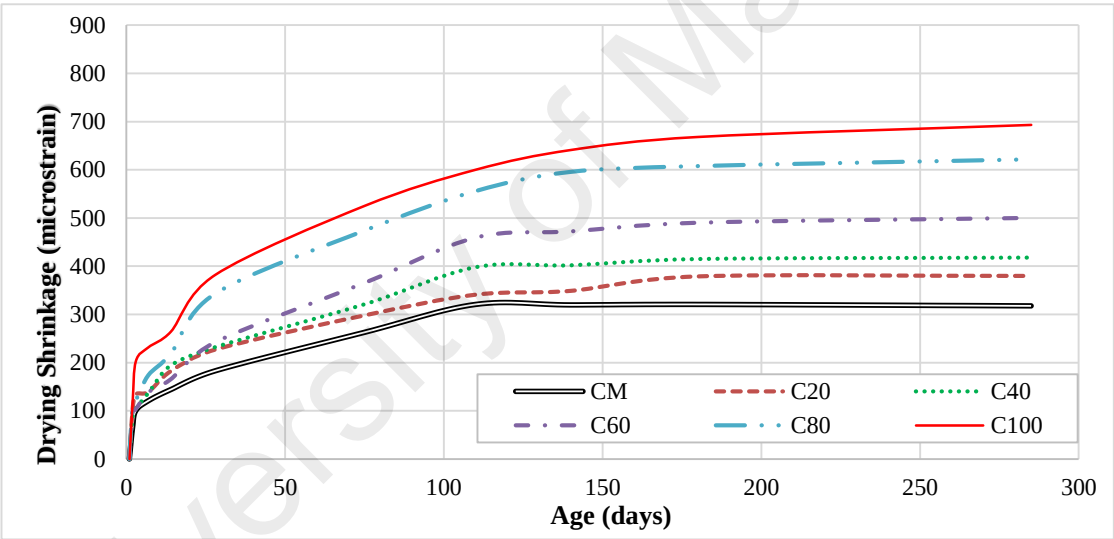

Figure 4.11: Development of drying shrinkage of all concrete mixes under air-drying condition

The surface texture and shape of OPS aggregates are the key factors for higher drying shrinkage of concrete containing OPS. Basically, surface texture of the crushed granite is rough which provides a strong bond with the cement matrix. In contract, OPS aggregates are flaky and smooth in the surface texture. Therefore, by the blend of both NWA and OPS aggregate in concrete, higher drying shrinkage strain is expected. Al-Attar (2008) studied the shrinkage behaviour of conventional concrete by considering crushed and uncrushed gravel aggregate. He highlighted that the drying shrinkage of concrete

using uncrushed gravel aggregates with smooth texture was higher than concrete made crushed aggregates. Aslam et al. (2016b) investigated the drying shrinkage behaviour of blended coarse LWAC. They reported that drying shrinkage of the OPSC could be decreased significantly by contribution of rough surface textured oil-palm-boiler clinker (OPBC) aggregate in OPS concrete.

Another important factor that affects the drying shrinkage of concrete, is the type of aggregate and its stiffness. Normally, elastic modulus of NWC is in the range of 14 to 41 GPa (Shafigh et al., 2014). However, elastic modulus of OPSC was found much lower compared to the NWC, in the range of 5.3 to 10.9 GPa (Alengaram et al., 2013). Neville (1971) revealed that modulus of elasticity of concrete is depending on the elastic modulus of its constituents and their proportions by volume in concrete. Therefore, by using of OPS in conventional concrete, the elastic modulus of the concrete might be reduced due to the low elastic moduli of OPS aggregate. On the other hand, it should be noted that, concrete containing aggregate with low modulus of elasticity has higher shrinkage strain compared to conventional aggregate concrete (Neville, 2008). It was pointed out by Shafigh et al. (2012a and 2012b) that, the expanded clay lightweight aggregate concrete with about 30% lower compressive strength than OPS concrete showed approximately 40% greater modulus of elasticity.

Another cause of high concrete's drying shrinkage is the moisture content of aggregates. Al-Attar (2008) revealed that the use of the dry aggregate in concrete mixture resulted lower drying shrinkage compare to saturated aggregates. In this research, crushed granite aggregates were replaced with saturated OPS aggregates, and therefore it is expected that concrete containing higher saturated OPS aggregates show higher drying shrinkage.

The drying shrinkage development of the OPS concrete up to the age of 9 months under air drying condition has been investigated. For this, six different mixed OPS concretes were selected from the literature to compare the experimental drying shrinkage measurements. Based on the result presented in Figure 4.11, it is recommended that in concretes under air-drying condition, incorporation of OPS should be limited to 60% of total volume of coarse aggregate.

4.6.2 Drying shrinkage of cured specimens

To control initial cracks and shrinkage, the adequate duration of curing plays an important role in concrete (Carlson, 1938). At the early-ages, a proper long period of curing significantly improves the efficiency of materials. Also, it can postpone and reduce the long-term drying shrinkage. In Figures 4.12 and 4.13, the growth of drying shrinkage for all concrete mixes under 7 and 28 days curing are indicated. As shown in Figure 4.12, the control conventional concrete showed drying shrinkage of about 270 microstrain at later-ages which was significantly low (on average 64%) compared to the C80 and C100 mixes with the shrinkage strain in the range of 700-800 microstrain. However, at long-term ages, the C20, C40, and C60 mixes showed greater drying shrinkage strain of about 20%, 38%, and 49%, respectively, in comparison with CM under 7-day of moist curing. Compare to the air-dried conditions, 7-day moist-cured specimens showed on average about 5% lower drying shrinkage results at early-ages. Similarly, the progress of drying shrinkage strain under 28-day moist curing is shown in Figure 4.13. At the early-ages, all the mixes showed the similar trend for 7 days moist-cured specimens with consistent increment in shrinkage. At long-term age (275 days), higher drying shrinkage of about 33% was recorded for concrete mixes containing OPS up to 60%, compared to the CM. Whereas for mixes containing OPS beyond 60% the increment in shrinkage was significantly higher (about 64%). Shrinkage values of CM to C60 mixes were found almost constant after 75 days. However, the constant trend for same mixes was observed at about 110

days' age for the 7-day moist-cured specimens. Nilsen and Aitcin (1992) measured the drying shrinkage of low-density concrete made of expanded shale aggregate and reported a shrinkage value of 160 microstrain at about 4 months' age under 7-day moist curing. Few years later, Al-Khaiat and Haque (1998) studied the drying shrinkage behaviour of lytag LWC under 7-day moist curing and reported a long-term (3 months) drying shrinkage value of about 640 microstrain. They concluded that, the type of lightweight aggregate in the mixture directly affects the drying shrinkage. Furthermore, Kayali et al. (1999) reported the value of shrinkage about 450 microstrain at 90 days for lightweight sintered fly ash aggregate concrete. They also showed that shrinkage of NWC was constant and stable after 400 days, while for LWC after a same period of drying, shrinkage had an upward trend. Aslam et al. (2016c) studied the impact of lightweight aggregate type on concrete's drying shrinkage. They reported that LWAC mixes containing OPS and OPBC showed lower drying shrinkage in comparison with structural LWCs made of expanded shale, lytag and sintered fly ash. Concrete mixes containing 20-60% of OPS showed drying shrinkage in the range of 280-450 and 350-460 microstrain for 7-day and 28-day cured specimens respectively at 90 days' age. These ranges are lower compared to the lightweight concretes made with expanded shale, lytag and sintered fly ash. However, the C80 and C100 mixes showed remarkably higher drying shrinkage against the same concretes at the same ages.

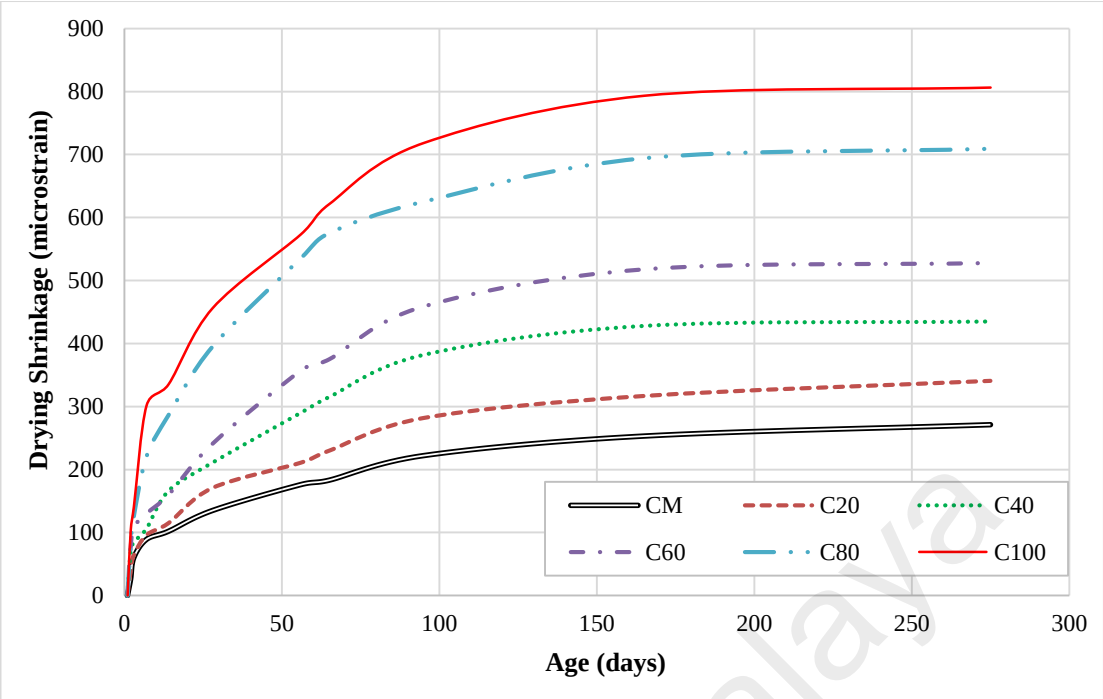

Figure 4.12: Development of drying shrinkage strain under 7-day moist curing

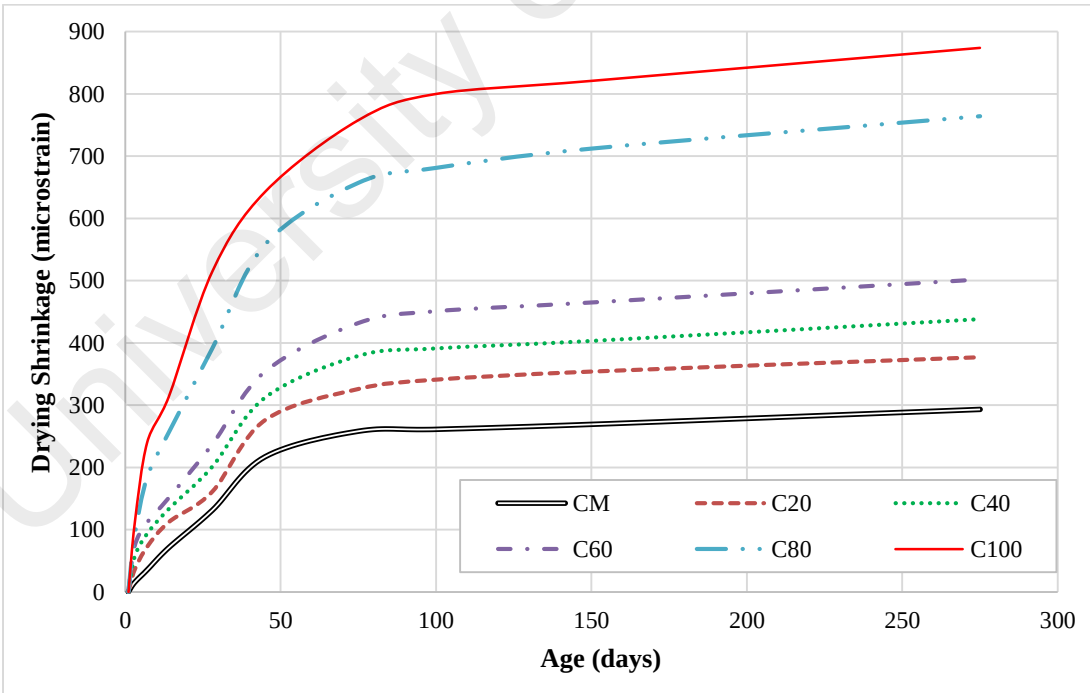

Figure 4.13: Development of drying shrinkage strain under 28-day moist curing

4.6.3 Effect of curing conditions on drying shrinkage

From the previous studies, it was found that curing has significant effect on reduction of crack and shrinkage of concrete (Maslehuddin et al., 2013; Tongaroonsri & Tangtermsirikul, 2009). Oliveira et al. (2015) indicated that the curing could control drying of concrete which causes delaying effect in the shrinkage as well as allowing the natural growth of concrete's mechanical properties. Therefore, two different curing conditions were considered in this study to evaluate the drying shrinkage of concrete samples in order to control the drying process of concrete. The relationship between air-dried and moist-cured specimens at early-ages for drying shrinkage is given in Table 4.4. It was observed that under 7-day moist curing, the CM to C60 mixes showed a reduction in drying shrinkage at early ages. Whereas, the C80 and C100 mixes showed higher drying shrinkage than air-dried specimens. This was mainly because of high volume of OPS aggregates. Table 4.4 shows the effect of curing as well as curing period which is essential to control drying shrinkage of concrete specially at early-ages. In general, more curing time results lower drying shrinkage. However, the impact of curing period on short-term drying shrinkage was more significant on concretes containing less volume of OPS. Concrete containing 80 to 100% coarse OPS aggregate showed high drying shrinkage under both 7 and 28-day moist curing conditions.

West (2010) pointed out that if there is not enough moisture for curing, existing moisture is consumed due to hydration process and shrinkage would occur. Furthermore, inadequate water on concrete's surface caused more shrinkage and crack.

Table 4.4: Effect of curing at early ages on the drying shrinkage

Mix ID	Drying shrinkage (× 10^{-6})									Compared average (7 days)	Compared average (28 days)
	Uncured			Cured (7 days)			Cured (28 days)				
	Age (days)			Age (days)			Age (days)				
	3	7	14	3	7	14	3	7	14	(%)	(%)
CM	100	121	144	60 (-40%)	89 (-26%)	102 (-29%)	15 (-85%)	35 (-71%)	71 (-51%)	-32	-69%
C20	134	139	182	64 (-52%)	96 (-31%)	115 (-37%)	35 (-74%)	72 (-48%)	112 (-38%)	-40	-54%
C40	104	137	194	85 (-18%)	106 (-23%)	166 (-14%)	56 (-46%)	93 (-32%)	133 (-31%)	-18	-37%
C60	103	138	165	108 (5%)	130 (-6%)	160 (-3%)	73 (-29%)	111 (-20%)	151 (-8%)	-01	-19%
C80	121	174	218	125 (3%)	220 (26%)	286 (31%)	89 (-26%)	183 (5%)	256 (17%)	+20	-01%
C100	203	232	264	141 (-31%)	301 (30%)	335 (27%)	110 (-46%)	240 (3%)	314 (19%)	+09	-08%

(+) Represents the positive shrinkage development in cured specimens in comparison with uncured specimens.

(-) Represents the negative shrinkage development in cured specimens in comparison with uncured specimens.

The long-term drying shrinkage under different curing conditions for all the mixes are shown in Table 4.5. It is found that the CM had the lowest drying shrinkage results among the mixes under both curing conditions compared to air-dried specimens. The consistent reduction in shrinkage was also observed for concretes with low substitution of OPS up to 40% (C20 & C40 mixes). Furthermore, on average, the C80 and C100 mixes showed higher shrinkage strain under both 7 and 28-day moist curing conditions of about 16% and 25%, respectively, compared with air-dried specimens. Neville (1996) reported that, the shrinkage at early-ages delayed by long-term moist curing. However, the magnitude of shrinkage will be higher at later ages. Furthermore, Carlson (1938) specified the contrary influences of long-term moist curing. Firstly, it increases the hardness of cement matrix which improves the restraining effect against the shrinkage. Secondly, it initiates more hydrated cement which causes higher drying shrinkage strain. Some other studies (Mehta & Monteiro, 2006; Neville, 2008) revealed that after curing, in case of

low relative humidity, diminution in volume would be occurred due to the force generated by moisture migration from the materials. Similarly, the increase moisture of material could be caused the swelling. Aslam et al. (2016c) investigated the drying shrinkage behavior of structural LWAC under 7-day moist curing. They highlighted that the saturated aggregates in the concrete mixes could minimize the early-age drying shrinkage and postpone it; nonetheless, higher shrinkage was recorded in long-term. Bogas et al. (2014) compared the behavior of lightweight and conventional concretes under 7-day moist curing. It was concluded that the long-term shrinkage could be reduced and delayed by proper curing, by about 16.5% for lightweight and 12% for conventional concretes. Furthermore, they specified that, the long-term shrinkage should be considered for low-density concrete due to its slow drying process.

Table 4.5: Effect of curing on long-term drying shrinkage

Mix ID	Drying shrinkage ($\times 10^{-6}$)									Compared average (7 days)	Compared average (28 days)
	Uncured			Cured (7 days)			Cured (28 days)				
	Age (days)			Age (days)			Age (days)				
	28	100	275	28	100	275	28	100	275	(%)	(%)
CM	183	321	318	135 (-26%)	222 (-31%)	271 (-15%)	131 (-28%)	261 (-19%)	293 (-08%)	-24	-18
C20	227	341	380	171 (-25%)	282 (-17%)	341 (-10%)	161 (-29%)	341 (0%)	377 (01%)	-17	-10
C40	232	398	418	211 (-09%)	382 (-04%)	435 (04%)	201 (-13%)	391 (-02%)	438 (05%)	-03	-03
C60	242	459	500	21 (0%)	459 (0%)	528 (06%)	237 (-2%)	451 (-02%)	502 (0%)	+02	-01
C80	343	556	622	395 (15%)	625 (12%)	709 (14%)	391 (14%)	681 (22%)	764 (23%)	+14	+20
C100	382	600	693	456 (19%)	718 (20%)	806 (16%)	515 (35%)	800 (33%)	874 (26%)	+18	+31

(+) Represents the positive shrinkage development in cured specimens in comparison with uncured specimens

(-) Represents the negative shrinkage development in cured specimens in comparison with uncured specimens

4.7 Drying shrinkage prediction model

For prediction of drying shrinkage of the oil palm shell concrete and comparison of the actual and predicted results, twelve different mix proportions in two groups with the same volume of binder and aggregate were designed by using of crushed granite (NWA) and OPS aggregates. In both groups, the NWC with only crushed granite aggregate was considered as control mix. Partially replacement of the normal-weight aggregate for the conventional concrete at an interval of 20% was applied for both groups. The type of the binder was the only difference between group (1) and group (2). Class F fly ash with dosage of 25% by weight of binder was used for group (2). Generally, the optimum level of the fly ash can be determined by evaluating its effect on mechanical properties, workability, setting time and durability of concrete. According to ACI 211.1-91(1991) the recommended substation level of class F fly ash is ranging from 15 to 25% of total cementitious material. The designed mix proportions, slump, density and 28-day compressive strength for all concrete mixes are shown in Table 4.6.

Table 4.6: Concrete mix proportions

Groups	Mix ID	Binders (kg)		Water (litre)	SP (kg/m^3)	Sand (kg/m^3)	Coarse aggregate (kg/m^3)		Slump (mm)	Density (kg/m^3)	f_{cu}*
		OPC	FA				Granite	OPS			
Group (1)	CM	480	0	163	4.8	819	898	0	205	2340	74.4
	C20						715	81	130	2205	64.2
	C40						540	163	90	2110	54.4
	C60						359	244	70	2015	50.1
	C80						179	325	65	1990	44.8
	C100						0	406	40	1900	40.5
Group (2)	FM	360	120	162	4.8	819	898	0	245	2255	59.1
	F20						715	81	110	2180	51.3
	F40						540	163	110	2100	48.8
	F60						359	244	105	1990	40.5
	F80						179	325	125	1815	35.5
	F100						0	406	90	1715	31.2

*f_{cu} is the 28-day compressive strength in MPa

In construction industry and for structural engineers, prediction of the time-dependent strain of the hardened concrete is an approach to predict serviceability of the concrete structure and assess the risk of deflection and cracking. Based on the experimental results from drying shrinkage and relevant theories, several mathematical models were generated and added to the standards and codes of practices for the prediction of drying shrinkage strain. Generally, they were designed on the basis of two main factors namely, mathematical form of the model relating to the time, and fitting of the parameters and resulting expressions. In this study, five prediction model such as ACI-209R, EN1992 (EC2), Gardner and Lockman (GL2000), Bazant and Baweja (B3) and Sakata (SAK) were applied to predict drying shrinkage behavior of the normal weight, and low-density concretes. The selected set of values considered for the prediction of drying shrinkage strain of the different concretes is shown in Table 4.7. Furthermore, the summary to different factors and parameters considered by the selected prediction models are presented in Table 4.8.

Table 4.7: Selected parameters used for prediction models in this study

Factors / Items	Input data
Age of concrete	7 days
Relative humidity (%)	70.0 to 76.0
Compressive strength (28-day, MPa)	30.0 to 75.0
Type of cement	Normal OPC
Cement content (kg/m^3)	400 - 550
Slump (mm)	40 to 245
Dimension of specimen (mm)	100 × 100 × 300

Table 4.8: Selected factors for the prediction of drying shrinkage

Factors	Drying shrinkage prediction models				
	ACI-209R	EN1992	GL2000	B3	SAK
Compressive strength (MPa)	*	*	*	*	*
Curing condition	*	-	-	*	-
Relative humidity	*	*	*	*	*
Volume to surface ratio (v/s)	*	-	*	*	*
Concrete slump	*	-	-	-	-
Fine agg. to total aggregate (Af /A)	*	-	-	-	-
Cement type	*	*	*	*	*
Water	-	-	-	-	*
Air content	*	-	-	-	-
Cross-section	-	*	*	*	*
Environmental	-	-	-	-	-
Lightweight concrete	-	*	-	-	-

4.7.1 ACI- 209R shrinkage model

The ACI 209.2R-08 (2008) is an empirical model which has been used by designers since 1971 for prediction of drying shrinkage strains for lightweight and normal weight concretes with low to moderate strength, under controlled environmental conditions. Furthermore, this model was not designed to predict the shrinkage phenomena or any specific coefficient to penalize the long-term shrinkage of LWC. According to ACI-209.2R-08 (2008), the shrinkage strain as S (t,tc) is calculated as shown in Equations 11 to 14. Where, t (days) is the age of concrete at the time of shrinkage, tc (days) the age of concrete at beginning of drying, and S_∞ is the ultimate shrinkage.

$$S_{(t,t_c)} = \frac{(t - t_c)}{f + (t - t_c)} \times S_\infty \quad (11)$$

$$f = 26.0 \times e^{\left[1.42*10^{-2}\left(\frac{V}{S}\right)\right]} \quad (12)$$

$$S_{\infty} = 780\times10^{-6}\times(Y_{sh}) \quad (13)$$

$$Y_{sh} = Y_{tc} \times Y_{RH} \times Y_{vs} \times Y_s \times Y_{\psi} \times Y_c \times Y_{\alpha} \quad (14)$$

An average value for *f* of 35 under 7 days moist curing condition and 55 for up to 3 days' steam curing is recommended by ACI, while f also can be computed from Eq. (2). The volume-surface ratio is represented as V/S. The Y_{sh} represents the product of seven applicable correction factors that take into consideration as follow;

Y_{tc} = curing time coefficient
Y_{RH} = relative humidity coefficient
Y_{vs} = factor depends on volume-surface ratio
Y_s = slump factor (mm)
Y_{ψ} = ratio of fine aggregate to total aggregates
Y_c = cement content in kg/m3
Y_{α} = air content (%).

The ACI 209.2R-08 (2008) prediction model almost covers all the effective factors with direct or indirect impact on drying shrinkage of concrete, as shown in Table 4.8. The ACI model was individually applied to each mix to estimate the shrinkage strain, although each mix has different compressive strength at 28-day. The comparison of the experimental development of drying shrinkage strain and the ACI predicted values for concrete mixes in group (1) are shown in Figure 4.14. Also table 4.9 shows a comparison between drying shrinkage strain of experimental and predicted results at early-ages. It was found that all the mixes in group (1) gained sharp shrinkage strain during the first week of drying. However, the rate of increasing in shrinkage was lower at 14 days' age for CM and C20 mixes. The difference between the predicted and experimental results for conventional concrete (CM) was found about 66%, 50% and 22% for 3-day, 7-day and 14-day, respectively. Furthermore, it was observed that as the substitution of OPS in NWC increased, the drying shrinkage strain sharply increased. The sharpest increment in

shrinkage strain and remarkable difference between the predicted and experimental test result was recorded for C100 mix.

At early-ages, the model showed under-estimated shrinkage value with increasing of drying period. At later-ages, the ACI model presented a similar trend to the CM and C20 mixes. It over-estimated (about 17%) for CM mix, and under-estimated (about 5%) for C20 mix. However, for all the remaining mixes, the ACI model predicted lower results. After 9 months of drying, for the C40, C60, C80 and C100 mixes, the model predicted lower values of shrinkage by about 26%, 39%, 54%, and 60% respectively. This shows that incorporation of OPS in conventional concrete significantly increases the rate of shrinkage development at early-ages which significantly resulted in higher drying shrinkage strain at long-term ages. Therefore, it can be concluded that due to the fast increment of drying shrinkage in concretes containing high volume of OPS, this type of aggregate cannot be used as total coarse aggregate in concrete mixtures. The optimum oil palm shell content as coarse aggregate in concrete based on mechanical and durability properties should be limited to 60% of total volume of the course aggregate in concrete mixture.

Table 4.9: Early-age measured and ACI predicted drying shrinkage strains

Groups	Mix code	Experiment			ACI predicted results *		
		3-day	7-day	14-day	3-day	7-day	14-day
Group (1)	CM	60	89	102	21 (-66%)	45 (-50%)	80 (-22%)
	C20	64	96	115	21 (-68%)	45 (-53%)	80 (-30%)
	C40	85	106	166	21 (-76%)	45 (-58%)	80 (-52%)
	C60	108	130	160	21 (-81%)	45 (-66%)	80 (-50%)
	C80	125	220	286	21 (-84%)	45 (-80%)	80 (-72%)
	C100	141	301	335	21 (-85%)	45 (-85%)	80 (-76%)
Group (2)	FM	55	98	135	27 (-51%)	58 (-41%)	102 (-25%)
	F20	76	115	158	27 (-64%)	58 (-50%)	102 (-36%)

	F40	93	119	184	27 (-71%)	58 (-51%)	102 (-45%)
	F60	102	144	199	27 (-73%)	58 (-60%)	102 (-49%)
	F80	120	151	222	27 (-77%)	58 (-62%)	102 (-54%)
	F100	161	249	386	27 (-83%)	58 (-77%)	102 (-74%)

* Value in parenthesis presents ratio of the predicted results to the experimental values.

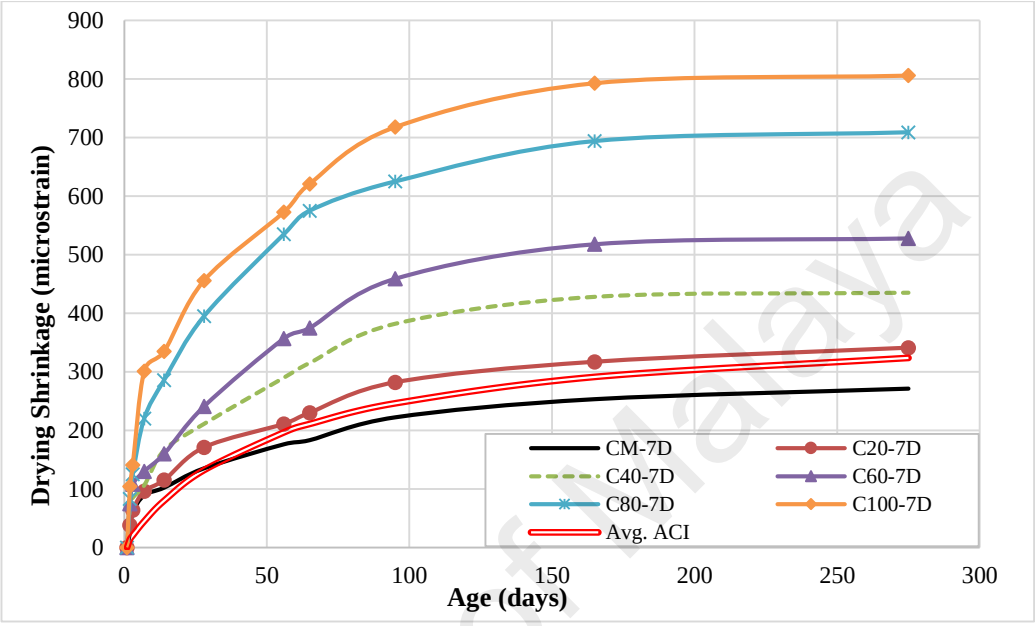

Figure 4.14: Development of the drying shrinkage for group (1) mixes with ACI-209.2R-08 (2008) model

Similar to group (1), the comparison of the drying shrinkage strain development of the experimental result and ACI predicted values for group (2) is presented in Figure 4.15. The ACI model was individually applied to each mix to estimate the shrinkage strain. Despite of different 28-day compressive strength for each mix, the model predicted almost similar results for each concrete mix with the average difference in the range of 3-5%. Therefore, the average values for the ACI model were considered and indicated in Figure 4.15. The comparison between experimental and predicted results at early-ages is shown in Table 4.9. It was observed that, the rate of increasing in shrinkage for group (2) mixes (containing fly ash) was higher than group (1) mixes.

For the conventional concrete (CM) drying shrinkage strain was recorded about 9% lower comparing to the same mix containing fly ash (FM) at 7-day age. However, for

both mixes, the ACI model predicted different results because of different compressive strengths. In general, it was found that as the substitution of OPS increased, sharper drying shrinkage strain was observed in group (2) concretes. F40 mix at 14 days' age showed about 45% higher drying shrinkage strain compared to the predicted values. Mix F6 showed a sharp increase in shrinkage strain which is almost similar to the C100 mix with average difference between the experimental and predicted results about 75%.

In general, at early ages it was observed that as drying period increases, the predicted model under-estimated the shrinkage values for all mixes in group (2), as shown in Figure 4.15. In later-ages of about 9 months of drying, predicted values of the ACI model were approximately 12%, 25%, 30%, 42%, 55%, and 62% lower than the experimental values for the mixes FM, F20, F40, F60, F80, and F100, respectively. In addition, the group (2) mixes showed higher experimental drying shrinkage strains compared to group (1) mixes. Test result in group (2) show that the addition of OPS in fly ash concrete has a significant effect on the rate of shrinkage development in early ages for all mixes, which also resulted in higher drying shrinkage strain at long-term ages.

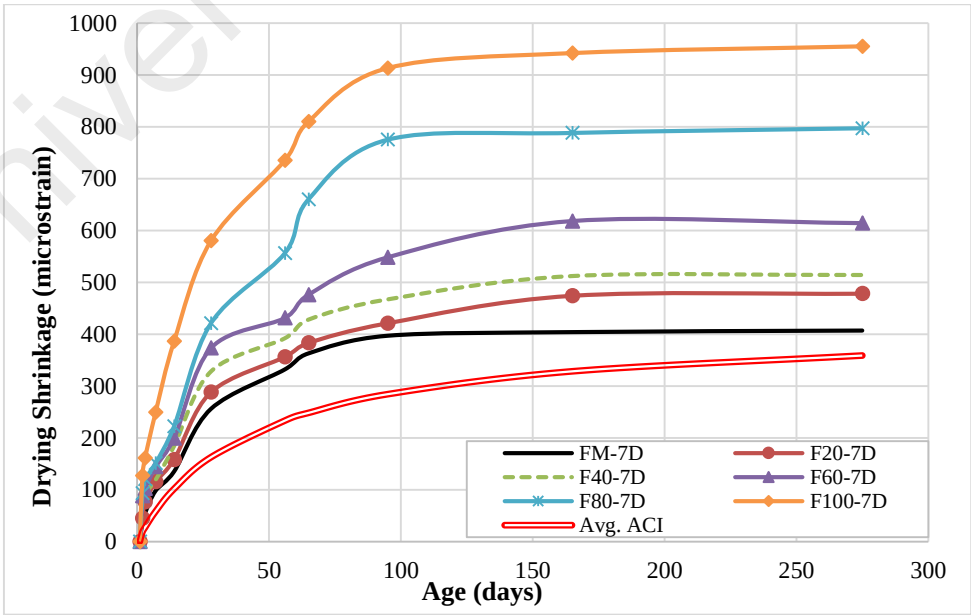

Figure 4-15: Development of the drying shrinkage for group (2) mixes with ACI-209.2R-08 (2008) model

4.7.2 Eurocode (EC2) drying shrinkage model

It has been specified by European Standards (EN 1992-1-1.,2010) that the drying shrinkage of the low-density concretes can be estimated by some expressions defined for NWC. In this model the final drying shrinkage of LWC is modified by an observational factor of 1.2. As represented in Eqs. 15 to 19 total shrinkage considered by EN1992 prediction model is composed of two components, the drying shrinkage strain and the autogenous shrinkage strain (EN 1992-1-1., 2010). Autogenous shrinkage in LWC with pre-soaked aggregates was assumed considerably smaller than normal-weight concrete, However, there is a lack of suggestions related to its prediction.

$$\varepsilon_{cs} = \varepsilon_{cd} + \varepsilon_{ca} \tag{15}$$

Where, ε_{cs} is the total shrinkage, ε_{cd} and ε_{ca} show the autogenous shrinkage and the drying shrinkage, respectively. The estimated model of drying shrinkage is also measured as follows:

$$\varepsilon_{cd} = \beta_{ds}(t, t_s).k_h.\varepsilon_{cd,0} \tag{16}$$

$$\varepsilon_{cd,0} = 0.85.\beta_{RH}.\left[(220 + 110.\alpha_{ds1}).\exp(\frac{-\alpha_{ds2}.f_{ck}}{10})\right] \tag{17}$$

$$\beta_{ds}(t, t_s) = \frac{(t - t_s)}{(t - t_s) + 0.04\sqrt{h_0^3}} \tag{18}$$

$$\varepsilon_{cs}(t, t_s) = \eta_3 * \varepsilon_{cd} \tag{19}$$

Where k_h is coefficient that depends on the notional size (h_0), $\beta_{as}(t)$ factor is associated with the function of time (t) in days. $\beta_{ds}(t, t_s)$ is the age of the experimental samples, t (in days) is the age of concrete, t_s (in days) is the age of concrete at beginning of drying and h_0 is the notional size.

The development of the experimental drying shrinkage strain and the EC2 model predicted results for mixes in group (1) are shown in Figure 4.16. Similar to the ACI model, the EC2 model was applied individually to each mix to estimate the shrinkage strain. Although each mix had different 28-day compressive strength, the EC2 model predicted almost similar results for each concrete mix. This is the reason why, the average values for the EC2 model were selected and plotted in Figure 4.16. All the experimental drying shrinkage results were observed and studied at early and long-term ages. Sharp increase in drying shrinkage was recorded for all the mixes at early-ages as shown in Table 4.10. The EC2 showed similar trend to the experimental result for CM mix at 3 days. It was also observed that, as drying age of the concrete specimens increases from 3 to 14 days, the difference between the experimental and the predicted results was increased. For instance, the predicted results for C20 mix at the ages of 3 and 7 days showed the average difference of about 7% and 18%, respectively. While at the age of 14 days, the EC2 significantly overestimated the values with the average difference of about 48%. In general, it was found that the EC2 model is not giving appropriate results for CM and C20 mixes at 14 days. Nonetheless, as the substitution level of OPS increased, the reliable results were achieved for C40 and C60 mixes. The average difference between the experimental and predicted results for C40 mix at 7 and 14 days were about 7% and 2%, respectively. Similarly, for C60 mix the difference was found about 13% and 6% at 7, and 14 days, respectively. Furthermore, the C80 and C100 mixes experienced the sharpest increase in shrinkage strain at early-ages.

Figure 4.16 shows the development trend of drying shrinkage experimental and predicted results for mixes in group (1). At later-ages up to about 2 months of drying, the EC2 model presented similar trend to the C40 and C60 mixes. Same trend also was observed for C20 mix after 3 months. At 9 months of drying, the model showed about 17% higher shrinkage strain for CM mix, whereas at same age of drying, predicted values

for C40, C60, C80 and C100 mixes were approximately 25%, 38%, 54%, and 60% lower than the experimental values, respectively. It clearly shows that the incorporation of OPS in conventional concrete significantly increases the rate of shrinkage development at early and long-term ages.

Table 4.10: Early-age difference between experimental and EC2 predicted drying shrinkage strains

Groups	Mix code	Experimental drying shrinkage strain			EC2 predicted results *		
		3-day	7-day	14-day	3-day	7-day	14-day
Group (1)	CM	60	89	102	60 (00%)	113 (-27%)	170 (-67%)
	C20	64	96	115	60 (+07%)	113 (-18%)	170 (-48%)
	C40	85	106	166	60 (+30%)	113 (-07%)	170 (-02%)
	C60	108	130	160	60 (+45%)	113 (+13%)	170 (-06%)
	C80	125	220	286	60 (+52%)	113 (+49%)	170 (+41%)
	C100	141	301	335	60 (+58%)	113 (+62%)	170 (+49%)
Group (2)	FM	55	98	135	67 (-22%)	127 (-29%)	190 (-41%)
	F20	76	115	158	67 (+12%)	127 (-10%)	190 (-20%)
	F40	93	119	184	67 (+28%)	127 (-06%)	190 (-03%)
	F60	102	144	199	67 (+34%)	127 (+12%)	190 (+04%)
	F80	120	151	222	67 (+44%)	127 (+16%)	190 (+14%)
	F100	161	249	386	67 (+58%)	127 (+49%)	190 (+51%)

* Value in parenthesis presents ratio of the predicted results to the experimental values.

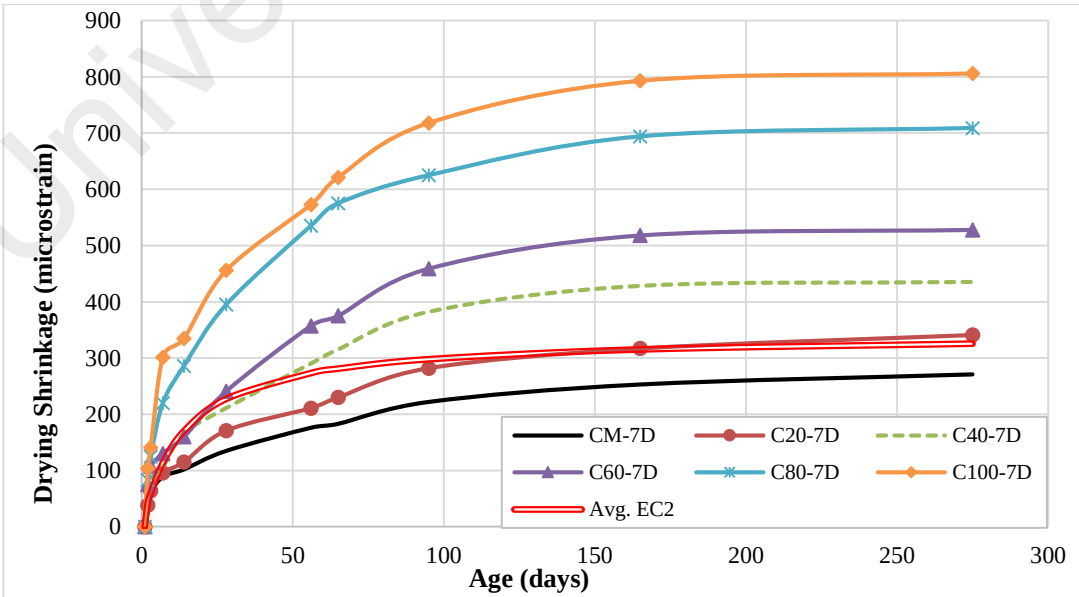

Figure 4.16: Development of the drying shrinkage for group (1) mixes with EC2 (EN 1992-1-1., 2010) model

The development of experimental drying shrinkage strain and the average EC2 predicted values for mixes in group (2) are presented in Figure 4.17. Comparing to the group (1), all mixes containing fly ash in group (2), gained sharp shrinkage strain at first week of drying. Meanwhile, as can be seen in Table 4.10, the rate of increase in shrinkage for group (2) mixes was higher compared to mixes in group (1). Consistent increase in shrinkage was also observed for group (2) mixes compared to group (1) at early-ages. The FM mix showed about 24% higher drying shrinkage at 14 days compared to CM mix. However, for the same mix, EC2 predicted significantly higher results of about 41% which was mainly because of sharp development of shrinkage strain in conventional concrete due to addition of fly ash. Furthermore, consistent increase in drying shrinkage was observed for F20 to F80 mixes as the contribution level of OPS aggregates increased from 20 to 80% with same amount of fly ash content. The predicted results for F100 mix were found significantly lower due to its higher shrinkage strain at early- and long-term ages.

The comparison of experimental and EC2 predicted results for group (2) mixes at long-term ages are shown in Figure 4.17. At later-ages of about 9 months of drying, the EC2 model underestimated the shrinkage values compared to the experimental results with the percentages of about 11%, 24%, 29%, 41%, 54%, and 62% for FM, F20, F40, F60, F80, and F100 mixes, respectively. This might be caused by sharp increase in drying shrinkage at early-ages for all mixes due to the addition of OPS and fly ash in NWC, which significantly showed higher long-term shrinkage strains.

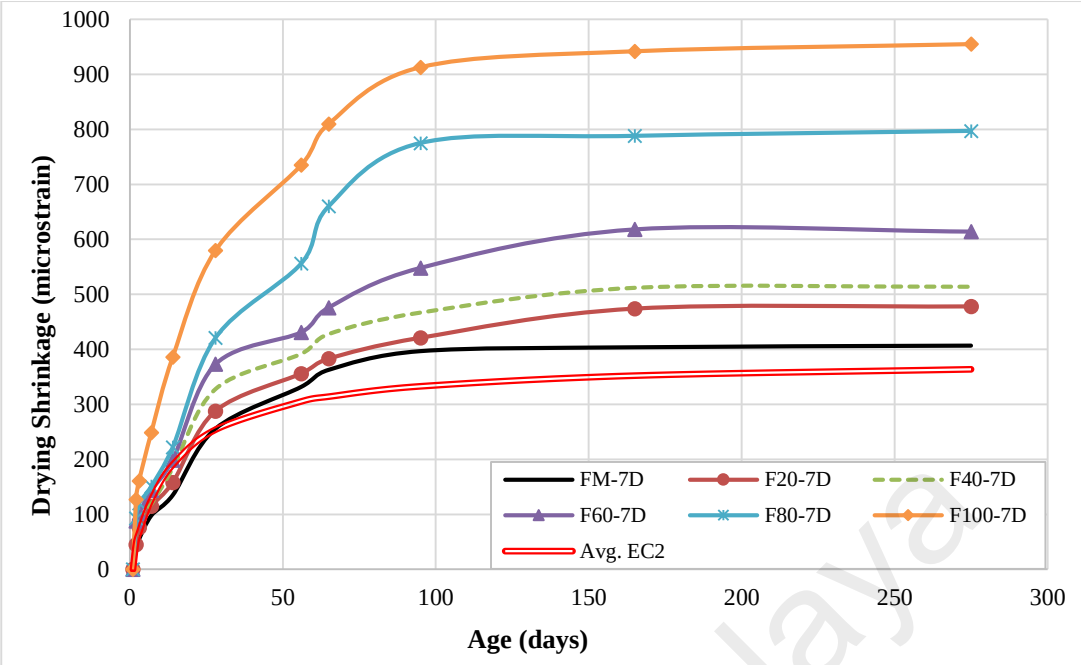

Figure 4.17: Development of the drying shrinkage for group (2) mixes with EC2 (EN 1992-1-1., 2010) model

4.7.3 Gardner and Lockman (GL-2000) model

In 2001, Gardner and Lockman (2001) proposed GL2000 model which was based on modification of Gardner and Zhao (GZ) model for prediction of drying shrinkage strain. This model is suitable to apply for conventional concrete having W/C in the range of 0.4 to 0.6 with 28 days' compressive strength up to 82 MPa. The effect of by product additive, chemical and mineral admixtures, curing method and casting temperature are not taken into consideration for this model.

The detailed expressions of this model for the prediction of drying shrinkage strain are explained below in equations 20 and 21.

$$\varepsilon_{sh}(t,t_0) = \varepsilon_{shu} * (1 - 1.18 * h^4) * \left[\frac{(t-t_0)}{(t-t_0)+0.15*(V/S)^2}\right]^{1/2} \quad (20)$$

$$\varepsilon_{shu} = 1000 * K * \left(\frac{30}{f_c'}\right)^{\frac{1}{2}} * 10^{-6} \quad (21)$$

Where ε_{sh} is the shrinkage strain, ε_{shu} ultimate shrinkage strain, t (in days) is the age of concrete, t_0 (in days) is the age of concrete at beginning of drying, h relative humidity in decimals, V volume of the specimen (mm^3), S surface area of the specimen surface (mm^2), K the cement type factor and f_c' compressive strength (MPa) at the age of 28 days. The selected parameters for the drying shrinkage prediction using GL2000 model were indicated in Table 4.8.

Figure 4.18 presents the comparative trends for the experimental and the average GL2000 predicted results of drying shrinkage strain for group (1) mixes. At early-ages, it was found that the GL2000 model predicted significantly higher results for CM and C20 mixes as can be seen in Table 4.11. This was mainly due to sharp prediction from the GL model. Furthermore, the over-estimated prediction results for C40 and C60 mixes were found much closer to the experimental results at 14 days' ages with the average difference of about 15%. For C80 and C100 mixes, the GL model under-estimated the results at all ages 3, 7 and 14 days with the increment percentages of about 30%, 46%, and 39%, respectively. For all mixes in group (1) it was observed that prediction results for minimum substitution of OPS (CM and C20 mixes) were significantly higher than the experimental results. Whereas, the mixes containing medium range of OPS substitution showed closer results. The prediction results were found significantly lower for mixes containing high volume of OPS aggregates.

Figure 4.18 shows the development trend of drying shrinkage experimental and predicted results for all mixes in group (1). Up to 2 months drying, the trend of GL2000 model was found much close to C40 and C60 mixes. However, at the same age, the experimental results for CM and C20 mixes were found significantly lower. At later ages, the GL model trend followed the trend of C40 mix. In general, at about 9 months of drying, the GL2000 model showed about 34% and 16% higher shrinkage strain for CM

and C20, respectively. While, at same age of drying, the predicted values were approximately 6%, 23%, 42%, and 49% lower than the experimental values for the C40, C60, C80 and C100 mixes, respectively.

Table 4.11: Early-age difference between experimental and GL2000 predicted drying shrinkage strains

Groups	Mix ID	Experimental drying shrinkage strain			GL2000 predictions *		
		3-day	7-day	14-day	3-day	7-day	14-day
Group (1)	CM	60	89	102	93 (-55%)	139 (-56%)	187 (-84%)
	C20	64	96	115	93 (-46%)	139 (-44%)	187 (-63%)
	C40	85	106	166	93 (-10%)	139 (-31%)	187 (-13%)
	C60	108	130	160	93 (+14%)	139 (-07%)	187 (-17%)
	C80	125	220	286	93 (+25%)	139 (+37%)	187 (+34%)
	C100	141	301	335	93 (+34%)	139 (+54%)	187 (+44%)
Group (2)	FM	55	98	135	118 (-114%)	175 (-79%)	237 (-75%)
	F20	76	115	158	118 (-55%)	175 (-52%)	237 (-50%)
	F40	93	119	184	118 (-27%)	175 (-47%)	237 (-29%)
	F60	102	144	199	118 (-15%)	175 (-21%)	237 (-19%)
	F80	120	151	222	118 (+2%)	175 (-16%)	237 (-07%)
	F100	161	249	386	118 (+27%)	175 (+30%)	237 (+39%)

* Value in parenthesis presents ratio of the predicted results to the experimental values

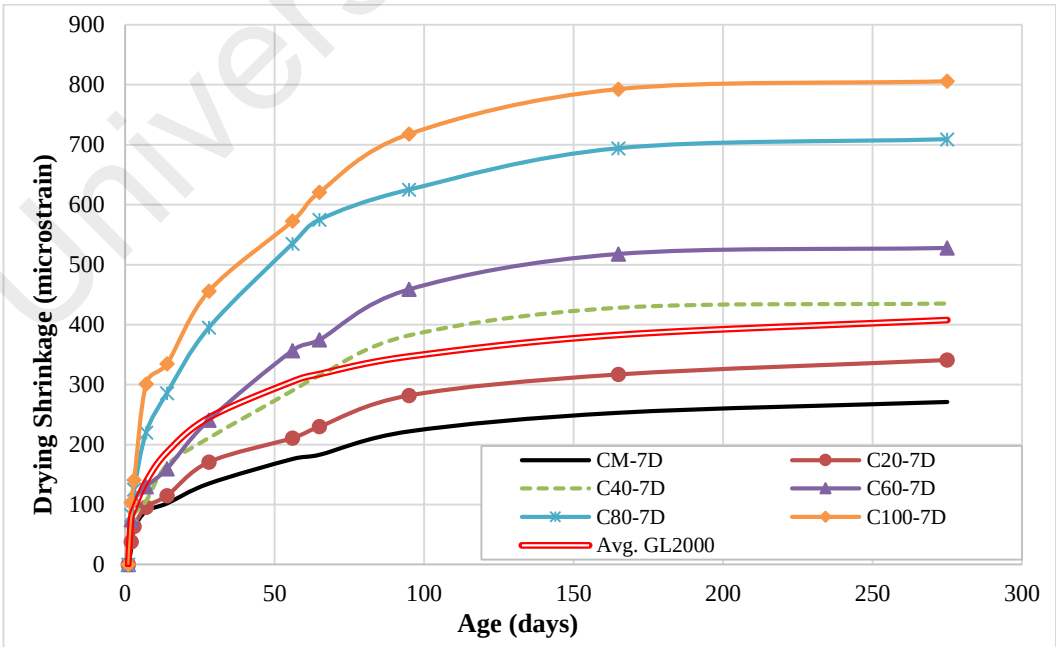

Figure 4.18: Development of the drying shrinkage for group (1) mixes with GL2000 (Gardner & Lockman, 2001) model

Table 4.11 shows the development of shrinkage strain at early-ages for mixes in group (1) and (2). It was found that the GL2000 model predicted significantly higher results for CM and C20 mixes, similar to FM and F20 mixes. Furthermore, the over-estimated prediction results for F80 mix was found much closer to the experimental results at 14 days' ages with the difference of about 7%. For C100 and F100 mixes, the GL model under-estimated the results at all ages 3, 7 and 14 days.

The development of the drying shrinkage strain and the theoretical results for group (2) mixes is shown in Figure 4.19. At first 60 days of drying, for FM to F60 mixes almost similar results of predicted and experimental shrinkage value were observed. At later ages, F60 mix gained a sharp increase in shrinkage, while FM mix experienced lower shrinkage strain compare to the predicted model. The difference between the experimental and predicted results for F1 mix was found about 21%. At 9 months of drying, the GL2000 model showed similar results for F20 and F40 mixes. Whereas, at same age of drying, the predicted values were approximately 16%, 35%, and 46% lower than the experimental values for the F60, F80 and F100 mixes, respectively.

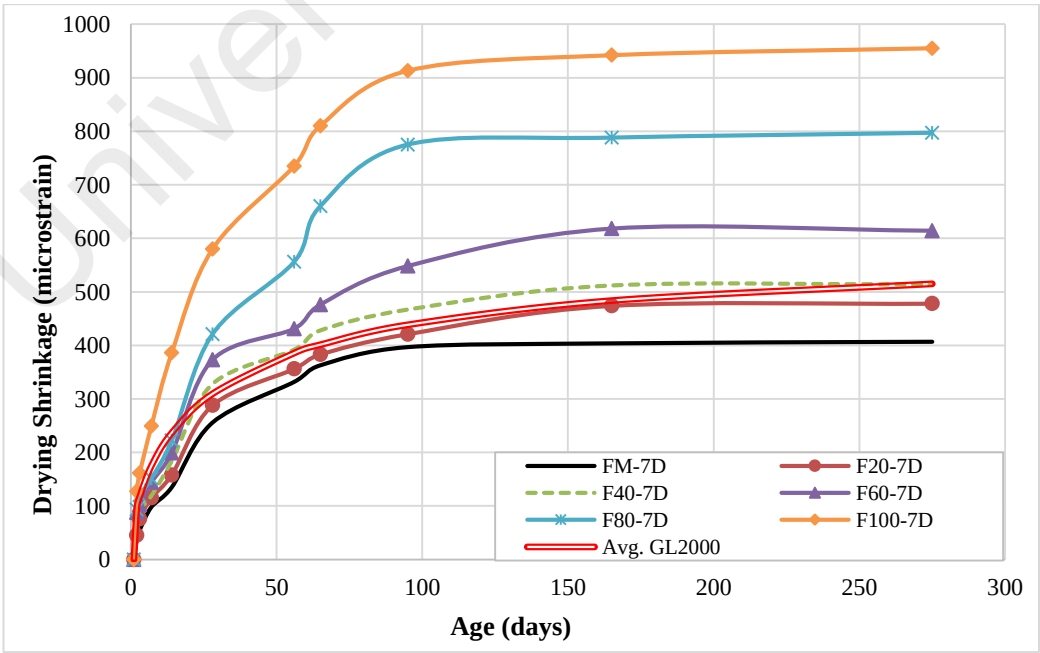

Figure 4.19: Development of the drying shrinkage for group (2) mixes with GL2000 (Gardner & Lockman, 2001) model

4.7.4 Bazant and Baweja (B3) shrinkage model

B3 model which is based on a mathematical description of several physical phenomena related to time-dependant creep and shrinkage, was developed by Bazant and Baweja (2000). This model was "calibrated by a computerized data bank comprising practically all the relevant test data obtained in various laboratories throughout the world". It was stated by Bazant and Baweja (2000) that B3 model has very low coefficient of variations compared to the ACI209R and EN1992 model. The model applies the compliance function which reduce the risk of errors due to inaccurate values related to modulus of elasticity. The proposed prediction equations for the drying shrinkage strain are as follows:

$$\varepsilon_{sh}(t, t_0) = -\varepsilon_{sh\infty} * k_h * \tan h \sqrt{\frac{t-t_0}{\tau_{sh}}} \quad (22)$$

$$\varepsilon_{sh\infty} = -\alpha_1 * \alpha_2 * [0.00856 * w^{2.1} * (145 * f_c')^{-0.28} + 270] * \frac{\left(\frac{607}{4+0.85*607}\right)^{1/2}}{\left(\frac{t_0+\tau_{sh}}{4+0.85*(t_0+\tau_{sh})}\right)^{1/2}} \quad (23)$$

where,

ε_{sh} = drying shrinkage strain,
$\varepsilon_{sh\infty}$ = ultimate shrinkage strain,
t = age of concrete (days),
t_0 = age of concrete at the beginning of drying (days),
α_1 = cement type factor,
α_2 = curing factor,
w = water content (kg/m^3),
f_c' = 28-day compressive strength (MPa),
k_h = humidity dependent factor,
τ_{sh} = size and shape dependent factor.

The selected parameters for prediction of drying shrinkage using B3 model are presented in Table 5.2.

The comparison between experimental and B3 analytical model results at early-ages is shown in Table 4.12. This model significantly under-estimated the results for all the mixes in both groups at early-ages. The development of shrinkage strain comparison at long-term ages are shown in Figures 4.20 and 4.21. For both groups, not suitable correlation between the experimental and predicted results was observed. This might be due to the factors which have been covered by this model. Therefore, this model cannot be considered as designed model for the mixes prepared in this study.

Table 4.12: Early-age difference between experimental and B3 predicted drying shrinkage strains

Groups	Mix ID	Experimental drying shrinkage strain			B3 predicted results *		
		3-day	7-day	14-day	3-day	7-day	14-day
Group (1)	CM	60	89	102	32 (+47%)	48 (+46%)	66 (+35%)
	C20	64	96	115	32 (+50%)	48 (+50%)	66 (+43%)
	C40	85	106	166	32 (+63%)	48 (+55%)	66 (+60%)
	C60	108	130	160	32 (+71%)	48 (+63%)	66 (+59%)
	C80	125	220	286	32 (+75%)	48 (+78%)	66 (+77%)
	C100	141	301	335	32 (+77%)	48 (+84%)	66 (+80%)
Group (2)	FM	55	98	135	30 (+45%)	46 (+53%)	63 (+53%)
	F20	76	115	158	30 (+60%)	46 (+60%)	63 (+60%)
	F40	93	119	184	30 (+67%)	46 (+62%)	63 (+66%)
	F60	102	144	199	30 (+70%)	46 (+68%)	63 (+68%)
	F80	120	151	222	30 (+75%)	46 (+70%)	63 (+71%)
	F100	161	249	386	30 (+81%)	46 (+82%)	63 (+84%)

* Value in parenthesis presents ratio of the predicted results to the experimental values

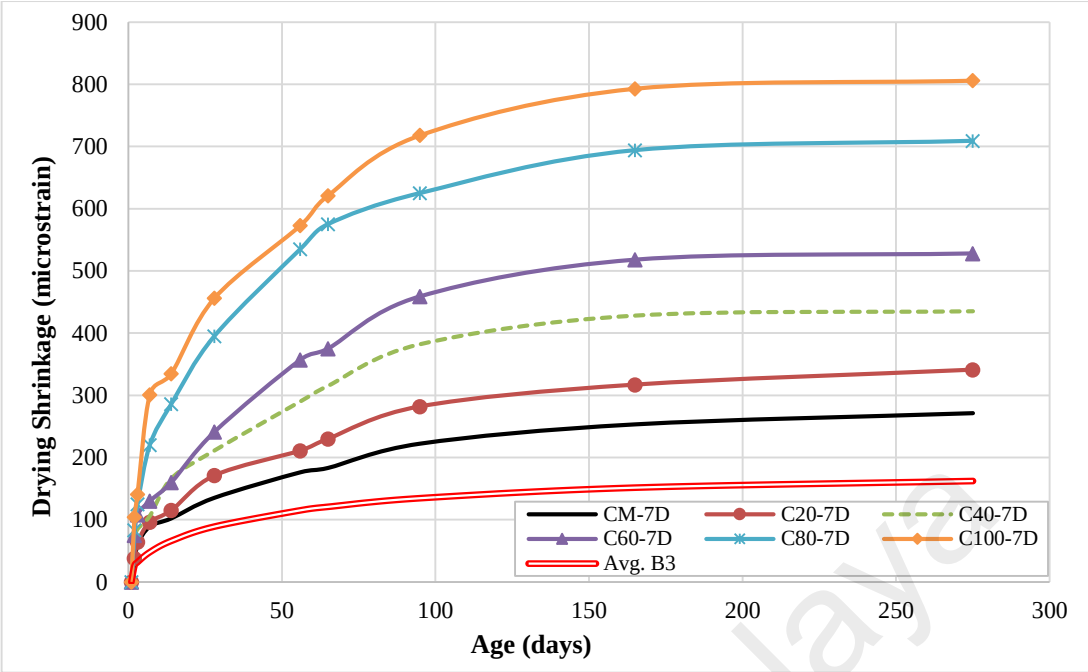

Figure 4.20: Development of the drying shrinkage for group (1) mixes with B3 (Bazant & Baweja, 2000) model

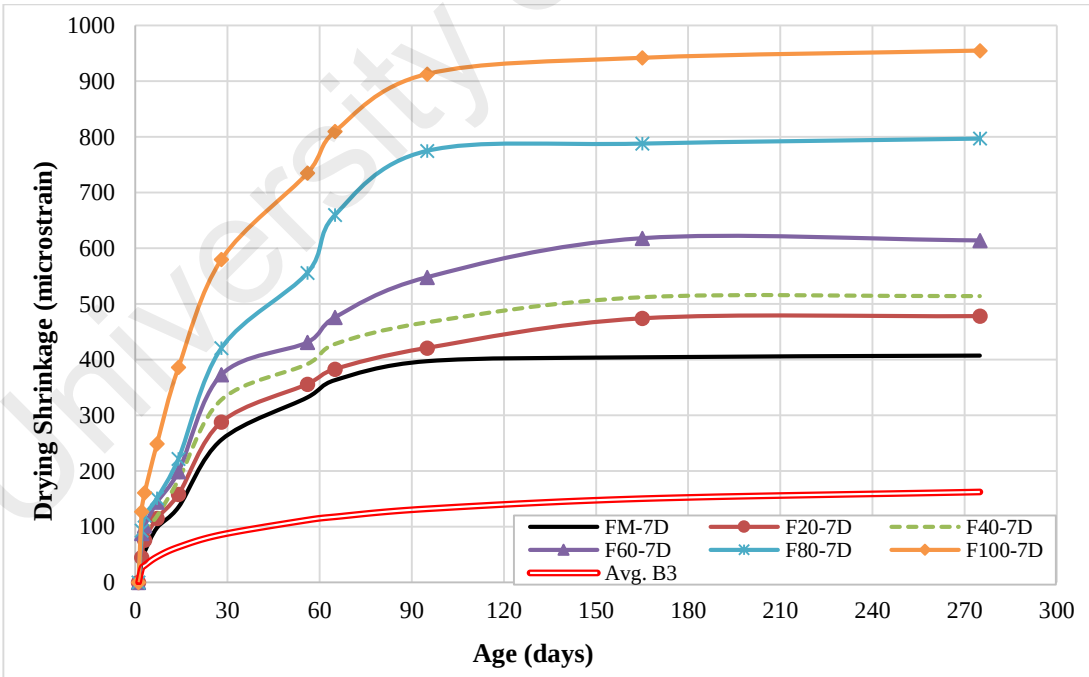

Figure 4.21: Development of the drying shrinkage for group (2) mixes with B3 (Bazant & Baweja, 2000) model

4.7.5 Sakata (SAK) shrinkage prediction model

Since the early 1980s Sakata has been working on a research project to develop a prediction model based on statistical method from many experimental data. He proposed new prediction equations of creep and shrinkage of concrete which was published in 1996 by Japan society of civil engineers in the standard specification for design and construction of concrete structure. The 1996 revision of the JSCE specification was noteworthy as for the first time it was presenting an original Japanese shrinkage model. For this model the creep and shrinkage tests were carried out corresponding to the actual and controlled ambient conditions (Sakata et al., 2001). The effect of temperature during casting of concrete also was taken into consideration. The detailed expressions of the model are presented as follows:

$$\varepsilon_{sh}(t, t_0) = \frac{\varepsilon_{sh\infty} * (t - t_0)}{\beta + (t - t_0)} \tag{24}$$

$$\varepsilon_{sh\infty} = \frac{\varepsilon_{sh\rho}}{1 + \eta * t_0} \tag{25}$$

$$\varepsilon_{sh\rho} = \frac{\alpha\,(1 - h)W}{1 + 150 exp\left\{-\frac{500}{f'_{c(28)}}\right\}} \tag{26}$$

where,

ε_{sh} = final value of shrinkage strain,
$\varepsilon_{sh\infty}$ = ultimate shrinkage strain,
t = age of concrete (days),
t_0 = age of concrete at the beginning of drying (days),
α = cement type factor,
h = relative humidity
W = water content (kg/m^3),
f'_c = 28-day compressive strength (MPa),

The selected parameters for prediction of the drying shrinkage using SAK model are summarized in Table 4.13. The early-age differences between the results are highlighted in Table 4.13. For conventional concrete (CM), the SAK model predicted

closer results at 7 days' age while, the difference was higher for 14 days. However, the model showed reliable results for mixes containing 20 to 60% OPS (C20 to C60), with the average difference in the range of 15 to 21%. Furthermore, due to sharp gain of shrinkage for C80 and C100 mixes, the SAK model predicted significantly lower results with the average difference of about 58%.

Figure 4.22 shows the development trend of drying shrinkage experimental and SAK predicted results for all mixes in group (1). At later-ages, the SAK model showed similar trend to the experimental values of C20, C40 and C60 mixes up to 30 days, whereas, the C60 mix due to sharper gain in shrinkage left the trend. At about 9 months of drying, the SAK model showed about 28% and 10% higher shrinkage strain for CM and C20 mixes, respectively, whereas, at same age of drying, the predicted values for C40, C60, C80 and C100 mixes were approximately 13%, 28%, 47%, and 53%, respectively, lower than the experimental values.

Table 4.13: Early-age difference between experimental and SAK model drying shrinkage strains

Groups	Mix ID	Experimental drying shrinkage strain			SAK predicted results *		
		3-day	7-day	14-day	3-day	7-day	14-day
Group (1)	CM	60	89	102	38 (+37%)	78 (+12%)	132 (-29%)
	C20	64	96	115	38 (+41%)	78 (+18%)	132 (-15%)
	C40	85	106	166	38 (+56%)	78 (+26%)	132 (+21%)
	C60	108	130	160	38 (+65%)	78 (+40%)	132 (+18%)
	C80	125	220	286	38 (+70%)	78 (+64%)	132 (+54%)
	C100	141	301	335	38 (+73%)	78 (+74%)	132 (+61%)
Group (2)	FM	55	98	135	39 (+29%)	82 (+17%)	138 (-02%)
	F20	76	115	158	39 (+49%)	82 (+29%)	138 (+13%)
	F40	93	119	184	39 (+58%)	82 (+31%)	138 (+25%)
	F60	102	144	199	39 (+62%)	82 (+43%)	138 (+31%)
	F80	120	151	222	39 (+67%)	82 (+46%)	138 (+38%)
	F100	161	249	386	39 (+76%)	82 (+67%)	138 (+64%)

* Value in parenthesis presents ratio of the predicted results to the experimental values

At early ages for FM mix, the predicted results were found almost similar at 14 days' age, while the 3 and 7 days' results were under-estimated by the model. Similar behaviour was also found for F20 mix, the average difference between the results was about 13% at 14 days' age. Furthermore, as the substitution of OPS increased beyond 20% in the mixes, the average difference between the experimental and predicted values was also increased. Due to sharp gain of shrinkage for F100 mix, the SAK model predicted remarkably lower results at 14 days' age with the difference of about 64%.

Figure 4.23 shows the development trend of the experimental drying shrinkage and SAK predicted results for all mixes in group (2). At later-ages, the SAK model presented similar trend to the experimental values of FM to F40 mixes up to 30 days. At later ages, the trend of the model was closer for FM mix. At about 9 months of drying, the model predicted lower results than the experimental values with the differences of about 18%, 23%, 36%, 51%, and 59% for F20, F40, F60, F80, and F100 mixes respectively, lower than the experimental values.

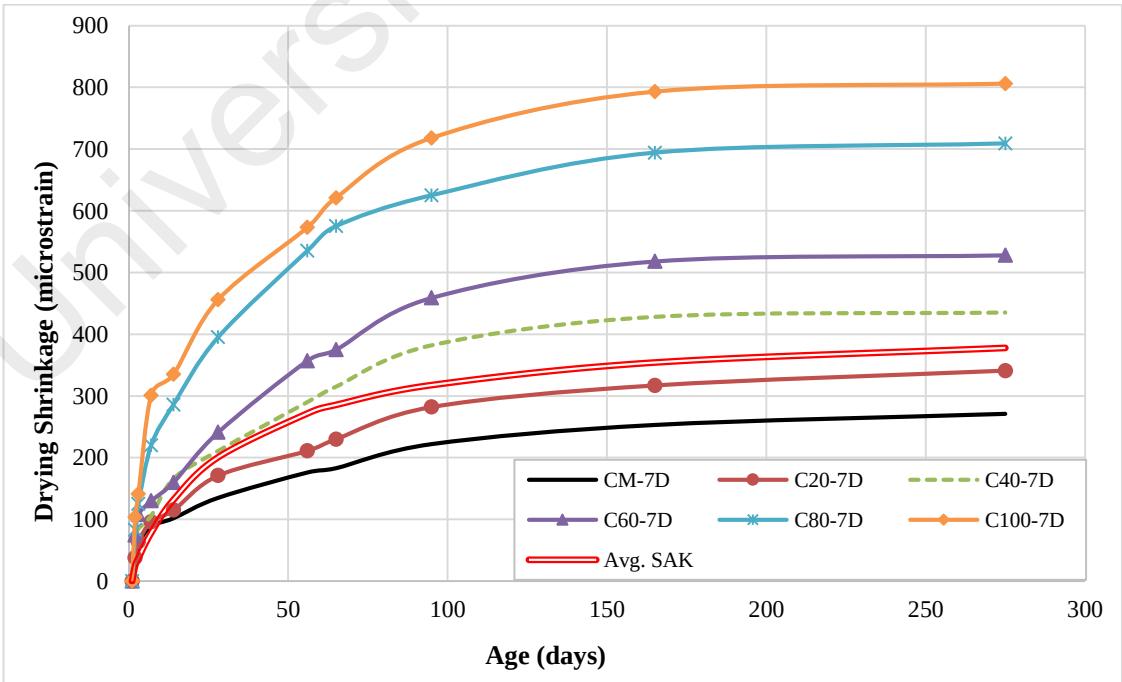

Figure 4.22: Development of the drying shrinkage for group (1) mixes with SAK (Sakata et al., 2001) model

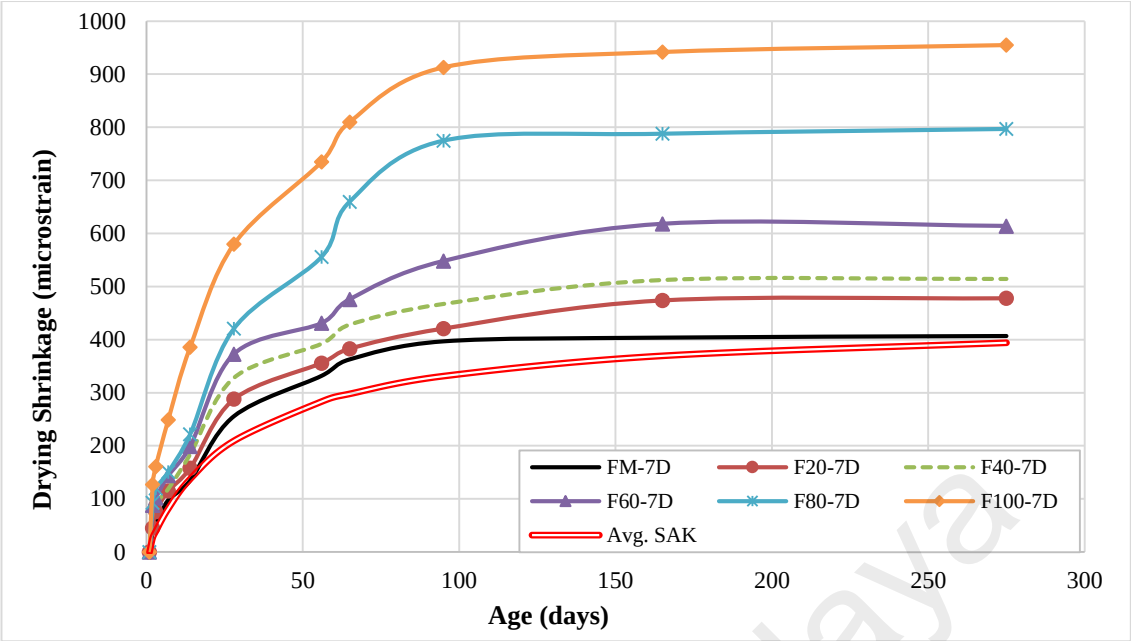

Figure 4.23: Development of the drying shrinkage for group (2) mixes with SAK (Sakata et al., 2001) model

4.8 The accuracy of the prediction models

The development of the drying shrinkage strains for the conventional concrete containing OPS as coarse aggregate (group (1)) and the same mixes with the replacement of cement with fly ash (group (2)) were compared with five prediction models (ACI 209R, EN1992, GL2000, B3 and SAK) as shown in Figures 4.14 to 4.23. Generally, it was observed that most of prediction models showed much lower results compared to the experimental values, which was mainly due to sharp gain of drying shrinkage strain for the mixes containing OPS aggregates. Therefore, to observe the accuracy of the prediction models for the prepared concrete mixes, two analyses were performed: an error percentage analysis (EP) and coefficient of variation (CV). For EP analysis, the residual values were calculated at the early age (14 days) and the long-term age (275 days). From the calculations, the positive residual values indicate that the model overestimated the data, and the negative values specify the model underestimation compared to the experimental data (Khanzadeh, 2010). In the EP analysis, the model with the minimum average error

percentage can be considered the best predictor and the best model for the CV test and this is the model with the lowest value.

The summarized results of the EP and the CV for the mixes in both groups at the age of 14-day are indicated in Table 4.14 and 4.15, respectively. In group (1) mixes, for CM concrete mixture, based on the EP and CV tests the ACI209R model was found as the best predictor for the drying shrinkage, although, it underestimates the results with the average error percentage of about 22%. The ascending rank of the other models for the conventional concrete (CM) was found as SAK, B3, EC2 and GL2000. Furthermore, the SAK model was found as better predictor for C20 concrete mixture, followed by ACI209, B3, EC2 and GL2000 models. For C40 and C60 mixes, the EC2 model was found as best predictor at early-ages for both mixes with the average difference in the range of about 2-6%, followed by the GL2000, SAK, ACI and B3 models. The higher substitution of OPS from 80 to 100% (C80 and C100) in conventional concrete showed sharp increase in the drying shrinkage, therefore, no other suitable models were found to predict better results for such concretes. Although, all the models selected in this study showed a significant difference between the experimental the predicted results with the average difference in the range of about 35 to 80%.

Similarly, in group (2) mixes, for FM concrete mixture, based on the EP and CV tests, the SAK model was found as the best predictor for the drying shrinkage at early-ages. It predicted almost 100% similar results. The ascending rank of the remaining models for the conventional concrete containing fly ash (FM) was found as ACI, EC2, B3 and GL2000. Furthermore, the SAK model was also found as a better predictor for F20 mix, followed by EC2, ACI209, GL2000 and B3 models. Similar to C40 and C60 mixes, the EC2 model was also found as best predictor at early-ages for both F40 and F60 mixes with the average difference in the range of about 3-4%, followed by the GL2000,

SAK, ACI and B3 models. The GL2000 and the EC2 models were found as good predictor for the F80 mix, the average difference between results was found in the range of 7-14%, whereas, the other models predicted significantly lower results. The OPS concrete (F100) showed sharp increase in the drying shrinkage, therefore, no other suitable models were found to predict better results for such concrete.

Table 4.14: Error percentage analyses for the mixes at early-ages (14 days)

Groups	Mix ID	Prediction models				
		ACI209	EC2	GL2000	B3	SAK
Group (1)	CM	-21.56	+66.66	+83.33	-35.29	+29.41
	C20	-30.43	+47.82	+62.60	-42.60	+14.78
	C40	-51.80	+02.40	+12.65	-60.24	-20.48
	C60	-50.00	+06.25	+16.87	-58.75	-17.50
	C80	-72.02	-40.55	-34.61	-76.92	-53.84
	C100	-76.11	-49.25	-44.17	-80.29	-60.60
Group (2)	FM	-24.44	+40.74	+75.55	-53.33	+02.22
	F20	-35.44	+20.25	+50.00	-60.12	-12.65
	F40	-44.56	+03.26	+28.80	-65.76	-25.01
	F60	-48.74	-04.52	+19.09	-68.34	-30.65
	F80	-54.05	-14.41	+06.75	-71.62	-37.83
	F100	-73.58	-50.77	-38.60	-83.67	-64.24

Table 4.15: Coefficient of variation analyses for the mixes at early-ages (14 days)

Groups	Mix ID	Prediction models				
		ACI209	EC2	GL2000	B3	SAK
Group (1)	CM	0.17	0.35	0.41	0.30	0.18
	C20	0.25	0.27	0.34	0.38	0.09
	C40	0.49	0.01	0.08	0.60	0.16
	C60	0.47	0.04	0.11	0.58	0.13
	C80	0.79	0.36	0.30	0.88	0.52
	C100	0.86	0.46	0.40	0.94	0.61
Group (2)	FM	0.19	0.23	0.38	0.51	0.01
	F20	0.30	0.13	0.28	0.61	0.10
	F40	0.40	0.02	0.17	0.69	0.20
	F60	0.45	0.03	0.12	0.73	0.26
	F80	0.52	0.10	0.04	0.79	0.32
	F100	0.82	0.48	0.33	1.01	0.66

Tables 4.16 and 4.17 present the summary of the EP and CV for both groups mixes at long-term ages (275 days). For conventional concrete (CM), the best prediction models were ACI and EC2. Although, they overestimated the results with the average difference of about 20%. This might be due to high strength of the conventional concrete. The ascending rank of the other models for the conventional concrete (CM) were found as SAK, B3 and GL2000. However, the same models (ACI and EC2) were also found as the best predictors for the C20 mix with the accuracy of approximately 96%-100%. Meanwhile, the SAK and GL2000 models predicted the shrinkage results for C20 concrete mixture with the error percentage of 11% and 20%, respectively. At long-term ages, the GL2000 model was found as best predictor for mix C40, it showed the accuracy of about 94%, followed by SAK which can predict the results with the accuracy in the range of 87-90%. The ascending rank of other models for mix C40 was EC2, ACI and B3. Furthermore, the mixes containing high volume OPS aggregates (C60 to C100) showed significantly higher experimental results. Therefore, no any accurate prediction model can be suggested for those mixes.

In group (2) mixes, for FM concrete mixture, based on the EP and CV tests, the SAK model was found to be the best predictor for the long-term drying shrinkage as it predicted almost 97% similar results. The ascending rank of the other models for the conventional concrete containing fly ash (FM) was found as EC2, ACI, GL2000 and B3. Furthermore, the GL2000 model showed a better correlation between experimental and predicted values for F20 mix, although, the difference was found about 8%, followed by SAK, EC2, ACI209 and B3 models. However, the same model GL2000 showed almost similar results for mix F40 and under-estimated with the difference of about 16% for F60 concrete mixture, whereas, the predicted values from other models were not found in suitable range for both mixes. The concretes containing high volume of OPS (F80 and

F100) showed sharp increase in the drying shrinkage, therefore, no other suitable models were found.

Table 4.16: Error percentage analyses for the mixes at long-term ages (275 days)

Groups	Mix ID	Prediction models				
		ACI209	EC2	GL2000	B3	SAK
Group (1)	CM	+19.56	+19.92	+50.55	-40.22	+39.48
	C20	-04.98	-04.62	+19.64	-52.49	+10.85
	C40	-25.51	-25.28	-06.20	-62.75	-13.10
	C60	-38.63	-38.44	-22.72	-69.31	-28.40
	C80	-54.30	-54.16	-42.45	-77.15	-46.68
	C100	-59.80	-59.67	-49.37	-79.90	-53.10
Group (2)	FM	-11.79	-10.81	26.53	-59.95	-03.19
	F20	-24.90	-24.05	07.74	-65.89	-17.57
	F40	-30.15	-29.37	00.19	-68.28	-23.34
	F60	-41.53	-40.87	-16.12	-73.45	-35.83
	F80	-54.95	-54.45	-35.38	-79.54	-50.56
	F100	-62.41	-61.98	-46.07	-82.93	-58.74

Table 4.17: Coefficient of variation analyses for the mixes at long-term ages (275 days)

Groups	Mix ID	Prediction models				
		ACI209	EC2	GL2000	B3	SAK
Group (1)	CM	0.12	0.12	0.28	0.35	0.23
	C20	0.03	0.03	0.12	0.50	0.07
	C40	0.20	0.20	0.04	0.64	0.09
	C60	0.33	0.33	0.18	0.75	0.23
	C80	0.52	0.52	0.38	0.89	0.43
	C100	0.60	0.60	0.46	0.94	0.51
Group (2)	FM	0.08	0.08	0.16	0.60	0.02
	F20	0.20	0.19	0.05	0.69	0.13
	F40	0.25	0.24	0.00	0.73	0.18
	F60	0.37	0.36	0.12	0.82	0.30
	F80	0.53	0.52	0.30	0.93	0.47
	F100	0.64	0.63	0.42	1.00	0.59

CHAPTER 5: CONCLUSION AND RECOMMENDATION

5.1 Conclusion

In this research, in order to achieve the optimum level of oil palm shell (OPS) contribution in concrete mixture for production of the lightweight aggregate concrete, six concrete mixes with different level of OPS as replacement of crushed granite from 20 to 100% (by volume) with interval of 20% were produced. The obtained results of the mechanical properties and drying shrinkage are represented as follow:

1. Replacement level of OPS from 60 to 100% in normal-weight concrete transformed it into lightweight concrete, whereas concrete mixes containing 20 to 60% of OPS aggregate, with oven-dry density between 2100 to 2200 kg/m^3 are categorized as semi-lightweight aggregate concretes.

2. In improper curing condition, concrete containing OPS aggregates has higher loss of compressive strength compared to conventional aggregate concrete. Under partial early curing (7D), concretes containing OPS showed 9% higher compressive strength in comparison with air-drying curing condition (AC). At least 7 days moist curing is recommended for OPS concrete.

3. Control mix (CM) showed the initial water absorption lower than 3%. However, since normal weight aggregate was replaced with OPS aggregate, the water absorption was consistently increased. In order to achieve a good quality concrete with final water absorption less than 5%, incorporation of OPS as coarse aggregate in concrete should be less than 50% of the total volume of coarse aggregate.

4. Under air-drying curing condition and up to 275 days' age, CM showed the long-term shrinkage strain of 318 microstrain, while drying shrinkage consistently increased by incorporation of OPS in conventional concrete up to 693 microstrain

for the mix containing just OPS as coarse aggregate. Almost similar drying shrinkage at early age (7-day) was obtained with contribution of OPS up to 60% in normal weight concrete (CM). However, the significant increase in shrinkage strain was observed even after 2 days of drying for concrete mixes containing 80 and 100% OPS. At later ages (around 10 months), the mixes containing 20, 40, 60, 80 and 100% OPS showed about 16%, 24%, 36%, 49%, and 54%, higher drying shrinkage strain compared to the control mix, respectively.

It is recommended that in concretes under air-drying condition, incorporation of OPS as coarse aggregate should be limited to 60% of total volume of the coarse aggregate in concrete mixture. Mixes containing coarse OPS more than 60% have high drying shrinkage and therefore they are not recommended to be used in structural elements.

Under moist curing condition and up to 275 days' age, CM showed the shrinkage strain of 270 microstrain compared to the mixes containing 80 and 100% OPS lightweight concretes with the shrinkage strain in the ranging from 700 to 800 microstrain. Compare to air-dried conditions, 7-day moist-cured specimens showed on average about 5% lower drying shrinkage results at early-ages, whereas at later ages, the average difference was not significant (about 2%). However, under 28 days moist curing condition, mixes containing 80 and 100% OPS showed remarkably greater drying shrinkage in comparison with the same concretes at the same ages but under 7-day moist curing condition.

5. Up to 60% replacement of crushed granite aggregates with OPS, structural lightweight aggregate concrete with maximum drying shrinkage strain of approximately 500 microstrain can be produced which is still in allowable limit for drying shrinkage.

The conventional control concrete showed lowest drying shrinkage results among the mixes under both 7 and 28 days moist curing conditions compared to air-dried specimens.

For low substitution levels of OPS (up to 40%), consistent reduction in drying shrinkage was observed when concrete specimens were cured. However, the difference between moist-cured and air-dried specimens reached to almost zero percent for the mix containing 60% OPS. The mixes containing 80 and 100% OPS showed higher shrinkage strain under both moist curing conditions of about 14% and 20%, respectively, compared to air-dried specimens.

6. Most prediction models in this study showed much lower results of drying shrinkage strain compared to the experimental values at long-term ages (275 days). It was mainly due to the sharp gaining of drying shrinkage strain for the mixes containing OPS aggregates.

   The error percentage (EP) and coefficient of variation (CV) equations were used to achieve the best prediction model for all the mixes in group (1) and (2). In general, based on EP and CV values, EC2 was the best prediction model at early-ages for both groups, same as GL2000 at long-term ages. In contrast, the B3 model exhibited poor and non-conservative results of the drying shrinkage prediction for all mixes in both groups at early and long-term ages.

   In group (1) (mixes without fly ash) and at early-ages (14 days), the best models for prediction of drying shrinkage were ACI209R, SAK for CM and C20 mixes, respectively. EC2 model was found as a practical predictor for mixes C40 and C60 with the average difference in the range of about 2-6%. However, no any accurate prediction model was found for the C80 and C100 mixes with higher substitution

of OPS from 80 to 100% in conventional concrete. In group (2) (mixes with fly ash), for FM and F20 mixes, the SAK model was considered as the best predictor with 100% and 90% similarity in results, respectively. The EC2 was the most accurate model among others for both mixes F40 and F60 with the average difference in the range of about 3-4%. For mix F80, GL2000 and EC2 models were selected with average difference in the range of 7-14%. The F6 mix with 100% OPS substation of aggregate showed the highest rate of drying shrinkage, as a result none of the models in this study could predict the drying shrinkage value for such concrete.

In group (1) and at long-term ages (275 days), both ACI and EC2 models were found as reliable predictors with accuracy of about 80% and 96% for CM and C20 mixes, respectively. The GL2000 model was selected for mix C40 with accuracy of about 94% while, no suitable prediction model was found to predict the drying shrinkage of C60 to C80 mixes. In group (2), the SAK model predicted the drying shrinkage strain with accuracy of about 97% for FM mix. A good correlation between experimental and predicted values with a difference of about 8% was observed by the GL2000 model for F20 mix. The same model showed almost similar results for F40 mix; and under-estimated the drying shrinkage with the difference of about 16% for F60 concrete mix. However, due to the sharp increase in drying shrinkage for F80 and F100 mixes, no any suitable model can be proposed.

5.2 Recommendation for further research

The present study identifies few subjects for further research as below:

1- To develop a proper drying shrinkage model to predict drying shrinkage strain of the concrete containing the optimized OPS lightweight aggregate. In present research, the maximum substitution level of the OPS was suggested 60% in normal-weight concrete.

2- Further investigation on using different types of cementitious material such as silica fume, ground granulated blast-furnace slag (GGBS), metakaolin in OPS concrete and propose drying shrinkage prediction model. The effect of fly ash on drying shrinkage of the OPS concrete was investigated in this study for mixes in group (2). By having different results from varies types of cementitious material in OPS concrete, prediction models can be proposed for drying shrinkage strain of this type of concrete.

REFERENCES

Abdullah, A. A. (1996). Palm oil shell aggregate for lightweight concrete *Waste Materials Used in Concrete Manufacturing* (pp. 624-636).

Abouhussien, A. A., Hassan, A. A., & Ismail, M. K. (2015). Properties of semi-lightweight self-consolidating concrete containing lightweight slag aggregate. *Construction and Building Materials, 75*, 63-73.

ACI 308. (1980). Proposed ACI standard: standard practice for curing concrete (pp. 45-55): *American Concrete Institute*; 2(11).

ACI 209.2R-08. (2008). Guide for modeling and calculating shrinkage and creep in hardened concrete. *American Concrete Institute*.

ACI 318M-05. (2005). Proposed ACI-Standard: Building code requirements for structural concrete and commentary: *American Concrete Institute*, Farmington Hills, Michigan, USA.

ACI 209R-97. (1997). Prediction of Creep, Shrinkage, and Temperature Effects in Concrete Structures. ACI Manual of Concrete Practice. *American Concrete Institute*, Farmington Hills, MI, pp. 209R.201-209R.247.

ACI 211-91. (1991). Standard practice for selecting proportions for normal, heavy weight and mass concrete (Reaproved 2009), *American Concrete Istitute*, Farmington Hills, MI, USA

Ahmad, H., Hilton, M., & Mohd Noor, N. (2007). Physical properties of local palm oil clinker and fly ash.

Ahmed, E., & Sobuz, H. R. (2011). Flexural and time-dependent performance of palm shell aggregate concrete beam. *KSCE Journal of Civil Engineering, 15*(5), 859-865.

Al-Attar, T. S. (2008). Effect of coarse aggregate characteristics on drying shrinkage of concrete. *Engineering and Technology Journal, 26*(2), 146-153.

Al-Khaiat, H., & Haque, M. N. (1998). Effect of initial curing on early strength and physical properties of a lightweight concrete. *Cement and Concrete Research, 28*(6), 859-866.

Alengaram, U. J., Al Muhit, B. A., & bin Jumaat, M. Z. (2013). Utilization of oil palm kernel shell as lightweight aggregate in concrete–a review. *Construction and Building Materials, 38*, 161-172.

Alengaram, U. J., Jumaat, M. Z., & Mahmud, H. (2008). Ductility behaviour of reinforced palm kernel shell concrete beams. *European Journal of Scientific Research, 23*(3), 406-420.

Alengaram, U. J., & Awam, U. M. J. K. (2009). Mechanical Properties and Structural Behaviour of Palm Kernel Shell Foamed and Non-foamed Concrete: *Jabatan Kejuruteraan Awam*, Fakulti Kejuruteraan, Universiti Malaya.

Alengaram, U. J., Jumaat, M. Z., Mahmud, H., & Fayyadh, M. M. (2011). Shear behaviour of reinforced palm kernel shell concrete beams. *Construction and Building Materials, 25*(6), 2918-2927.

Alimohammadi, V., Sedighi, M., & Jabbari, E. (2017a). Experimental study on efficient removal of total iron from wastewater using magnetic-modified multi-walled carbon nanotubes. *Ecological Engineering, 102*, 90-97.

Alimohammadi, V., Sedighi, M., & Jabbari, E. (2017b). Optimization of sulfate removal from wastewater using magnetic multi-walled carbon nanotubes by response surface methodology. *Water Science and Technology*, wst2017424.

Aminur, M. R., Harunur, M. R., Teo, D. C. L., & MM, A. Z. (2010). Effect of aggregates and curing conditions on the compressive strength of concrete with age. *Journal of Civil Engineering, Science and Technology*, 1(2), 1-6.

Arioglu, N., Girgin, Z. C., & Arioglu, E. (2006). Evaluation of ratio between splitting tensile strength and compressive strength for concrete up to 120 MPa and its application in strength criterion. *ACI Materials Journal, 103*(1), 18-24.

Aslam, M., Shafigh, P., & Jumaat, M. Z. (2015). Structural Lightweight Aggregate Concrete by Incorporating Solid Wastes as Coarse Lightweight Aggregate. *Applied Mechanics & Materials, 749*.

Aslam, M., Shafigh, P., & Jumaat, M. Z. (2016a). Drying shrinkage behaviour of structural lightweight aggregate concrete containing blended oil palm bio-products. *Journal of cleaner production, 127*, 183-194.

Aslam, M., Shafigh, P., & Jumaat, M. Z. (2016b). Effect of replacement of oil-palm-boiler clinker with oil palm shell on the properties of concrete. Paper presented at the *AIP Conference Proceedings*.

Aslam, M., Shafigh, P., & Jumaat, M. Z. (2016c). Oil-palm by-products as lightweight aggregate in concrete mixture: a review. *Journal of cleaner production, 126*, 56-73.

Aslam, M., Shafigh, P., & Jumaat, M. Z. (2018). Drying Shrinkage Strain of Palm-oil by-products Lightweight Concrete: A Comparison between Experimental and Prediction Models. *KSCE Journal of Civil Engineering, 22*(12), 4997-5008.

Aslam, M., Shafigh, P., Jumaat, M. Z., & Lachemi, M. (2016). Benefits of using blended waste coarse lightweight aggregates in structural lightweight aggregate concrete. *Journal of cleaner production, 119*, 108-117.

ASTM. (2008). Standard test method for length change of hardened hydraulic-cement mortar and concrete.

ASTM, C. (2006). 330. Standard specification for lightweight aggregates for structural concrete. *Annual Book of ASTM Standard, ASTM, West Conshohocken, PA.*

Atiş, C., Özcan, F., Kılıc, A., Karahan, O., Bilim, C., & Severcan, M. (2005). Influence of dry and wet curing conditions on compressive strength of silica fume concrete. *Building and environment, 40*(12), 1678-1683.

Atis, C. D., Ozcan, F., Kilic, A., Karahan, O., Bilim, C., & Severcan, M. H. (2005). Influence of dry and wet curing conditions on compressive strength of silica fume concrete. *Building Environment, 40*(12), 1678-1683.

BS EN 206-1. (2001). 2000 Concrete. Specification, performance, production and conformity, 22.

Babu, K. G., & Babu, D. S. (2003). Behaviour of lightweight expanded polystyrene concrete containing silica fume. *Cement and Concrete Research, 33*(5), 755-762.

Badur, S., & Chaudhary, R. (2008). Utilization of Hazardous wastes and By-products as A Green Concrete material through S/S process: A Review. *Rev. Adv. Mater. Sci, 17*(1-2), 42-61.

Basri, H. B., Mannan, M. A., & Zain, M. F. M. (1999). Concrete using waste oil palm shells as aggregate. *Cement and Concrete Research*, 29, 619-622.

Batayneh, M., Marie, I., & Asi, I. (2007). Use of selected waste materials in concrete mixes. *Waste management, 27*(12), 1870-1876.

Bazant, Z., & Baweja, S. (2000). Creep and shrinkage prediction model for analysis and design of concrete structures: Model B3. *ACI Special Publications, 194*, 1-84.

Bhanja, S., & Sengupta, B. (2005). Influence of silica fume on the tensile strength of concrete. *Cement and Concrete Research, 35*(4), 743-747.

Bisschop, J., & Van Mier, J. (2002). Drying shrinkage microcracking in cement-based materials. *Heron*, 47 (3)

Bogas, J. A., Nogueira, R., & Almeida, N. G. (2014). Influence of mineral additions and different compositional parameters on the shrinkage of structural expanded clay lightweight concrete. *Materials & Design, 56*, 1039-1048.

Carlson, R. W. (1938). Drying shrinkage of concrete as affected by many factors. *American Soc Testing & Materials Proc*.

Cement and Concrete Association of Australia (2002), Drying Shrinkage of Cement and Concrete, P6.

Clarke, J. (2002). Structural lightweight aggregate concrete. *Taylor & Francis e-Library, CRC Press*, London, United Kingdom.

Davis, H. E. (1940). Autogenous volume change of concrete. *Proc. ASTM, 40*, 1103-1110.

EN 1992-1-1., (2010). Eurocode 2: Design of concrete structures – Part 1–1: General rules and rules for buildings. *European Committee for standardization CEN*.

FA, O. (1991). Prediction of concrete tensile strength from compressive strength: evaluation of existing relations for normal weight concrete. *ACI Materials Journal, 83*(3), 302-309.

Fujji, K., Adachi, S., Takeuchi, M. T., Kakizaki, M., Edahiro, H., & lnoue, T. e. a. (1998). Properties of high-strength and high-fluidity lightweight concrete. *ACI Spec Publ, 179*, 65-84.

Gao, J., Sun, W., & Morino, K. (1997). Mechanical properties of steel fiber-reinforced, high-strength, lightweight concrete. *Cement and Concrete Composites, 19*(4), 307-313.

Gardner, N., & Lockman, M. (2001). Design Provisions for Drying Shrinkage and Creep of Normal-Strength Concrete. . *ACI Materials Journal,, 98,* , 159-167.

Gesoglu, M., Ozturan, T., & Guneyisi, E. (2004). Shrinkage cracking of lightweight concrete made with cold-bonded fly ash aggregates. *Cement and Concrete Research, 34*(7), 1121-1130.

Gribniak, V., Kaklauskas, G., Kliukas, R., & Jakubovskis, R. (2013). Shrinkage effect on short-term deformation behavior of reinforced concrete–when it should not be neglected. *Materials & Design, 51*, 1060-1070.

Gündüz, L., & Uğur, İ. (2005). The effects of different fine and coarse pumice aggregate/cement ratios on the structural concrete properties without using any admixtures. *Cement and Concrete Research, 35*(9), 1859-1864.

Hansen, W. (1987). Drying shrinkage mechanisms in Portland cement paste. *Journal of the American Ceramic society, 70*(5), 323-328.

Haque, M. (1996). Strength development and drying shrinkage of high-strength concretes. *Cement and Concrete Composites, 18*(5), 333-342.

Harimi, M., Harimi, D., Kurian, V. J., & Nurmin, B. (2005). Evaluation of the thermal performance of metal roofing under tropical climatic conditions. *Center of Mineral and Materials, Universiti Malaysia Sabah, Malaysia*.

Hassanpour, M., Shafigh, P., & Mahmud, H. B. (2012). Lightweight aggregate concrete fiber reinforcement–a review. *Construction and Building Materials, 37*, 452-461.

Holm, T. A., & Bremner, T. W. (2000). State of the art report on high strength, high durability structural low-density concrete for applications in severe marine environments. *US Army Corps of Engineers, Engineering Research and Development Center*, Erdc/Sl Tr-00-3.

Holt, E. E. (2001). Early age autogenous shrinkage of concrete. *Technical Research Centre of Finland Espoo, (Vol. 446)*, Finland.

Islam, M. M. U., Mo, K. H., Alengaram, U. J., & Jumaat, M. Z. (2016). Mechanical and fresh properties of sustainable oil palm shell lightweight concrete incorporating palm oil fuel ash. *Journal of cleaner production, 115*, 307-314.

Kayali, O., Haque, M. N., & Zhu, B. (1999). Drying shrinkage of fibre-reinforced lightweight aggregate concrete containing fly ash. *Cement and Concrete Research, 29*(11), 1835-1840.

Khairallah, R. S. (2009). Analysis of Autogenous and Drying Shrinkage of Concrete. *Doctoral dissertation.* Civil Engineering Department, McMaster university, Canada

Khanzadeh, M. (2010). Accuracy of Shrinkage Prediction Models in High Performance Concretes Containing Slag and Silica Fume. Paper presented at the In *Second International Conference on Sustainable Construction Materials and Technologies:* Ancona, Italy.

Kosmatka, S., Panarese, W., & Kerkhoff, B. (2002). Portland cement association. *Design and control of concrete mixtures, 5420*, 60077-61083.

Kosmatka, S. H., Kerkhoff, B., & Panarese, W. C. (2011). Design and control of concrete mixtures: *Portland Cement Assoc.*

Li, J., & Yao, Y. (2001). A study on creep and drying shrinkage of high performance concrete. *Cement and Concrete Research, 31*(8), 1203-1206.

Liu, M. Y. J., Alengaram, U. J., Jumaat, M. Z., & Mo, K. H. (2014). Evaluation of thermal conductivity, mechanical and transport properties of lightweight aggregate foamed geopolymer concrete. *Energy and Buildings, 72*, 238-245.

Lura, P., Jensen, O. M., & van Breugel, K. (2003). Autogenous shrinkage in high-performance cement paste: An evaluation of basic mechanisms. *Cement and Concrete Research, 33*(2), 223-232.

Mannan, M., & Ganapathy, C. (2001). Long-term strengths of concrete with oil palm shell as coarse aggregate. *Cement and Concrete Research, 31*(9), 1319-1321.

Mannan, M. A., Basri, H. B., Zain, M. F. M., & Islam, M. N. (2002). Effect of curing conditions on the properties of OPS-concrete. *Building Environment, 37*(11), 1167-1171.

Mannan, M. A., & Ganapathy, C. (2002). Engineering properties of concrete with oil palm shell as coarse aggregate. *Construction and Building Materials, 16*(1), 29-34.

Maslehuddin, M., Ibrahim, M., Shameem, M., Ali, M. R., & Al-Mehthel, M. H. (2013). Effect of curing methods on shrinkage and corrosion resistance of concrete. *Construction and Building Materials, 41*, 634-641.

Mehta, P. K., & Monteiro, P. J. (2006). Microstructure and properties of hardened concrete. *Concrete: Microstructure, properties and materials*, 41-80.

Mehta, P. K., & Monteiro, P. J. M. (2006). Concrete: Microstructure, Properties and Materials. *Third ed. McGraw-Hill*, USA, New York.

Meyer, C. (2009). The greening of the concrete industry. *Cement and Concrete Composites, 31*(8), 601-605.

Mo, K. H., Alengaram, U. J., Jumaat, M. Z., & Yap, S. P. (2015). Feasibility study of high volume slag as cement replacement for sustainable structural lightweight oil palm shell concrete. *Journal of cleaner production, 91*, 297-304.

Müller, H., Bažant, Z., & Kuttner, C. (1999). Data base on creep and shrinkage tests, *Rilem Subcommittee 5 report Rilem Tc 107-Csp*: Paris: Rilem.

Neville, A. (2000). Properties of Concrete (Fourth and Final ed.). Essex, England: *Pearson Education*: Longman Group.

Neville, A. (2008). Properties of concrete,(CTP-VVP): *Kuala Lumpur*, Malaysia.

Neville A.M., B. J. J. (2008). Concrete technology. *Pearson Education Asia Pte Ltd, PP(CTP), Malaysia*.

Neville, A. M. (1971). Hardened Concrete: Physical and Mechanical Aspects: ACI Monograph No. 6. *American Concrete Institute.* Iowa State University Press, Detroit, USA.

Neville, A. M. (1995). Properties of Concrete, Longman Group Limited. *Harlow Essex, England,*, 346-350.

Neville, A. M. (1996). Properties of concrete: *John Wiley & Sons.*

Neville, A. M. (2008). Properties of Concrete: *fourteenth ed. CTP-VVP*, Malaysia.

Nilsen, U. A., & Aitcin, P. C. (1992). Properties of high-strength concrete containing light-,normal-, and heavyweight aggregate. *Cement, Concrete and Aggregate, 14*(1), 8-12.

Okafor, F. O. (1991). An investigation on the use of superplasticizer in palm kernel shell aggregate concrete. *Cement and Concrete research*, *21*(4), 551-557.

Oliveira, M. J., Ribeiro, A. B., & Branco, F. G. (2015). Curing effect in the shrinkage of a lower strength self-compacting concrete. *Construction and Building Materials, 93*, 1026-1215.

Omar W., Makhtar A.M., Lai T.P., Omar R., and Kwong N.M. (2008), Creep, Shrinkage and Elastic Modulus of Malaysian Concrete, *Final Report-Project*, No: LPIPMlCREAMiUPP 02-02-06-09-23.

Ramezanianpour, A., Mahdikhani, M., & Ahmadibeni, G. (2009). The effect of rice husk ash on mechanical properties and durability of sustainable concretes. *International Journal of Civil Engineering, 7(2), 83-91*.

Ranjbar, M. M., Madandoust, R., Mousavi, S. Y., & Yosefi, S. (2013). Effects of natural zeolite on the fresh and hardened properties of self-compacted concrete. *Construction and Building Materials, 47*, 806-813.

Rosković, R., & Bjegović, D. (2005). Role of mineral additions in reducing CO2 emission. *Cement and Concrete Research, 35*(5), 974-978.

Sakata, K., tsubaki, T., inoue, S., & Ayano, T. (2001). Prediction Equations of Creep and Drying Shrinkage Strain for Wide-Ranged Strength Concrete. *Doboku Gakkai Ronbunshu, 2001*(690), 1-19.

Salam, S. A., & Abdullah Ali, A. (1987). Lightweight concrete using oil palm shells as aggregates. *IPMKSM*

Sarabèr, A., Overhof, R., Green, T., & Pels, J. (2012). Artificial lightweight aggregates as utilization for future ashes–A case study. *Waste management, 32*(1), 144-152.

Satish, C., & Berntsson, L. (2002). Lightweight aggregate concrete, science, technology, and applications. *Published in the USA by Noyes Publications/William Andrew Publishing*.

Satish, C., & Berntsson, L. (2003). Lightweight Aggregate Concrete, Science, Technology, and Applications. *Retrieved from Noyes Publications*, New York.

Shafigh, P., Alengaram, U. J., Mahmud, H. B., & Jumaat, M. Z. (2013). Engineering properties of oil palm shell lightweight concrete containing fly ash. *Materials & Design, 49*, 613-621.

Shafigh, P., Ghafari, H., Mahmud, H. B., & Jumaat, M. Z. (2014). A comparison study of the mechanical properties and drying shrinkage of oil palm shell and expanded clay lightweight aggregate concretes. *Materials & Design, 60*, 320-327.

Shafigh, P., Jumaat, M., & Mahmud, H. (2012). Effect of Replacement of Normal Weight Coarse Aggregate with Oil Palm Shell on Properties of Concrete. *Arabian Journal for Science & Engineering, 37*(4), 955-964.

Shafigh, P., Jumaat, M. Z., & Mahmud, H. (2010). Mix design and mechanical properties of oil palm shell lightweight aggregate concrete: a review. *International journal of the physical sciences, 5*(14), 2127-2134.

Shafigh, P., Jumaat, M. Z., & Mahmud, H. (2011). Oil palm shell as a lightweight aggregate for production high strength lightweight concrete. *Construction and Building Materials, 25*(4), 1848-1853.

Shafigh, P., Jumaat, M. Z., Mahmud, H., & Norjidah, A. A. (2012). Lightweight concrete made from crushed oil palm shell: tensile strength and effect of initial curing on compressive strength. *Construction and Building Materials, 27*(1), 252-258.

Shafigh, P., Jumaat, M. Z., Mahmud, H. B., & Alengaram, U. J. (2011). A new method of producing high strength oil palm shell lightweight concrete. *Materials & Design, 32*(10), 4839-4843.

Shafigh, P., Mahmud, H., Jumaat, M. Z., Ahmmad, R., & Syamsul, B. (2014). Structural lightweight aggregate concrete using two types of waste from the palm oil industry as aggregate. *Journal of Cleaner Production, 80*, 187-196.

Shafigh, P., Mahmud, H. B., & Jumaat, M. Z. (2012). Oil palm shell lightweight concrete as a ductile material. *Materials & Design (1980-2015), 36*, 650-654.

Shafigh, P., Mahmud, H. B., Jumaat, M. Z. B., Ahmmad, R., & Bahri, S. (2014). Structural lightweight aggregate concrete using two types of waste from the palm oil industry as aggregate. *Journal of cleaner production, 80*, 187-196.

Silva, R. V., de Brito, J., & Dhir, R. K. (2016). Establishing a relationship between modulus of elasticity and compressive strength of recycled aggregate concrete. *Journal of cleaner production, 112*, 2171-2186.

Slate, F. O., Nilson, A. H., & Martinez, S. (1986). Mechanical properties of high strength lightweight concrete. *ACI Journal Proceeding, 83*(7), 606-613.

Smadi, M., & Migdady, E. (1991). Properties of high strength tuff lightweight aggregate concrete. *Cement and Concrete Composites, 13*, 129-135.

Smadi, M. M., Slate, F. O., & Nilson, A. H. (1987). Shrinkage and creep of high-, medium-, and low-strength concretes, including overloads. *Materials Journal, 84*(3), 224-234.

Swamy, R. (2007). *Design for sustainable development of concrete construction. Pap*er presented at the Proceedings of the Fourth International Structural Engineering and Construction Conference (ISEC 4), *Taylor & Francis Ltd England.*

Tazawa, E.-i. (2014). Autogenous shrinkage of concrete: *CRC Press.*

Tazawa, E., Miyazawa, S., & Sato, T. (1993). Influence of cement composition on autogenous shrinkage. Paper presented at the *JCA Proceedings of Cement & Concrete.*

Teo, D., Mannan, M., & Kurian, V. (2010). Durability of lightweight OPS concrete under different curing conditions. *Materials and structures, 43*(1-2), 1.

Teo, D., Mannan, M. A., Kurian, V., & Ganapathy, C. (2007). Lightweight concrete made from oil palm shell (OPS): structural bond and durability properties. *Building and environment, 42*(7), 2614-2621.

Teo, D. C., Mannan, M. A., & Kurian, J. V. (2006). Flexural behaviour of reinforced lightweight concrete beams made with oil palm shell (OPS). *Journal of advanced concrete technology*, 4(3), 459-468.

Teo, D. C. L., Mannan, M. A., & Kurian, V. J. (2006). Structural concrete using oil palm shell (OPS) as lightweight aggregate. *Turkish Journal of Engineering and Environmental Sciences, 30*(4), 251-257.

Tongaroonsri, S., & Tangtermsirikul, S. (2009). Effect of mineral admixtures and curing periods on shrinkage and cracking age under restrained condition. *Construction and Building Materials, 23*, 1050-1056.

West, M. B. (2010). Effect of Materials and Curing Period on Shrinkage of Concrete. *(M.S Thesis),* University of Kansas Center for Research, Kansas, Project No. TPF-5(051)-SM Report No. 98.

Wilson, H., Malhotra, V. . (1988). Development of high strength lightweight concrete for structural applications. *International Journal of Cement Composites and Lightweight Concrete, 10*(2), 79-90.

Yaşar, E., Atiş, C. D., & Kiliç, A. (2004). High strength lightweight concrete made with ternary mixtures of cement-fly ash-silica fume and scoria as aggregate. *Turkish Journal of Engineering and Environmental Sciences*, 28(2), 95-100.

Zia, P., Ahmad, S., & Leming, M. (1997). High-performance concretes: a state-of-art report (1989-1994). *Retrieved from*